Diabetes *mellitus* is characterized by a loss of whole-body glucose homeostasis resulting from impaired insulin secretion (type 1 diabetes *mellitus* -T1DM) and/or insulin sensitivity (type 2 diabetes *mellitus* - T2DM). The liver plays a key role in glucose homeostasis through a metabolic network that converts glucose and other carbohydrates to glycogen during feeding and sustains whole body glucose demands during fasting. Since these activities are tightly controlled by insulin, a deficiency or inaction of insulin results in deregulated hepatic glucose metabolism that is incompatible with the supply and demand of whole body glucose over the daily feeding-fasting cycle.

In this Thesis, normal and deregulated liver glucose metabolism in human subjects was characterized by stable isotope tracers and noninvasive assays of hepatic metabolite enrichments from these tracers using Nuclear Magnetic Resonance (NMR) spectroscopy.

Cristina Barosa

Noninvasive Measurements of Human Hepatic Metabolism Using Deuterated Water

2011

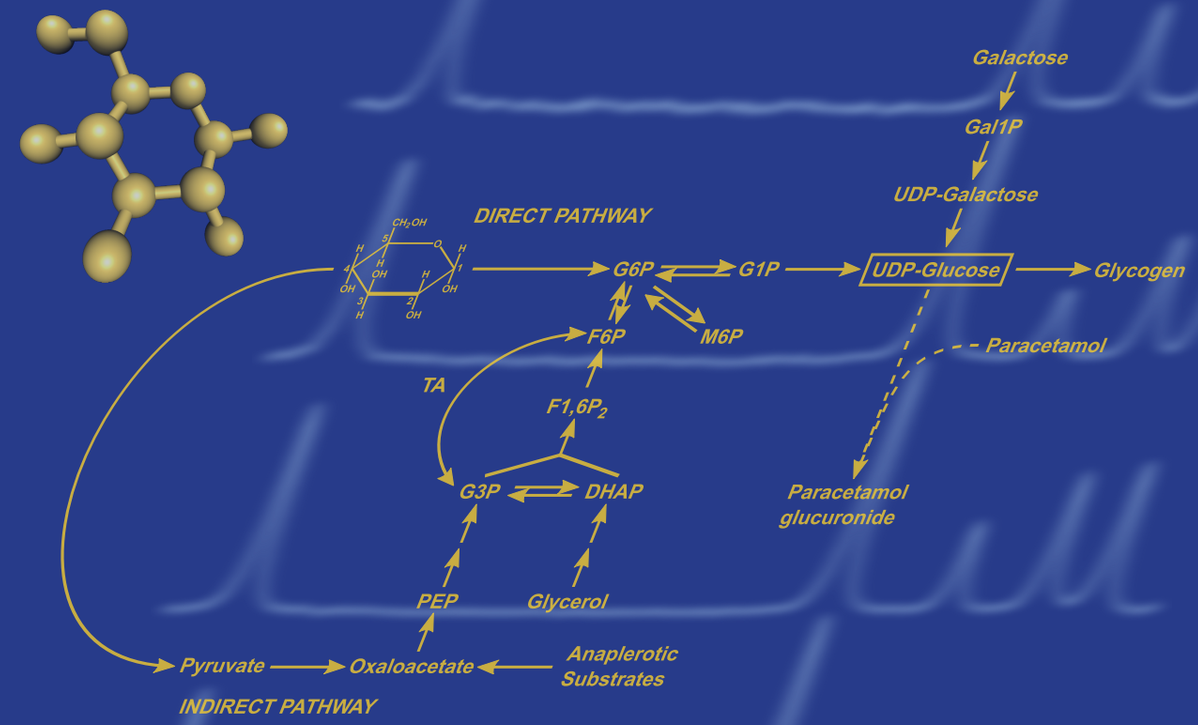

Noninvasive Measurements of Human Hepatic Metabolism Using Deuterated Water

Influence of Deuterium Exchange Processes on Metabolic Flux Estimates

Cristina Barosa

2011

UNIVERSIDADE DE COIMBRA

Noninvasive Measurements of Human Hepatic Metabolism Using Deuterated Water

Influence of Deuterium Exchange Processes on Metabolic Flux Estimates

Cristina Barosa
Universidade de Coimbra
2011

I am very grateful for the access to the facilities of the Laboratory of Nuclear Magnetic Resonance of the Center for Neurosciences and Cell Biology (LabRMN-CNC) and of the Laboratory of the Chemistry Department of the Faculty of Sciences and Technology where all these studies were carried out.

I acknowledge the Rede Nacional de RMN for access to the facilities. The Varian VNMRS 600 MHz spectrometer is part of the National NMR Network and was purchased in the framework of the National Program for Scientific Re-equipment, contract REDE/1517/RMN/2005, with funds from POCI 2010 (FEDER) and Fundação para a Ciência e a Tecnologia (FCT).

I also acknowledge the Nuclear Magnetic Resonance Laboratory of the Coimbra Chemistry Centre (www.nmrccc.uc.pt), Universidade de Coimbra, supported in part by grant REEQ/481/QUI/2006 from FCT, POCI-2010 and FEDER, Portugal.

Print Version:
Cover design: Emeric Wasielewski
Printed by: OGAMI, Serviços Multimédia, Coimbra, Portugal

Departamento das Ciências da Vida
Faculdade de Ciências e Tecnologia
Universidade de Coimbra

Noninvasive Measurements of Human Hepatic Metabolism Using Deuterated Water: Influence of Deuterium Exchange Processes on Metabolic Flux Estimates

Dissertation presented to the Faculty of Sciences and Technology of the University of Coimbra for attribution of a Ph.D. degree in Biochemistry, speciality of Technology in Biochemistry.

Dissertação apresentada à Faculdade de Ciências e Tecnologia da Universidade de Coimbra para prestação de provas de Doutoramento em Bioquímica, na especialidade de Tecnologia Bioquímica.

Cristina Barosa

2011

Supervised by:
John Griffith Jones, Ph.D.
Madalena Caldeira, Ph.D.

CONTENTS

Abbreviations		VIII
Summary		XIII
Resumo		XVII
Chapter 1	General Introduction	1
Chapter 2	Sources of Hepatic Glycogen Synthesis Following a Mixed Breakfast Meal in Healthy Subjects	57
Chapter 3	Significant Transaldolase Exchange Activity in Human Liver: Implications for Deuterated Water Measurements of Gluconeogenesis	89
Chapter 4	Contribution of Proteolytic and Metabolic Sources to Hepatic Glutamine	113
Chapter 5	Concluding Remarks	147
Acknowledgdments/Remerciements/Agradecimentos		153

ABBREVIATIONS

[^{18}F]FDG	Fluorine-18-labeled 2-fluoro-2-deoxy-D-glucose
[^{18}F]FTHA	Fluorine-18-labeled 6-thia-hepta-decanoic acid
^{11}C	Carbon 11
^{12}C	Carbon 12
^{13}C	Carbon 13
^{14}C	Carbon 14
^{18}F	Fluorine-18
^{1}H	Proton
^{2}H	Deuterium
$^{2}H_2O$	Deuterated water
^{3}H	Tritium
$^{3}H_2O$	Tritiated water
ADA	American Diabetes Association
ATP	Adenosine triphosphate
BMI	Body mass index
BW	Body water
C^2H_3CN	Deuterated acetonitrile
CH_3CN	Acetonitrile
CSII	Continuous subcutaneous insulin infusion pumps
D_1	Pulse delay
DHAP	Dihydroxyacetone phosphate
DMSO	Dimethylsulfoxide
E4P	Erythrose-4-phosphate
EGP	Endogenous glucose production
F1,6P_2	Fructose-1,6-bisphosphate

$F1,6P_2ase$	Fructose-1,6-bisphosphatase
F6P	Fructose-6-phosphate
FFA	Free fatty acids
fid	Free induction decays
G1P	Glucose-1-phosphate
G3P	Glyceraldehyde-3- phosphate
G6P	Glucose-6- phosphate
G6Pase	Glucose-6- phosphatase
$G6P_{\mathbf{Direct}}$	Direct pathway contribution to glycogen synthesis
$G6P_{\mathbf{F6P}}$	Glucose-6-phosphate fraction participating in G6P-F6P exchange
$G6P_{\mathbf{Indirect}}$	Indirect pathway contribution to glycogen synthesis
$G6P_{\mathbf{TA}}$	Glucose-6-phosphate fraction that experienced TA exchange
GK	Glucokinase
GLUT2	Hepatic non-insulin sensitive glucose transporters
GP	Glucose production
GS	Glycogen synthase flux
$GS_{\mathbf{G6P}}$	Glycogen synthase flux from G6P
$GS_{\mathbf{Gal}}$	Glycogen synthase flux from galactose
HbA1c	Glycosylated hemoglobin
HDL	High density lipoprotein
Hz	Hertz
I	Spin quantum number
IFG	Impaired fasting glucose
IGT	Impaired glucose tolerance
IRS-1	Insulin receptor substrate-1
IRS-2	Insulin receptor substrate-2

$LiBH_4$	Lithium borohydride
M6P	Mannose-6-phosphate
MAG	Monoacetone glucose
MAGL	Monoacetoneglucuronolactone
MHz	Mega Hertz
MIDA	Mass isotopomer distribution analysis
MS	Mass Spectrometry
NADH	Reduced nicotinamide adenine dinicleotide
NFG	Normal fasting glucose
NGT	Normal glucose tolerance
NMR	Nuclear Magnetic Resonance
NOE	Nuclear Overhauser Effect
OAA	Oxaloacetate
OGTT	Oral glucose tolerance test
PAGN	Phenylacetylglutamine
PEP	Phosphoenolpyruvate
PEPCK	Phosphoenolpyruvate carboxykinase
PET	Positron Emission Tomography
PI3-kinase	Phosphatidylinositol 3-kinase
PPAR-γ	Peroxisome proliferator-activated receptor-gamma
R_a	Rate of appearance
S7P	Sedoheptulose-7-phosphate
SEM	Standard error of the mean
SH2	Src homology 2
SNR	Signal to noise ratio
SPE	Solid phase extraction
T_1	Longitudinal relaxation times

T1DM	Type 1 diabetes mellitus
T2DM	Type 2 diabetes mellitus
TA	Transaldolase
THF	Tetrahydrofuran
TNF-α	Tumor necrosis factor-alpha
TPI	Triose phosphate isomerase
TZDs	Thiazolidinediones
UDP-glucose	Uridine diphosphate-glucose
WHO	World Health Organization

SUMMARY

Diabetes *mellitus* is characterized by a loss of whole-body glucose homeostasis resulting from impaired insulin secretion (type 1 diabetes *mellitus* -T1DM) and/or insulin sensitivity (type 2 diabetes *mellitus* -T2DM). The liver plays a key role in glucose homeostasis through a metabolic network that converts glucose and other carbohydrates to glycogen during feeding and sustains whole body glucose demands during fasting. Since these activities are tightly controlled by insulin, a deficiency or inaction of insulin results in deregulated hepatic glucose metabolism that is incompatible with the supply and demand of whole body glucose over the daily feeding-fasting cycle.

In this Thesis, normal and deregulated liver glucose metabolism in human subjects was characterized by stable isotope tracers and noninvasive assays of hepatic metabolite enrichments from these tracers using Nuclear Magnetic Resonance (NMR) spectroscopy.

Chapter 1: A general introduction is presented in this Chapter focused in Diabetes *mellitus*. Hepatic glucose metabolism and an overview to its regulatory aspects are presented. Disruption of glucose fluxes in T1DM, T2DM and Insulin Resistance are described. Molecular mechanisms of insulin signaling and T2DM therapy are briefly overviewed. The use of isotopes to study the hepatic metabolism is underlined in this Chapter as well the importance of the use of xenobiotics to noninvasively address glucose and protein metabolism.

Chapter 2: Hepatic glycogen synthesis following a breakfast meal that included milk was evaluated in healthy subjects using deuterated water (^2H_2O) and [1-^{13}C]glucose tracers for resolving the contributions of galactose, direct, and indirect pathways to glycogen synthase flux.

The completeness of hepatic glucose-6-phosphate-fructose-6-phosphate (G6P-F6P) exchange was confirmed using [U-$^{2}H_{7}$]glucose hence the dilution of the ^{2}H label in position 2 could be completely attributed to galactose metabolism. Transaldolase (TA) exchange activity was also measured. Its influence on the direct and indirect pathway contributions derived from the $^{2}H_{2}O$ method was evaluated and compared with data obtained from [1-^{13}C]glucose – this latter tracer being insensitive to TA exchange activity. Analysis of carbon-13 (^{13}C) and deuterium (^{2}H) was addressed by NMR spectroscopy.

Chapter 3: The presence of hepatic TA exchange activity was determined in a group with normal fasting glucose/normal glucose tolerance (NFG/NGT) subjects, in a group with impaired fasting glucose/impaired glucose tolerance (IFG/IGT) and in a group with impaired fasting glucose/normal glucose tolerance (IFG/NGT) subjects. TA measurements were determined by infusing [1-^{13}C]acetate. Glucose and glucuronide ^{13}C-enrichments were analyzed by ^{13}C NMR. TA increases the label of position 5 of glucose independently of gluconeogenic activity when deuterated water method is used. This overestimates the contribution of gluconeogenic fraction to glucose production. The contribution of gluconeogenesis and glycogenolysis to endogenous glucose production (EGP) was determined after an overnight fasting for the three groups using $^{2}H_{2}O$. The values obtained were corrected for TA exchange activity resulting in a significantly decreased gluconeogenic fraction and a significantly increased glycogenolytic contribution. Also $^{2}H3/^{2}H2$ ratios were compared with the $^{2}H5/^{2}H2$ ratios corrected for TA exchange.

Chapter 4: Recently, whole-body protein turnover kinetics have been shown to be altered in the insulin resistant state resulting in an increased availability of amino acids such as glutamine for hepatic gluconeogenesis and therefore an increased potential for excessive hepatic glucose production. A reduction in the anabolic action

of insulin is anticipated to result in elevated appearance of whole-body glutamine from proteolysis compared to its metabolic synthesis from the Krebs cycle.

The contribution of proteolytic and metabolic sources to hepatic glutamine was determined in healthy subjects. They were studied after ingestion of $^{2}H_2O$ following an overnight fast and hepatic glutamine was noninvasively sampled as urinary phenylacetylglutamine (PAGN) using phenylbutyrate. The enrichment of this sampled glutamine from $^{2}H_2O$ provided a measure of metabolic and proteolytic contributions. These studies demonstrate that even for healthy insulin sensitive subjects, proteolysis accounts for a significant fraction of hepatic glutamine.

Finally, in the last Chapter, the main results obtained in this Thesis were summarized.

RESUMO

A diabetes *mellitus* caracteriza-se pela perda da regulação da homeostase da glicose devido a alterações na secreção de insulina (diabetes *mellitus* tipo 1 -T1DM) e/ou na sensibilidade à insulina (diabetes *mellitus* tipo 2-T2DM). O fígado desempenha um papel chave nesta regulação através de uma rede metabólica que converte a glicose e outros hidratos de carbono em glicogénio no estado pós-prandial enquanto durante o jejum assegura as necessidades fisiológicas de glicose. Sendo estes processos estritamente controlados pela insulina, a deficiência em insulina ou alterações na sua acção, resultam na perda da regulação do metabolismo hepático da glicose durante o ciclo diário de pós-prandial/jejum.

Nesta Tese, o metabolismo hepático da glicose foi caracterizado em indivíduos saudáveis ou pacientes com alterações da acção da insulina, por espectroscopia de Ressonância Magnética Nuclear (RMN) usando marcadores de isótopos estáveis e métodos não invasivos.

Capítulo 1: Uma introdução geral é apresentada neste Capítulo, focando a Diabetes *mellitus*. O metabolismo hepático da glicose e uma visão geral da sua regulação são apresentados. Alterações dos fluxos hepáticos da glicose em T1DM, T2DM e na insulino-resistência são descritos. Os mecanismos da sinalização da insulina e da terapia em T2DM são brevemente abordados. O uso de isótopos no estudo do metabolismo hepático foi sublinhado neste Capítulo assim como a importância do uso de xenobióticos para estudar de um modo não invasivo o metabolismo da glicose e proteico.

Capítulo 2: A síntese hepática de glicogénio após ingestão de um pequeno almoço que inclui leite, foi avaliada em indivíduos saudáveis usando o método da

água deuterada (^2H_2O) e o método da [1-^{13}C]glicose, para determinar a contribuição da galactose, via directa e indirecta para o fluxo a nível da enzima glicogénio sintetase.

A completa extensão da inter-conversão entre a glicose-6-fosfato e a frutose-6-fosfato (G6P-F6P) hepáticas foi confirmada usando [U-$^2H_7$]glicose e assim a diluição da marcação em deutério na posição 2 pode ser completamente atribuída ao metabolismo da galactose. A actividade da transaldolase (TA) foi também determinada. A sua influência na contribuição das vias directa e indirecta para a síntese de glicogénio foi avaliada através do método da ^2H_2O e os resultados foram comparados com os valores obtidos com o método da [1-^{13}C]glicose, que é insensível à acção da TA. A análise de carbono-13 (^{13}C) e deutério (^{2}H) foi feita por espectroscopia de RMN.

Capítulo 3: A presença da actividade da TA hepática foi determinada num grupo de indivíduos com valores normais de glicose em jejum/tolerância normal à glicose (NFG/NGT), num grupo com valores alterados da glicose em jejum/alteração da tolerância à glicose (IFG/IGT) e num grupo com valores alterados da glicose em jejum/tolerância normal à glicose (IFG/NGT). As medições da actividade da TA foram determinadas por infusão de [1-^{13}C]acetato. Os enriquecimentos em ^{13}C e em ^{2}H da glicose e do glucuronato foram analisados por espectroscopia de RMN. A actividade da TA aumenta a marcação da posição 5 da glicose independentemente da actividade gliconeogénica resultando numa sobrestimava da contribuição da fracção gliconeogénica na produção de glicose. A contribuição da gliconeogénese e da glicogenólise para a produção endógena de glicose foi determinada após um jejum nocturno nos três grupos de indivíduos pelo método da ^2H_2O. Os valores obtidos foram corrigidos tendo em conta o efeito da actividade da TA resultando numa redução significativa da fracção gluconeogénica num aumento significativo da contribuição da glicogenólise. Também as razões

$^{2}H3/^{2}H2$ foram comparadas com as razões $^{2}H5/^{2}H2$ previamente corrigidas para a actividade da TA.

Capítulo 4: Recentemente verificou-se que a cinética de turnover proteico global está alterada em situações de insulino-resistência. Esta alteração resulta num aumento da disponibilidade de aminoácidos, tais como a glutamina, para a gliconeogénese hepática e num potencial aumento da produção hepática de glicose. Provavelmente, o aumento do aparecimento de glutamina dever-se-á principalmente a uma elevada proteólise relativo à sua síntese metabólica derivada do ciclo de Krebs. As contribuições de fontes proteolíticas e metabólicas para a glutamina hepática foram determinadas de uma forma não-invasiva em indivíduos saudáveis utilizando água deuterada e fenilbutirato. Após um jejum nocturno, a glutamina hepática foi obtida a partir de fenilacetilglutamina urinária e o enriquecimento proveniente da $^{2}H_{2}O$ quantificado por espectroscopia de RMN. Estes estudos demonstraram que mesmo em indivíduos saudáveis e sensíveis à insulina, a proteólise contribui com uma fracção significativa para a glutamina hepática.

Finalmente, no último Capítulo, os principais resultados obtidos nesta Tese foram resumidos.

Chapter 1

General Introduction

1.1 General Introduction 5

1.1.1 Diabetes *mellitus* 5

1.2 Hepatic glucose metabolism 9

1.3 Hepatic metabolic fluxes and T1DM 13

1.3.1 Hepatic metabolic flux defects in the fasting state 13

1.3.2 Hepatic metabolic flux defects in the fed state 14

1.3.3 Effect of treatments: intensive insulin therapy 14

1.4 Hepatic metabolic fluxes and T2DM 16

1.4.1 Hepatic insulin resistance 16

1.4.2 Hepatic metabolic flux defects in the fasting state 18

1.4.3 Hepatic metabolic flux defects in fed state: 19

1.4.4 Effect of treatments on hepatic insulin resistance: drug therapy 19

1.5 The use of tracers in the study of hepatic intermediary metabolism 22

1.5.1 Short- and long-lived radioactive tracers of hepatic metabolism 23

1.5.2 Analysis of stable isotope tracer enrichment 24

1.5.3 Analysis and quantification of Carbon-13 and Deuterium enrichments by NMR 26

1.6 The use of xenobiotics to assess enrichment of hepatic metabolites from stable isotope tracers 29

1.7 Nonsteady- and steady-state metabolic flux measurements 31

1.8 Tracing hepatic glucose metabolism with stable isotopes in fasting and fed states 33

1.8.1 Fasting state 33

1.8.2 Fed state 36

1.9 Confounding factors of the deuterated water measurements of gluconeogenesis and glycogen synthesis: 38

1.9.1 Transaldolase exchange activity 38

1.9.2 Glycogen cycling 39

1.9.3 Galactose metabolism 40

1.10 References 41

1.1 General Introduction

1.1.1 Diabetes *mellitus*

Incidence and epidemiology: diabetes *mellitus* is one of the most common chronic diseases in nearly all the countries and it is in a continuous increasing incidence. According to the World Health Organization (WHO) the worldwide total number of people with diabetes was 171 million in 2000 and estimated to rise to 366 million in 2030 (Setacci *et al.* 2009) increasing from 2.8% in 2000 to 4.4% in 2030 (Wild *et al.* 2004).

A first study in estimating the global mortality attributable to diabetes was estimated to 2.9 million deaths, equivalent to 5.2% of all world deaths in 2000. Thus diabetes becomes the fifth globally leading cause of death (Roglic *et al.* 2005). A recent study referred that deaths attributable to diabetes worldwide was estimated in 3.96 million in the age group 20-79 years old, which is 6.8% of global (all ages) cause of mortality in 2010 (Roglic *et al.* 2010). The multiple complications and mortality accounts for at least 10% of the total health care budgets in many countries (Roglic *et al.* 2005).

Diabetes *mellitus* is considered as a group of metabolic diseases characterized by hyperglycemia resulting from deficiencies in insulin secretion, insulin action or both. The chronic hyperglycemia is associated with a long term damage, dysfunction and failure of various organs and tissues particularly the eyes, kidneys, nerves, heart, and blood vessels.

The pathogenic processes involved in the development of the disease divide diabetes in two main categories: type 1 diabetes *mellitus* (T1DM) caused by autoimmune destruction of the β-cells of the pancreas with a consequent absolute insulin secretion deficiency and type 2 diabetes *mellitus* (T2DM), caused by metabolic abnormalities resulting in a combination of resistance to insulin action and inadequate compensatory insulin secretory response.

Table 1.1: Etiologic classification of diabetes *mellitus* (American Diabetes Association 2011) (Genuth *et al.* 2003; Inzucchi *et al.* 2010).

I.	**Type 1 diabetes *mellitus* (T1DM)**
	(β-cell destruction, usually leading to absolute insulin deficiency)
A.	Immune mediated
B.	Idiopathic
II.	**Type 2 diabetes *mellitus* (T2DM)**
	(May range from predominantly insulin resistance with relative insulin deficiency to a predominantly secretory defect with insulin resistance)
III.	**Other specific types**
A.	Genetic defects of β-cell function
B.	Genetic defects in insulin action
C.	Diseases of the endocrine pancreas
D.	Endocrinopathies
E.	Drug-or chemical-induced
F.	Infections
G.	Uncommon forms of immune-mediated diabetes
H.	Other genetic syndromes sometimes associated with diabetes
IV.	**Gestational diabetes *mellitus* (GDM)**

T2DM is the most prevalent form of diabetes, accounting for 90-95% of people with diabetes while T1DM immune-mediated diabetes accounts only for 5-10% (Inzucchi *et al.* 2010).

T2DM results from the interaction between a genetic predisposition and behavioural risk factors. While the genetic basis for of T2DM has not be identified, there is an evidence that risk factors, characteristic of the modern society, as obesity, sedentary life-style and the consumption of high-caloric diets, are important determinants of the disease. Most of the patients are obese and even those who are

not considered obese by the body mass index (BMI) criteria may have altered body fat distribution such as increased visceral or abdominal fat that may predispose them to T2DM.

Clinical characteristics: many T2DM subjects remain undiagnosed. Blood glucose levels can rise without significant symptoms. In several situations, when diabetes is diagnosed, patients already have developed complications such retinopathy, a consequence of the damage on small blood vessels (microvascular disease). The main risk in undiagnosed T2DM is the increased risk of cardiovascular disease, mainly ischemic heart disease due to damage in the arteries (macrovascular disease). Early diagnosis of diabetes allows early interventions, such as an adequate diet and exercise and if necessary, drugs to reduce the cholesterol and glucose levels, reducing the risk of heart disease and hyperglycemia. Microvascular disease such as retinopathy is specific to diabetes, while macrovascular disease is not. However, T2DM patients are at an increased risk in developing macrovascular disease. The increased risk in developing retinopathy begins even before the plasma glucose levels reach diabetic levels.

More recently, people who have impaired glycemic control but are not clinically diagnosed with T2DM can be classified according to Table 1.2 on the basis of fasting plasma glucose levels and/or 2-hours glucose levels after an oral glucose tolerance test (OGTT), (Gavin *et al.* 1997; Genuth *et al.* 2003; American Diabetes Association 2011).

Impaired fasting glucose (IFG) and impaired glucose tolerance (IGT) subjects are related to an increased risk to develop T2DM, especially those who are obese. Obesity is associated with an increased risk of mortality, particularly form cardiovascular disease. Hypertension, diabetes and dyslipidemia are all factors individually associated with the increased risk for mortality from cardiovascular disease. Low levels of high-density lipoprotein cholesterol (HDL), high triglyceride levels and fasting glucose levels are risks associated (Nguyen *et al.* 2008). The risk of

heart disease is slightly increased in IFG but about 60% in IGT subjects (Waugh *et al.* 2007). The early diagnosis in crucial not just for T2DM detection but also for this intermediate group, particularly for IGT subjects. Heart disease is the most life-threatening consequence of diabetes increasing cardiovascular morbidity and mortality and accounts for up to 65% of deaths (Ferdinand 2006). Lifestyle interventions can reduce the progression from IGT to T2DM, and glycemic control improves postprandial plasma glucose levels.

T2DM is characterized by insulin resistance in major insulin-sensitive organs/tissues such as skeletal muscle, liver and adipocytes, and a failure of pancreatic β-cells to compensate the increased demands for insulin secretion due to insulin resistance. Populations based studies revealed a prevalence of peripheral arterial disease in diabetic populations to be about 30% (Setacci *et al.* 2009). The increasing worldwide diabetes prevalence will result in an increasing proportion of deaths from cardiovascular disease and an increased prevalence in other complications related to diabetes.

Table 1.2: Categories of fasting plasma glucose (FPG) concentrations and 2-h after an OGTT (American Diabetes Association 2011).

Fasting plasma glucose
normal fasting glucose (NFG): FPG < 100 mg/dl (5.6 mmol/l)
impaired fasting glucose (IFG): FPG 100-125 mg/dl (5.6-6.9 mmol/l)
provisional diagnosis of diabetes: FPG ≥ 126 mg/dl (7.0 mmol/l)
Plasma glucose 2-h after an OGTT
normal glucose tolerance (NGT): 2-h post load glucose <140 mg/dl (7.8 mmol/l)
impaired glucose tolerance (IGT): 2-h post load glucose 140–199 mg/dl (7.8–11.1mmol/l)
provisional diagnosis of diabetes: 2-h post load glucose ≥200 mg/dl (11.1 mmol/l)

1.2 Hepatic glucose metabolism

Since this Thesis is primarily focused on the study of hepatic glucose and glycogen metabolism in T1DM and T2DM, hepatic glucose metabolism and its regulation by insulin will be described in more depth.

The liver is a key organ in regulating glucose metabolism, maintaining the systemic glucose concentration within physiological ranges by producing or storing glucose depending on the nutritional state. Insulin and glucagon reciprocally regulate hepatic glucose storage and glucose production.

The liver is the predominant site of glucose production (GP) in both the postabsorptive and prolonged fasted state. The kidney is the other principal source of GP and it contributes ~5% of endogenous glucose production (EGP) in the overnight-fasted state rising to 20-25% after 60 hours of fasting (Ekberg *et al.* 1999). For the studies and conditions discussed in this Thesis, hepatic and endogenous glucose production are considered to be equivalent hence EGP will be defined as both hepatic and endogenous glucose production.

In the fasting state, blood glucose levels decrease and insulin secretion is reduced. Glucagon is released from pancreatic α-cells increasing the levels relative to those of insulin, glycogen phosphorylase is activated and glycogen is hydrolysed to glucose which is then released in the circulation. Glycogen phosphorylase breaks down glycogen to form glucose-1-phosphate (G1P) which is then converted to glucose-6-phosphate (G6P) by phosphoglucomutase. Glucose is then formed from G6P by glucose-6-phophatase and released into circulating blood. This pathway of glucose production is supplemented by gluconeogenesis, where glucose is synthesized *de novo* from non-carbohydrate precursors.

For overnight-fasted healthy adults, the contribution of gluconeogenesis and glycogenolysis to EGP are approximately equal (Jones *et al.* 2006b). After a prolonged fast, the hepatic stores of glycogen are diminished and the contribution of

gluconeogenesis to hepatic glucose production increases relative to glycogenolysis (Rothman *et al.* 1991; Landau *et al.* 1996; Ekberg *et al.* 1999).

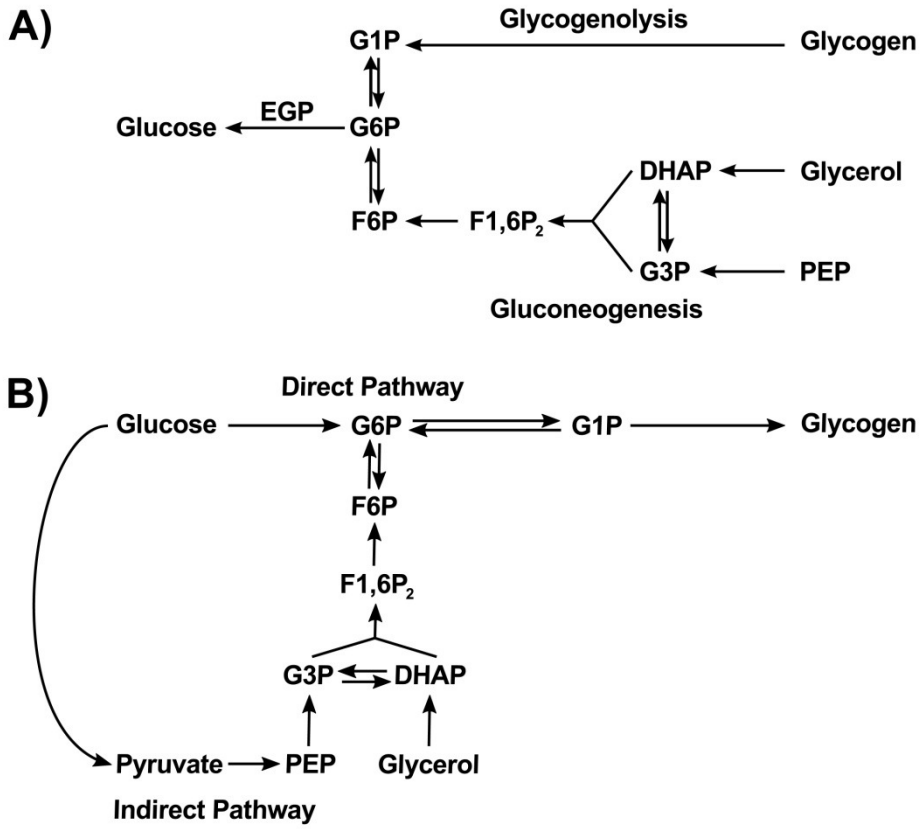

Figure 1.1: Hepatic metabolic model of carbohydrate fluxes during: **A)** fasting and **B)** feeding. PEP (phosphoenolpyruvate), G3P (glyceraldehyde-3-phosphate), DHAP (dihydroxyacetone phosphate), $F1,6P_2$ (fructose-1,6,-bisphosphate), F6P (fructose-6-phosphate), G6P (glucose-6-phosphate), G1P (glucose-1-phosphate), EGP (endogenous glucose production).

In the fed state, glucose is absorbed from the intestine resulting in elevated hepatic portal vein glucose levels. This results in stimulation of insulin secretion and repression of glucagon production by the pancreas. The liver, being immediately downstream of the pancreatic duct, therefore sees a combination of high glucose and high insulin levels and a reduction in glucagon concentrations.

Glucose is taken up from the portal vein circulation by the liver through the hepatic non-insulin sensitive glucose transporters (GLUT2). The increased glucose concentration and insulin levels induce the phosphorylation of the hepatic glucose to G6P by glucokinase (GK). Insulin rapidly promotes GK activation *via* the glucokinase regulatory protein hence providing a fast response to increased portal vein glucose levels. Unlike hexokinase, the other constitutive glucose phosphorylating enzyme, GK is not inhibited by its G6P product hence it is able to continually convert glucose into G6P in the face of rising G6P levels. Elevated levels of G6P in turn inactivate glycogen phosphorylase, preventing glycogen hydrolysis to glucose, and along with insulin, activate glycogen synthase. As a consequence, the liver switches from the net production of glucose (that occurs in the fast state) to net glucose uptake and hepatic glycogen stores are repleted. After a meal, one fifth of the glucose absorbed into the liver is stored as glycogen (Petersen *et al.* 2001; Jones *et al.* 2006b). The liver capacity to store glycogen is 5-6% of its wet weight corresponding to approximately 100 grams.

Hepatic glycogen can be synthesized by a direct pathway from intact glucose units and by an indirect pathway were glucose is first metabolized *via* glycolysis to 3-carbon intermediates and metabolized to G6P *via* the gluconeogenic pathway. In its original definition, the indirect pathway refers to hepatic glucose metabolism but in the whole organism, glucose that is metabolized *via* the Cori cycle is also effectively a component of the indirect pathway, with the glycolytic phase taking place in peripheral tissues followed by export of the glycolytic products to the liver for G6P synthesis. The indirect pathway also allows glycogen to be synthesized *de novo* from gluconeogenic precursors such as glycerol. The contributions of the direct and indirect pathways have been measured under different routes of tracer administration including oral glucose load ingestion, together with a mixed meal and under hyperinsulinemic glucose clamps. In healthy subjects presented with oral or intravenous glucose loads, the direct pathway contributes to 50-75% to hepatic glycogen synthesis. For an oral glucose load ingested after an overnight fast, the direct

contribution increases with the amount of the load. For a glucose load of 75 grams, used in standard OGTT, the direct pathway contribution was ~50% (Napoli *et al.* 1992; Delgado *et al.* 2009) and with a larger load of 98 grams its contribution was ~64% (Petersen *et al.* 2001). When glucose is ingested as part of a mixed meal, the direct pathway contribution increases over time: at 2-4 hours after the meal its contribution was 46 ± 5% increasing to 68 ± 8% at 4-6 hours (Taylor *et al.* 1996).

After an overnight fasting and during a hyperglycemic clamp a direct pathway contribution measured after 2-4 hours was 54 ± 6% increasing to 59 ± 5% at 4-6 hours and reached 63 ± 4% at 6-8 hours (Stingl *et al.* 2006). When glucose was administered by intravenous infusion after overnight fasting, the direct pathway contributed 50% at the start of the infusion increasing to approximately 70% when measured 4 hours after a ingestion of a breakfast meal (Shulman *et al.* 1990). Presumably, the shift towards higher direct pathway contributions reflects the increase in portal vein glucose levels as the meal carbohydrate is absorbed or as the hyperglycemia is established in the clamp procedure. The initially high indirect pathway contributions may be a reflection of the preceding gluconeogenic activity that was sustaining EGP immediately before the meal (Landau *et al.* 1996; Chandramouli *et al.* 1997; Perdigoto *et al.* 2003a) and illustrates the persistence of gluconeogenic G6P production even in fed insulin-sensitive subjects.

In summary, the fasting state is characterized by net glucose production from both glycogenolysis and gluconeogenesis. Flux through these pathways are promoted through increased transcription of key gluconeogenic enzymes such as glucose-6-phosphatase (G6Pase), fructose-1,6,-bisphosphatase ($F1,6P_2ase$) and phosphoenol-pyruvate carboxykinase (PEPCK) and increased availability of free fatty acids (FFA) for synthesis of adenosine triphosphate (ATP) and reducing equivalents to drive the anaplerotic conversion of pyruvate and other anaplerotic substrates to phosphoenolpyruvate (PEP). In addition, the opposing glycolytic and glycogen synthesis pathway enzyme activities are transcriptionally and allosterically repressed.

The transition of fasting to feeding involves the reversal of glucose fluxes so that the liver becomes a net glucose consumer with glycogen synthesis and glycolysis fluxes becoming dominant. The signaling actions of insulin play a central role in this transition. In the liver, insulin signaling is initiated by the activation of the insulin receptor tyrosine kinase, leading to the phosphorylation of intracellular receptor substrates, including insulin receptor substrates-1 and -2 (IRS-1 and IRS-2). Following phosphorylation, IRS-1 and IRS-2 can associate with proteins containing Src homology 2 (SH2) domains through specific tyrosyl phosphorylation sites. This association leads to activation of the enzyme phosphatidylinositol 3-kinase (PI3-kinase) (Saad *et al.* 1995) Activation of PI3-kinase and further downstream signaling pathway has been reported to play an important role in insulin-induced glycogen synthesis and suppression of PEPCK expression in hepatocytes (Gabbay *et al.* 1996). Activated PI3-kinase phosphorylates Akt which then shuts down the transcription factors for gluconeogenic and β-oxidation enzymes.

1.3 Hepatic metabolic fluxes and T1DM

1.3.1 Hepatic metabolic flux defects in the fasting state

Hepatic glycogen is an important short-term reserve of glucose that can be rapidly mobilized to maintain fasting blood glucose levels within the physiological range. T1DM with poor control of blood glucose levels have low postprandial hepatic glycogen stores and are therefore over-reliant on gluconeogenesis for sustaining EGP and glucose homeostasis. The reduced availability of hepatic glycogen may impair the rapid response of glucose production to hypoglycaemic episodes during fasting (Bischof *et al.* 2002). As a result of low glycogen stores and glycogenolytic fluxes, the gluconeogenic contribution to EGP after an overnight fasting is higher for T1DM than for healthy control subjects (Jones *et al.* 2006b).

1.3.2 Hepatic metabolic flux defects in the fed state

Net hepatic glycogen synthesis is the result of simultaneous fluxes of glycogen synthase and phosphorylase which are regulated by glucose, insulin and glucagon. Chronic alterations in regulatory enzymes such glucokinase may contribute to reduced glycogen synthesis. When T1DM patients with poor glycemic control were compared with healthy controls during normal-life day both groups presented similar fasting hepatic glycogen stores but at the end of the day, T1DM had synthesized only ~30% of glycogen compared with the control subjects. Also the contribution of the indirect pathway relative to that of the direct pathway was higher when measured over the 5 hours after the breakfast relative to controls, although in both groups the direct pathway contribution increased with time (Hwang *et al.* 1995). The indirect pathway plays a more important role for hepatic glycogen synthesis in T1DM which is shown by the ~60% contribution measured at the end of the breakfast compared with ~35% for control subjects. In another study, after an overnight fast following a breakfast meal the indirect contribution was ~64% while for matched controls it was ~53% (Jones *et al.* 2006b). The low insulin to glucagon ratio in T1DM relative to normal subjects may have an important role in the prevalence of the indirect over direct pathway contribution.

1.3.3 Effect of treatments: intensive insulin therapy

The pancreatic β-cells produce very little or no insulin at all in subjects with T1DM. Insulin administration replaces or supplements the lack of own body insulin secretion, restoring normal or near-normal blood glucose levels.

Intravenous insulin infusion administration is not a routine or suitable procedure for day-to-day self-administration. Instead, glycemic control is optimized by frequent subcutaneous insulin injections or by continuous subcutaneous insulin

infusion pumps (CSII). However, in clinic research studies, intravenous infusions are applied for to achieve blood glucose control.

Long-term and short-term intravenous insulin therapies result in a near normoglycemia in poorly controlled T1DM and in a decreased fasting EGP.

After a long-term (~1 year) near normoglycemia T1DM patients were administered a variable intravenous insulin infusion to maintain plasma glucose levels within a normal range (Bischof *et al.* 2002). An overnight intravenous insulin infusion resulted in normalization in fasting plasma glucose concentrations while a further intravenous infusion along with mixed meals ingestion resulted in slightly increased plasma glucose levels during meal ingestion relative to non-diabetic subjects. These interventions restored net hepatic glycogen synthesis and breakdown rates to those of non-diabetic controls. However, the direct and indirect pathway contributions to glycogen synthesis were not restored to normal, hence the indirect pathway remained the dominant source of glycogen synthesis in these patients (Bischof *et al.* 2002). The effect of short-term intensive insulin therapy by variable intravenous insulin infusion in moderately controlled T1DM established near-normoglycemia for 24 hours. However rates of overnight hepatic glycogen synthesis, while significantly improved, remained well below those of non-diabetic controls. In the overnight fasting phase, net glycogenolysis were also increased but did not attain those of controls (Bischof *et al.* 2001).

CSII technology is rapidly improving and in principle allows a more precise tailoring of insulin delivery to glycemic states while eliminating much of the discomfort of insulin injections. Poorly controlled T1DM patients placed on CSII pump therapy presented improvements in plasma glucose concentration and in HbA1c (Kacerovsky *et al. in press*). The method improved fasting hepatic glucose metabolism by more effective suppression of EGP, principally by a marked reduction in gluconeogenesis such that the fractional contributions of gluconeogenesis and glycogenolysis to EGP approached those of healthy controls (Kacerovsky *et al. in press*). In the postprandial state, CSII improved net rates of hepatic glycogen synthesis

but it was not determined if direct and indirect pathway contributions were also normalized (Kacerovsky *et al. in press*).

1.4 Hepatic metabolic fluxes and T2DM

T2DM is characterized by the initial development of an insulin resistant state where insulin-mediated control of glucose metabolism is less effective but nevertheless may be compensated by increased insulin secretion by the pancreatic β-cells. At later stages, β-cell function becomes impaired, resulting in insufficient insulin secretion for maintaining glucose homeostasis in these circumstances. Insulin resistance is defined as failure of insulin-sensitive tissues to respond to normal levels of insulin and ultimately resulting in loss of control of glucose homeostasis.

Insulin-stimulated glucose uptake is markedly reduced in skeletal muscle and other insulin-sensitive peripheral tissues contributing to a decrease in peripheral glucose disposal and elevated plasma glucose levels. Insulin-mediated disposal of triglycerides into adipocytes is also compromised resulting in chronically high levels of plasma FFA (Petersen *et al.* 2002; Krssak *et al.* 2004b; Roden 2006). Recent studies have also shown that insulin-stimulated amino-acid uptake into protein synthesis is also impaired in the insulin resistant state (Chevalier *et al.* 2006). Among other things, this may increase the availability of gluconeogenic amino acids such as glutamine and alanine for gluconeogenesis (Chevalier *et al.* 2006). These peripheral defects may contribute to both defective hepatic insulin actions and alterations in hepatic metabolic fluxes.

1.4.1 Hepatic insulin resistance

Hepatic insulin resistance in humans is characterized by inappropriately high rates of EGP during both fasting and postprandial states (Boden 2002) and a reduced capacity

for net hepatic glycogen synthesis during feeding. On a molecular level, hepatic insulin resistance is characterized by an impaired insulin-stimulated phosphorylation of IRS-1 and IRS-2 (serine is phosphorylated instead of tyrosine) which compromises the ability of insulin to activate glycogen synthase therefore diminishing the capacity to synthesize glycogen. Transcription of key gluconeogenic enzymes (PEPCK, pyruvate carboxylase, F1,6P_2ase and G6Pase) remain active, resulting in inappropriately high rates of gluconeogenesis and EGP (Samuel *et al.* 2004).

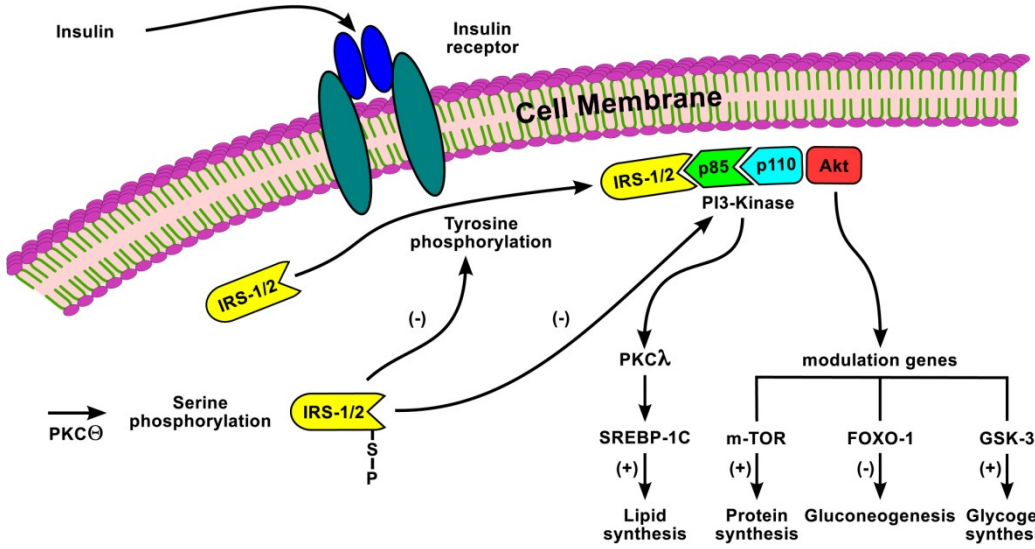

Figure 1.2: Insulin signaling involving tyrosine phosphorylation of IRS-1/2 influences metabolism of glucose, protein and lipids *via* transcription factor such as GSK-3, FOXO-1, m-TOR and SREBP-1C. In the insulin resistant state this is disrupted by serine phosphorylation of IRS-1/2 mediated by PKCΘ.

Elevated plasma FFA levels leads to intrahepatic accumulation of triglycerides, fatty acyl-CoA and diacylglycerol and ceramides (Gastaldelli *et al.* 2007). These latter triad of metabolites are associated with the activation of a serine kinase (protein kinase theta –PKCθ) which in turn phosphorylates the serine sites of IRS-1/IRS-2. This process disrupts the normal signaling sequence, which depends on the

tyrosine phosphorylation of IRS-1/IRS-2. Blockage of IRS-1/IRS-2 tyrosine phosphorylation in turn results in Akt not being phosphorylated and not silencing the transcription factors for gluconeogenic and β-oxidation enzymes (Dresner *et al.* 1999; Griffin *et al.* 1999; Roden 2006). As a result, gluconeogenic flux is unchecked. These same insulin signaling defects result in a failure of glycogen synthase activation and reduced rates of hepatic glycogen synthesis. The insulin resistant state is also associated with chronic low-grade inflammation. This is attributed to the release of pro-inflammatory cytokines such as tumor necrosis factor-alpha (TNF-α) from the adipose tissue and hepatic Kupffer cells. TNF-α desensitizes insulin signaling by activating the serine phosphorylation of IRS-1/IRS-2 (Yu *et al.* 2002).

1.4.2 Hepatic metabolic flux defects in the fasting state

T2DM is characterized by an increased rate of fasting EGP and this is largely accounted for an increased gluconeogenesis (Consoli *et al.* 1989). Decreased insulin sensitivity, increased lipolysis resulting in an increased availability of glycerol, a gluconeogenic precursor, and increased availability of gluconeogenic amino acids (Chevalier *et al.* 2006) all contribute to elevated gluconeogenesis. In the fasting state, both glycogenolysis and gluconeogenesis are active and are required to maintain normal rates of EGP. In T2DM patients, fasting hyperglycemia is strongly related to increased rates of EGP (Magnusson *et al.* 1992; Krssak *et al.* 2004a).

In the presence of hyperglycemia and defective insulin actions, hepatic autoregulation contributes to the regulation of EGP in mild and moderate T2DM. This process primarily acts on glycogen metabolism (Gastaldelli *et al.* 2001). Elevated hepatic G6P levels resulting from high levels of plasma glucose activate GS independently of insulin. This results in a decreased net glycogenolysis and an overall reduction in EGP. By stimulating glycogen synthesis in the face of glycogenolytic fluxes, hepatic autoregulation also promotes cycling between G6P and glycogen – a process referred to as "glycogen

cycling" (see Section 1.8.2 for further details). Among other things, this process can dilute the enrichment of G6P from gluconeogenic tracers such as ^2H_2O independently of net glycogenolytic flux resulting in overestimation of glycogenolysis and underestimation of gluconeogenesis (Hundal *et al.* 2000).

1.4.3 Hepatic metabolic flux defects in fed state:

After meal ingestion, hepatic glucose storage into glycogen is decreased in T2DM relative to healthy subjects (Magnusson *et al.* 1992; Woerle *et al.* 2006). Hepatic insulin resistance results in slower rates of glycogen synthesis and lower levels of postprandial glycogen through reduced plasma glucose uptake and glycogen synthase activities (Basu *et al.* 2000; Bischof *et al.* 2001).

After a meal T2DM have low plasma insulin but high glucagon and FFA concentrations which impair EGP suppression and the regulation of hepatic glucose metabolism. The insulin to glucagon (I/G) ratio at level of portal vein was ~50% lower after a meal in T2DM, along with a reduced hepatic insulin sensitivity, this lower I/G ratio may also contribute to the decrease of the net glycogen synthesis and EGP suppression. Both impaired net hepatic glycogen synthesis and deficient EGP suppression resulted in a decrease in hepatic glucose uptake and an increase of glucose released into the blood circulation (Krssak *et al.* 2004a). Postprandial EGP is defectively suppressed due to the reduced insulin action resulted from hepatic insulin resistance.

1.4.4 Effect of treatments on hepatic insulin resistance: drug therapy

Pharmacological interventions are designed to improve peripheral and hepatic actions of insulin. In advanced T2DM, where endogenous insulin secretion may be

compromised, insulin administration becomes an additional requirement for glycemic control.

Metformin (dimethylbiguanide) is an oral antidiabetic agent which decreases fasting plasma glucose concentrations by reducing EGP (Cusi *et al.* 1996; Inzucchi *et al.* 1998; Roden *et al.* 2001). It is believed to act by inhibiting hepatic gluconeogenesis, in part as a result of reduction in plasma FFA (Boden *et al.* 1998; Chen *et al.* 1999; Hundal *et al.* 2000; Roden 2006). Poor controlled T2DM patients treated for 3 months with metformin presented a 30% decrease in fasting plasma glucose concentration and in HbA1c. After treatment, glucose production in these patients was reduced by 25% without a significant increase in glucose clearance. Hepatic glycogen content and the rate of net hepatic glycogenolysis tended to increase. The rate of gluconeogenesis was 33% reduced. Also plasma FFA concentrations were decreased by 30% (Hundal *et al.* 2000).

Thiazolidinediones (TZDs) are currently one of the most commonly prescribed medications for T2DM and are effective in reducing both fasting HbA1c and hyperinsulinemia. TZDs are synthetic ligands that bind to the nuclear peroxisome proliferator-activated receptor-gamma (PPAR-γ) and exert their action by activating transcription of genes that, among others, regulate adipocyte differentiation and adipogenesis as well as glucose and lipid metabolism. There is also evidence TZDs improve pancreatic β-cell function (Gastaldelli *et al.* 2007). The molecular mechanism of TZDs involves the activation of PPAR-γ through the formation of a heterodimer with retinoid X receptor. This heterodimer binds to specific peroxisome proliferator response elements on a number of key target genes involved in the carbohydrate and lipid metabolism (Saltiel *et al.* 1996; Boden *et al.* 2006; Chiarelli *et al.* 2008). Although the primary insulin-sensitizing action is on peripheral tissues, TZDs also improve hepatic insulin sensitivity and inhibit hepatic gluconeogenesis (Gastaldelli *et al.* 2006). The insulin sensitizing effect of TZDs may, in part, be due to stimulation of

triglyceride synthesis in adipocytes. This results in the decrease of circulating FFA available for other tissues such as liver and muscle (Chiarelli *et al.* 2008).

PPAR-γ is also modestly expressed in pancreatic β-cells thus, hence the effects of TZDs may extend to these cells. In a T2DM animal model, TZD administration was shown to increase the insulin secretory capacity and preserve the integrity of β-cells (Shimabukuro *et al.* 1998; Finegood *et al.* 2001; Diani *et al.* 2004; Kawasaki *et al.* 2005; Gastaldelli *et al.* 2007). Several studies suggest that TZDs also exert beneficial effects on human β-cell function. TZDs slow the progression in humans with IGT to T2D by preventing the decline of β-cell function and improving insulin sensitivity. These effects were associated with lowered plasma FFA levels suggesting that β-cell function was preserved or improved by at least in part reducing its exposure to high circulating FFA levels (Gastaldelli *et al.* 2007). For a group of T2D patients, TZD treatment significantly decreased both fasting gluconeogenesis total flux and fractional contribution to EGP in values comparable to healthy control subjects. Also fasting plasma glucose concentration was decreased as result of a small decrease in EGP and of a 20% increase in fasting glucose clearance. Glycogenolysis was not affected by TZD treatment (Gastaldelli *et al.* 2006).

Sulfonylureas are a class of antidiabetic drugs that have long been used in T2DM treatment. They act by stimulating insulin secretion from the pancreatic β-cells in response to glucose levels. Sulfonylureas may induce hypoglycemia as a result of excesses in insulin production and release. After an initial improvement in blood glucose concentration control and a decrease in HbA1c sulfonylureas are associated with a progressive increase in HbA1c and progressive loss of β-cell function. The loss of plasma glucose concentration control with sulfonylureas occurs after the initial 18 months of therapy (DeFronzo 2009).

T2DM is a progressive disease characterized by insulin resistance and declining β-cell function, often leading to a requirement for insulin therapy to maintain good glycemic control and prevent diabetes-associated complications.

(Barnett 2007). In newly diagnosed T2DM subjects without acute or chronic complications, low-dose insulin therapy led to β-cell recovery (Bhattacharya *et al.* 2011). In more advanced T2DM, there is less capacity for pancreatic insulin secretion due to declining β-cell function often leading to a requirement for insulin therapy to improve glycemic control and retard diabetes-associated complications (Saisho *et al.* 2011).

1.5 The use of tracers in the study of hepatic intermediary metabolism

Hepatic metabolism is characterized by a dynamic extraction and secretion of metabolites from and to the circulation which is correlated with the synthesis and degradation of intrahepatic metabolites such as glycogen. Therefore, hepatic metabolism may be characterized by quantifying the changes in hepatic metabolite levels by needle biopsy and arterio-venous gradients of metabolites by catheter sampling of portal vein and hepatic vein blood. In practice, this approach is invasive and poses unacceptable risk-benefit ratios for diabetic subjects. While this approach has been successfully applied in medium to large animal models such as dogs and pigs (Chiasson *et al.* 1977; Adkins *et al.* 1984; Shiota *et al.* 1997; Lang *et al.* 1999) it is technically challenging for the more widely used rat and mouse models of diabetes. Tracers provide a mean of interrogating hepatic metabolic fluxes with less invasive methods. Importantly, they can be applied equally effectively to both mice and men allowing metabolic information from animal models and humans to be read in the same experimental format.

A tracer is a compound that is chemically identical to the naturally occurring compound of interest (tracee) but it is possible to detect and follow its metabolic fate in the body. In an isotopic tracer, one or more atoms in the molecule are substituted

for an atom of the same chemical element, but of a different isotope. Isotopes may be identified by radioactivity, or differences in mass and/or nuclear spin.

1.5.1 Short- and long-lived radioactive tracers of hepatic metabolism

Recently the short-lived positron emitting radioisotopes carbon-11 (^{11}C) and fluorine-18 (^{18}F) have also been applied in positron emission tomography (PET) studies of metabolism. The tracer is injected intravenously or inhaled as a gas and distributes throughout the body *via* blood circulation and enters into organs. An intravenous injection of less than one microgram is often sufficient for the performing of a PET study. Thus dose without any pharmacological effects can be used. The quantitation of glucose utilization, fatty acid uptake and oxidation are some possible use of PET. [^{18}F]FDG is a fluorine-18 labeled glucose analogue (fluorine-18-labeled 2-fluoro-2-deoxy-D-glucose) which is transported into the cell and phosphorylated (Sokoloff *et al.* 1977; Phelps *et al.* 1979; Halama *et al.* 1983). [^{18}F]FDG cannot enter glycolysis, thus initial steps in glucose uptake and metabolism can be traced with this radio-pharmaceutical. [^{18}F]FTHA (fluorine-18-labeled 6-thia-hepta-decanoic acid) is a long chain fatty acid analogue. After transport into mitochondria it undergoes the initial steps of β-oxidation (Degrado *et al.* 1991; Ebert *et al.* 1994). Both [^{18}F]FDG and [^{11}C]glucose has been applied to study myocardial glucose uptake in humans (Davila-Roman *et al.* 2002; Herrero *et al.* 2002). PET studies using [^{18}F]FDG uptake in liver have been performed to evaluate diffuse fatty acid infiltration of the liver (Abele *et al.* 2010), detection and staging of hepatocellular malignant tumours, and monitoring therapy response (He *et al.* 2008). In summary, PET has been well developed for measuring the dynamics of substrate uptake by tissues and organs but at present, it does not inform the subsequent metabolic fate of the substrate.

Carbon-14 and tritium (^{14}C and ^{3}H) are long-lived radioactive isotopes that were widely used in early metabolic studies of both animals and humans and their use

was fundamental in characterizing the main pathways of hepatic carbohydrate metabolism. The knowledge base that was derived with radioactive isotopes has been of great importance in informing later measurements with their stable isotope counterparts, carbon-13 and deuterium (^{13}C and ^{2}H). Radioactive tracers have been largely replaced by their stable isotope counterparts in human studies while they are remain in relatively widespread use for animal studies. One key advantage of radioactive tracers is that they are easily detected by scintillation counting and background radioactivity is very low in comparison to metabolite specific activity. For certain applications, such as simple isotope dilution measurements or substrate uptake studies, the study protocols are simple and straightforward. Moreover, ^{14}C and ^{3}H are relatively weak β-particle emitters hence the radiation can be contained and managed without specialized materials or facilities.

Translation of tracer studies from radioactive to stable isotope tracers presents two main challenges, firstly stable isotopes do not spontaneously emit radiation and their detection is dependent on more interactive and inherently less sensitive modes of spectroscopy and secondly, background levels of stable isotopes are much higher compared to their radioactive counterparts. The transition from radioactive to stable isotope tracers has been accelerated by simplifications and improvements in spectroscopic (Nuclear Magnetic Resonance-NMR and Mass Spectrometry-MS) methods of analysis.

1.5.2 Analysis of stable isotope tracer enrichment

Measurement of stable isotope tracer enrichment levels are typically performed by MS or NMR spectroscopy. MS is more established and widespread due to lower instrumentation costs and higher sensitivity relative to NMR, but it also has inherent limitations compared to NMR. Stable isotope tracers are heavier than their tracee counterparts and MS detects and quantifies their presence by resolving heavier labeled

molecules from lighter unlabeled ones. Both ^{2}H and ^{13}C increase the molecular mass by ~1 atomic unit and conventional bench-top MS instruments are unable to distinguish which isotope contributes to the mass increase. Also the position of the isotope in the molecule is not identified directly but can be inferred from fragmentation and analysis of the mass of the daughter fragments (MS-MS). Fragmentation can also help identify specific multiply-enriched molecules of a given isotope (isotopomers) (Katz *et al.* 1989; Katz *et al.* 1993). However, fragmentation is dependent on the molecule´s chemical structure and may or may not isolate the label of interest. It may also result in the removal or transfer of the label to a different position. When fragmentation is not informative, chemical degradations that were previously developed for analyzing radioactive tracers are used, for example the analysis of glucose ^{2}H-enrichment from $^{2}H_2O$ (Landau *et al.* 1995b; Landau *et al.* 1996).

With NMR, positional information for any given isotope is inherent in the chemical shift dispersion of signals from specific nuclei in the molecule. Moreover, since each isotope has a characteristic resonance frequency, its signals can be uniquely detected with no interference from any other isotope that may be present. With isotopes such as ^{13}C, ^{13}C-^{13}C spin-spin coupling interactions inform the presence of neighbouring ^{13}C nuclei and allow metabolite isotopomers (isotope isomers) to be characterized. Isotopomer analysis is particularly powerful in detecting the incorporation of uniformly-^{13}C-enriched, 2- and 3-carbon precursors into product metabolites, such as acetyl-CoA incorporation into Krebs cycle metabolites (Jones *et al.* 1993; Jones *et al.* 1997; Jones *et al.* 2001b) or triose incorporation into glucose (Jones *et al.* 1994; Jones *et al.* 2008). For some nuclei such as ^{2}H, the limited signal dispersion requires the molecule to be derivatized in order to provide a more heterogeneous chemical environment thereby promoting differences in chemical shifts between the constituent nuclei (Schleucher *et al.* 1998; Jones *et al.* 2000; Kunert *et al.* 2003). This is particularly applicable for carbohydrates, where many of the

hydrogen and ^{13}C-signals are crowded together. Derivatization can further simplify NMR carbohydrate spectra by converting anomeric mixtures into a single species.

Low sensitivity and therefore, low throughput, is the main disadvantage of NMR compared to MS. However, the development of high magnetic field spectrometers, improved radiofrequency electronics, and reduction of thermal noise by cryogenic cooling have all contributed to substantial improvements in sensitivity over the past decade. For this Thesis work, all ^{13}C and ^{2}H tracer enrichments and metabolite levels were quantified by NMR.

1.5.3 Analysis and quantification of Carbon-13 and Deuterium enrichments by NMR

1.5.3.1 Carbon-13

The most abundant carbon isotope, ^{12}C, has a spin quantum number (I) of zero, no nuclear magnetic moment and is therefore not detectable by NMR. The magnetically active carbon isotope, ^{13}C isotope, has a natural abundance of 1.11% and a spin quantum number of ½ (I= ½). A low gyromagnetic ratio (only ¼ of that of ^{1}H), means that the ^{13}C NMR experiment is less sensitive than ^{1}H. The sensitivity of ^{13}C relative to ^{1}H NMR at the same magnetic field strength with the same number of nuclei is 0.0159 (Egan *et al.* 1977). ^{13}C yields sharp signals due to long longitudinal relaxation times (T_1) and ^{13}C chemical shifts are dispersed over a range of 200 ppm allowing good separation of signals. The intensity of a ^{13}C signal is related to both the degree of ^{13}C-enrichment and the total amount of the metabolite present in the sample. Hence, the degree of enrichment is quantitatively expressed as fractional enrichment ($^{13}C/^{13}C+^{12}C$), i.e. the ratio of the ^{13}C in a molecule to the total amount of carbon in that molecule. To the extent that ^{13}C NMR distinguishes between different

carbons within a molecule, fractional enrichments can be measured for these individual positions. In most human studies, these measurements require correction for the 1.11% background natural abundance ^{13}C since levels of excess ^{13}C-enrichments are typically comparable to the background level. ^{1}H-Decoupling eliminates all signal-splitting caused by ^{13}C-^{1}H couplings, and in addition, magnetization of the protons is transferred to the ^{13}C which they are attached. This results in an increased intensity of the ^{13}C NMR signal of that carbon due to Nuclear Overhauser Effect (NOE). Since NOE´s vary for each ^{13}C signal, it is not possible to estimate ^{13}C-enrichments directly from a signal acquired under these conditions. NOE can be avoided by performing ^{1}H decoupling during the acquisition only. Under these conditions, and allowing for full relaxation between pulses, ^{13}C signals that are directly proportional to the ^{13}C-enrichment level can be acquired.

In a molecule, a carbon can be either a ^{12}C or a ^{13}C hence for a molecule with n carbons, a maximum of 2^n different isotopomers can occur. During metabolism, pathway specific carbon rearrangements occur and, upon labeling with ^{13}C, a specific range of isotopomers is produced. Isotopomers that are generated from specific ^{13}C-enriched precursor can be precisely related to the alterations in metabolite carbon skeletons that define the formation of a product metabolite. This can apply even in cases where at least some of the intermediate metabolite carbons are considered to be "randomized", as for example in the Krebs cycle. Homonuclear ^{13}C-^{13}C coupling patterns allow metabolic isotopomers to be identified and quantified.

Both ^{13}C-enrichment (Basu *et al.*2010; Soares *et al.* 2010), (Barosa *et al. unpublished data*) and ^{13}C-isotopomers (Carvalho *et al.* 1998; Carvalho *et al.* 2001) are observable by ^{1}H-detection due to heteronuclear ^{1}H-^{13}C scalar coupling. Because of the higher gyromagnetic ratio of ^{1}H *versus* ^{13}C, the theoretical sensitivity of indirect ^{13}C detection is ~32 times that of direct ^{13}C detection. Experimentally, this is rarely achieved due to the multiplicity of the ^{1}H signal from ^{1}H-^{1}H coupling and signal losses through relaxation and imperfect selection of ^{13}C-^{1}H coherences by heteronuclear pulse sequences. However,

indirect detection does allow ^{13}C and ^{12}C levels to be directly compared since ^{1}H signals directly bonded to ^{13}C are fully resolved from those of ^{12}C due to the ^{1}H-^{13}C scalar coupling (Kunnecke 1999; Graaf *et al.* 2000; Jones *et al.* 2006a).

1.5.3.2 Deuterium

^{2}H has a spin quantum number of 1, and therefore a magnetic quadrupolar moment with characteristically shorter relaxation times and broader signals compared to its ^{1}H counterpart. The gyromagnetic ratio of ^{2}H is ~15% that of ^{1}H resulting in a correspondingly lower ^{2}H signal dispersion (Jones *et al.* 2006a). The inherent sensitivity of ^{2}H (at constant field and with an equivalent number of nuclei) is about 0.9% that of ^{1}H. ^{2}H NMR nuclei that are incorporated into metabolites have almost identical chemical shift values as their ^{1}H counterparts due to the same chemical environment. This property is highly useful for confirming the position of the ^{2}H resonance in a molecule by overlaying the ^{2}H and ^{1}H NMR spectra. ^{2}H-^{1}H couplings are 6.5 times smaller than ^{1}H-^{1}H couplings and are rarely observed directly in ^{2}H NMR spectra, but contribute to signal broadening hence ^{2}H spectra are routinely proton-decoupled. Unlike ^{13}C, there is no significant NOE effect from ^{1}H-decoupling, hence the ^{1}H-decoupled ^{2}H NMR signals are directly proportional to the number of ^{2}H nuclei. Replacement of ^{1}H by ^{2}H induces significant isotope shifts and spin-spin coupling with directly bound ^{13}C nuclei while neighboring ^{13}C nuclei also experience smaller, but measurable isotope shifts. These properties allow indirect detection of ^{2}H enrichment by ^{13}C NMR observation and have been applied in metabolic studies of animals, perfused organs and cells (Moldes *et al.* 1994; Rodrigues *et al.* 2005). Since this method relies on establishing relatively high enrichments of both ^{13}C-reporter and ^{2}H observed nuclei in metabolic intermediates, it has not been applied to human studies where ^{13}C and ^{2}H isotope enrichments are limited by both cost and safety factors.

1.5.3.3 Hydrogen

^{1}H has a spin of ½ and is the most sensitive nucleus for NMR due to its high gyromagnetic ratio and the high natural abundance (>99.9%). The chemical shifts range is more narrow (12 to -1 ppm) than that for ^{13}C. Due to its high natural abundance and the fact that almost all biological metabolites contain ^{1}H, ^{1}H NMR analysis provides a rich source of information on the identification and quantification of a wide range of metabolites.

1.6 The use of xenobiotics to assess enrichment of hepatic metabolites from stable isotope tracers

Xenobiotics are substances foreign to the body. There are xenobiotics that can be given safely to humans which conjugate with intermediates of glucose and other metabolites in liver and excreted into the urine. This process allows non-invasive sampling of hepatic intermediates of glucose and Krebs cycle metabolism.

Glucuronidation has been widely used to sample enrichment of the glucose moiety of hepatic UDP-glucose, a key intermediate of glucose metabolism. UDP-glucuronic acid is formed by first activating and oxidizing glucose in the form of G1P. UDP is phosphorylated to uridine triphosphate (UTP) which reacts with G1P forming UDP-glucose. The glucose moiety is activated and then oxidized and UDP-glucuronic acid is formed. The glucuronic acid can be transferred to an acceptor (functional groups include hydroxyl, carboxyl, amino and sulfate groups) leading to the formation of a glucuronide (Strominger 1964).

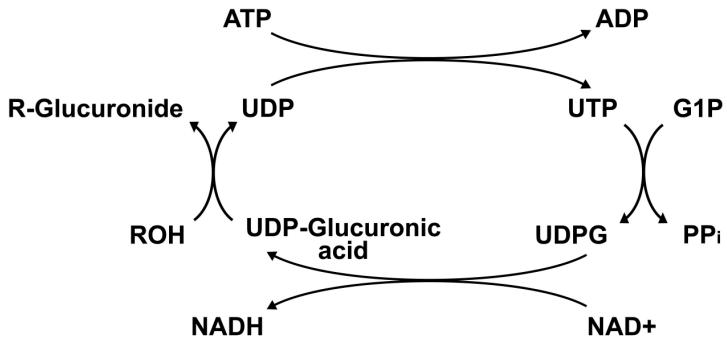

Figure 1.3: Conversion of UDP-glucose (UDPG) to glucuronide.

More than 90% of glucuronide is synthesised in the liver (Hellerstein *et al.* 1987). A pharmacological dose of paracetamol generates 200–800 μmol of paracetamol glucuronide over a 2-hours period of urine collection (Delgado *et al.* 2008b). This corresponds to about 4-12 times the amount of glucose obtained from 30 ml of blood (Burgess *et al.* 2003). Menthol can be safely ingested as enteric-coated capsules of peppermint oil and dosages of 200-400 mg, which are considered safe (Ribeiro *et al.* 2005), result in ~200 μmol of urinary menthol glucuronide. In human studies, the time resolution of urinary glucuronide sampling is 1-2 hours which is sufficiently brief to characterize hepatic glycogen synthesis during the 4-5 hour period of meal absorption. Diflusinal, an aspirin-like compound can be safely ingested in a 1 gram dose by an adult (Magnusson *et al.* 1987; Magnusson *et al.* 1988). A disadvantage of this compound is that only approximately one-half is excreted in the urine as its ether glucuronide with the remaining fraction being the unstable diflusinal ester glucuronide (Magnusson *et al.* 1987). With glucuronide sampling, it necessary to account for the lag time between formation in liver and appearance in urine. Urinary glucuronide collected over a certain interval represents its hepatic enrichment 30-60 min ahead of that interval (Hellerstein *et al.* 1987).

Hepatic glutamine can be non-invasively sampled as the urinary phenylacetylglutamine (PAGN) conjugate which can be generated by the ingestion of sodium phenylacetate or sodium phenylbutyrate (Yang *et al.* 1993; Dugelay *et al.* 1994; Yang *et al.* 1996; Jones *et al.* 2001b; Comte *et al.* 2002; Delgado *et al.* 2008b; Barosa *et al.* 2010). Ingestion of 300 mg of sodium phenylbutyrate yields approximately 600 μmoles of PAGN. Both glucuronide and PAGN probes can be given at the same time allowing analysis of hepatic UDP-glucose and Krebs cycle enrichments from [U-^{13}C]glycerol, [U-^{13}C]propionate and [U-^{13}C]glucose tracers (Jones *et al.* 1998; Jones *et al.* 2001b; Perdigoto *et al.* 2003b; Jones *et al.* 2009). PAGN enrichment from $^{2}H_2O$ was also measured and this is being developed as a method for resolving hepatic glutamine sources (see Chapter 4). In the liver, glutamine conjugation with phenylacetyl-CoA occurs predominantly in the hepatic perivenous zone (Jungermann 1986).

1.7 Nonsteady- and steady-state metabolic flux measurements

Tracer enrichment data are translated into metabolic information by the process of metabolic modeling. For mathematical purposes, the constituents of a living system can be represented as being located in distinguishable volumes called 'pools' or 'compartments' and metabolism of a particular substrate is defined by rates of appearance, disappearance and exchange between these various pools. Some assumptions govern tracer experiments but they are not always valid in all circumstances, thus appropriate corrections may be needed. One assumption is that the tracer has the same metabolic behaviour as its tracee. Another assumption is that for a given compartment, the tracer and tracee are uniformly distributed at all times. This implies instantaneous tracer and tracee mixing within the compartment. In reality, the time for this mixing process is not instantaneous and may be influenced by different morphological and physiological conditions. These include ingestion of a

glucose or meal load where plasma glucose levels are constantly changing due to the dynamics of glucose appearance from absorption and EGP on the one hand, and glucose disposal into glycogen and glycolytic pathways on the other. The appearance of tracer (for example from labeled glucose added to a meal) in this so-called nonsteady-state condition is dependent on the rate of mixing as well as that of glucose absorption and dilution from EGP and these parameters may all be changing over time. Metabolic modeling of these conditions requires frequent sampling to adequately define the time-dependent variables, coupled to a compartmental (Steele 1959; Radziuk *et al.* 1978; Cobelli *et al.* 1984) or circulatory model (Mari *et al.* 2003) that represents the various metabolite pool sizes, exchange between the pools, and net substrate input and output rates.

When rates of removal of the substances under study are equal to the rates of replacement, then concentrations and amounts of those substances are constant during the interval of the measurement. Under these conditions, the system is defined as being at metabolic steady-state. This situation is approximated by plasma glucose pool after an overnight fast, where plasma glucose levels are relatively constant, the glucose produced by the liver is equal to glucose uptake by peripheral tissues, and flux from the sources of hepatic glucose production (gluconeogenesis and glycogenolysis) are relatively constant. If, during this interval, enrichment of glucose from an administered tracer also reaches a constant value, then the system is a metabolic and isotopic steady-state. For this condition, the metabolic fluxes must be constant, enrichment of the precursor pool needs to be constant and the pool that is being sampled needs to be completely turned over. Steady-state conditions provide the simplest and most robust analyses because none of the enrichment parameters measured are time-dependent. The studies described in this Thesis are all based on assumptions of metabolic and isotopic steady state.

1.8 Tracing hepatic glucose metabolism with stable isotopes in fasting and fed states

1.8.1 Fasting state

The fasting state is characterized by a complete dependence of plasma glucose appearance on endogenous production. The liver is considered to be the principal supplier of EGP and the main contributing sources of hepatic glucose are glycogenolysis and gluconeogenesis. Present methodologies combine an isotope dilution measurement of EGP with tracer measurements of fractional glycogenolysis and gluconeogenesis. Alternatively, the EGP assay is combined with a direct real time measurement of hepatic glycogenolysis by *in vivo* ^{13}C NMR (Petersen *et al.* 1996; Hundal *et al.* 2000; Roden *et al.* 2001), (Kacerovsky *et al. in press*), with gluconeogenic flux being estimated as the difference of these two measurements. The *in vivo* ^{13}C NMR measurement requires specialized high-field clinical whole-body systems and is therefore less available in comparison to tracer assays.

The contribution of hepatic gluconeogenesis to EGP was previously measured by infusing ^{13}C- or ^{14}C-labeled gluconeogenic precursors such as lactate, pyruvate, gluconeogenic amino acids or glycerol and quantifying the enrichment or specific activity of glucose or glucuronide - the latter obtained by a glucuronidation agent (see section 1.6). Apart from the expense and inconvenience of a prolonged infusion of ^{13}C-enriched substrates, this method has a number of additional limitations and uncertainties. These include: 1) the measurement is limited to a single "representative" gluconeogenic substrate when in fact the liver can and does utilize a wide range of gluconeogenic substrates depending on their availability; 2) the inability to resolve tracer dilution from glycogenolysis *versus* that from other unlabeled gluconeogenic precursors (Alves *et al.* 2008); 3) the true hepatic precursor enrichment may be different to that measured in plasma and the tracer may also be preferentially

metabolized by periportal or perivenous zones resulting in a product enrichment that is biased towards the zone that metabolized the tracer (Ekberg *et al.* 1995); and 4) dilution and randomization of the tracer by exchange with hepatic Krebs cycle intermediates that is difficult to translate to a simple metabolic model.

Mass isotopomer distribution analysis (MIDA) is a technique for measuring the synthesis and turnover of polymers as carbohydrates, lipids and proteins. The technique is based on quantification of the relative abundances of different mass isotopomers in the polymer of interest that contains two or more units of a precursor monomeric subunit, after administration of a stable isotopically enriched precursor. The mass isotopomer distribution data are then fitted to a combinatorial probability model by comparing measured abundances to theoretical distributions predicted from the binomial or multinomial expansion. MIDA allows dilution in the monomeric (precursor) and polymeric (product) pools to be determined. Such polymers may be as simple as glucose synthesized from two triose units or as complex as proteins synthesized from amino acids or DNA made from nucleotides. (Hellerstein *et al.* 1999).

When applied to gluconeogenesis, MIDA allows the calculation of the triose-phosphate precursor ^{13}C-enrichment, following administration of a ^{13}C substrate such ^{13}C-glycerol. The difference between triose-P precursor and product glucose ^{13}C-enrichment is assigned to unlabeled glucose units derived *via* glycogenolysis. (Siler *et al.* 1998). The main drawbacks of this approach are 1) the relatively high levels of triose-P precursor enrichments that need to be established in order to generate a sufficient level of glucose molecules enriched in both triose units and 2) skewing of the glucose mass isotopomer distribution by metabolic zonation resulting in underestimates of the gluconeogenic fraction (Puchowicz *et al.* 1999; Bederman *et al.* 2001).

Deuterated water (^2H_2O) method was developed as an alternative to carbon tracers for quantifying the gluconeogenic contribution to EGP (Landau *et al.* 1995a; Landau *et al.* 1995b). ^2H_2O is a safe and inexpensive tracer and can be administered orally. As ^2H_2O rapidly equilibrates with total body water (BW), metabolites whose

hydrogens originate by BW exchange or addition become enriched with ^{2}H. BW precursor enrichment (plasma or urine ^{2}H-enrichments) can be easily and rapidly determined from small samples (Jones *et al.* 2001a). Once at isotopic steady-state, BW precursor enrichments are uniform across all tissues and are therefore unaffected by metabolic zonation or compartmentation. BW ^{2}H-enrichment levels for human studies range from 0.3-0.5% and this level of enrichment is achieved within 3-4 hours after drinking a loading dose consisting of 200-300 ml of 70-99% enriched $^{2}H_2O$. BW can then be maintained for extended periods by providing drinking water enriched with 0.3-0.5% ^{2}H. In the presence of $^{2}H_2O$ all glucose molecules derived *via* EGP, either by gluconeogenesis or glycogenolysis, will be enriched in position 2 to the same level as BW due to extensive glucose-6-phosphate-fructose-6-phosphate (G6P-F6P) exchange (Landau *et al.* 1996). Glucose derived from gluconeogenesis will also be enriched in position 5 due to the specific incorporation of solvent hydrogen at or below the triose phosphate isomerase (TPI) level. Therefore, the gluconeogenic contribution to EGP can be calculated by the ratio of enrichments in positions 5 and 2 ($^{2}H5/^{2}H2$). Position 5 is enriched regardless of whether the gluconeogenic source is glycerol or phosphoenolpyruvate (PEP) hence it represents all gluconeogenic activity. Enrichment of the prochiral position 6 hydrogens of glucose is almost all attributable to BW-hydrogen exchanges of PEP precursors, notably at the level of pyruvate and intervening Krebs cycle C4 metabolites. On this basis, the ratio of enrichments in positions 6 and 2 ($^{2}H6/^{2}H2$) provides the contribution of gluconeogenic PEP sources to EGP and include all anaplerotic substrates of the Krebs cycle. While both position 6 hydrogens are equally enriched from BW, there is uncertainty about the completeness of the BW-hydrogen exchange reactions. To the extent that these exchanges are incomplete, then the $^{2}H6/^{2}H2$ ratio underestimates contribution from the PEP precursors. Since these sites are not significantly enriched *via* glycerol gluconeogenesis, the difference between $^{2}H5/^{2}H2$ and $^{2}H6/^{2}H2$ can be attributed to the glycerol contribution. Incomplete exchange of the PEP precursors

will amplify the difference between $^{2}H5/^{2}H2$ and $^{2}H6/^{2}H2$ resulting in an overestimation of the glycerol contribution and a corresponding underestimation of the PEP fraction. Experimentally, the difference between $^{2}H5/^{2}H2$ and $^{2}H6/^{2}H2$ in healthy fasted subjects yields estimates of glycerol gluconeogenesis that are higher compared to those measured directly by glucose enrichment from ^{13}C-glycerol (Baba *et al.* 1995). However to date, the $^{2}H_2O$ and ^{13}C-glycerol measurements of glycerol gluconeogenesis have not been directly compared in the same subject.

The glycogenolytic contribution to EGP is calculated as the balance of the total gluconeogenesis contribution, i.e. $1-(^{2}H5/^{2}H2)$.

1.8.2 Fed state

The fed state is characterized by net hepatic glucose uptake and net synthesis of glycogen. These two parameters are not necessarily correlated since the liver can also synthesize glycogen from non glucose precursors *via* the indirect pathway. Net hepatic glycogen synthesis can be directly measured by *in vivo* ^{13}C NMR but is subject to the same limitations of equipment availability as described for *in vivo* ^{13}C NMR measurements of glycogenolysis. Alternatively, UDP-glucose flux can be measured by isotope dilution of infused labeled galactose (Hellerstein *et al.* 1997a; Hellerstein *et al.* 1997b), the UDP-glucose pool being sampled by glucuronidation probes as described earlier. These assays can then be coupled with tracer measurements of direct and indirect pathway contributions to hepatic glycogen synthesis flux.

Glucose tracers have been used to determine direct and indirect pathway contributions with the dilution of enrichment or specific activity between plasma glucose and hepatic UDP-glucose being attributed to indirect pathway flux. Both recyclable tracers such as [1-^{13}C]- or [6-^{14}C]glucose (Shulman *et al.* 1990; Bischof *et al.* 2002) and non-recyclable tracers such as [U-^{13}C]glucose and [5-^{3}H]glucose have been used (Katz *et al.* 1989; Stingl *et al.* 2006). [1-^{13}C]glucose has been widely used for to measure the

contribution of the direct pathway. However correction is needed for recycled ^{13}C-label, which will contribute to additional ^{13}C-enrichment to position 1. This recycled fraction is inferred from analysis of position 6 enrichment since recycling of [1-^{13}C]glucose will produce approximately equal populations of [1-^{13}C]- and [6-^{13}C]glucose (Landau *et al.* 1988; Shulman *et al.* 1990). With current protocols of direct/indirect pathway measurements that are based on a standard meal enriched with 5-10 grams of [1-^{13}C]glucose, this recycling fraction is relatively insignificant (see Chapter 2).

In the fed state the contribution of the direct and indirect pathways to glycogen synthesis can be also be measured using $^{2}H_2O$ and the metabolic information obtained by the analysis of a urine sample (Jones *et al.* 2006b). In presence of $^{2}H_2O$, both direct and indirect pathway intermediates become enriched in position 2 due to extensive G6P-F6P exchange, thus UDP-glucose and glycogen that is synthesized *via* both pathways are enriched in position 2. The indirect pathway also results in position 5 enrichment of UDP-glucose and glycogen. Hence, the indirect pathway fraction is given by the ^{2}H5/^{2}H2 ratio of UDP-glucose or glycogen, with the balance being attributed to the direct pathway fraction. This analysis is dependent on the assumption that position 2 enrichment of hepatic G6P is equivalent to that of BW. The advantages of the $^{2}H_2O$ method over glucose tracers for measuring direct and indirect pathway contributions are that stable precursor enrichment (BW) is easily established regardless of whether the glucose load is given intravenously, as an oral load or as part of a meal. By reading UDP-glucose enrichment with glucuronide probes, the measurement can be derived entirely from urine with no need for plasma glucose sampling. In animal studies, fractional glycogen synthesis can be directly measured from the ratio of glycogen position 2 enrichment to that of body BW (Soares *et al.* 2009). As with glucose tracers, the indirect pathway fraction is not resolved into contributions from intrahepatic glucose metabolism, Cori cycling of glucose or *de novo* gluconeogenesis.

1.9 Confounding factors of the deuterated water measurements of gluconeogenesis and glycogen synthesis

1.9.1 Transaldolase exchange activity

Transaldolase (TA) reversibly exchanges the carbons 4-5-6 of F6P with glyceraldehyde-3-phosphate (G3P). TA also catalyzes the transfer of DHAP moiety from sedoheptulose-7-phosphate (S7P) to G3P forming erythrose-4-phosphate (E4P) and F6P in the pentose cycle. Both carbon tracers and deuterated water method are affected by TA activity (Jones *et al.* 2008).

In presence of ^{2}H-enriched BW, the deuterium label from G3P is transferred to position 5 of unlabeled F6P derived from glycogenolysis, without net hexose synthesis. This occurs independently of gluconeogenic activity. Thus ^{2}H-enrichment of position 5 of G6P reflects the gluconeogenic contribution plus the fraction of G6P derived from unlabeled glucose or glycogen that underwent TA exchange. Therefore, glucose position 5 enrichment, and its ^{2}H5/^{2}H2 ratio, overestimates the gluconeogenic contribution to EGP.

^{2}H-enrichment of position 3 is not affected by TA. Position 3 enrichment is significantly less than that of position 5 which is consistent with TA activity (^{2}H3/^{2}H5<1).

With $^{2}H_2O$, TA exchange results in an increased ^{2}H-enrichment of position 5 and an increased ^{2}H5/^{2}H2 ratio, hence the indirect pathway contribution is overestimated (Barosa *et al. unpublished data*). Pathway contributions measured by glucose tracers such as [U^{13}C]glucose (Delgado *et al.* 2008a) or those labeled in positions 4, 5 or 6, i.e. [5-^{3}H]glucose, will also be modified by TA exchange. In these cases, TA exchange will remove the label resulting in an apparently higher dilution of the glucose tracer by indirect pathway flux. Thus, the indirect pathway contribution is overstated and that of the direct pathway correspondingly underestimated. Glucose

tracers that are labeled in positions 1, 2 or 3, such as [1-^{13}C]glucose, are not removed by TA exchange activity, hence their enrichment of UDP-glucose and glycogen is unaffected by this process.

1.9.2 Glycogen cycling

Under certain conditions the reciprocal regulation of glycogen synthase and phosphorylase activities is over-ridden and hepatic glycogen synthesis and glycogenolysis fluxes occur simultaneously. This mechanism facilitates exchange between hepatic G6P and glycogen glucosyl units and has important consequences on tracer enrichment of G6P and glucose. Glycogen cycling in the fasted state results in the uncoupling of glycogen phosphorylase and net glycogen breakdown fluxes, while in the fed state, rates of glycogen synthase and net glycogen accumulation are uncoupled. Since *in vivo* ^{13}C NMR methods measure net glycogen synthesis and hydrolysis, while tracers such as $^{2}H_2O$, measure glycogen phosphorylase and glycogen synthase fluxes, glycogen cycling is revealed as a discrepancy between tracer and *in vivo* ^{13}C-NMR-derived measurements of glycogen metabolism. To date, these measurements have only been performed simultaneously in fasted subjects (Hundal *et al.* 2000), (Kacerovsky *et al. in press*).Thus labeled units from G6P will be diluted from unlabeled glycosyl units resulted from glycogen breakdown. Glycogen cycling influences the ^{2}H-enrichment of G6P and the ^{2}H5/^{2}H2 ratio. In the fed state, glycogen cycling underestimates the indirect pathway by diluting the position 5 label of G6P formed from gluconeogenic precursors. In the fasting state the dilution of the position 5 ^{2}H-enrichment also occurs and underestimates the gluconeogenic contribution to glucose production (Stingl *et al.* 2006).

1.9.3 Galactose metabolism

Galactose is metabolized in liver and converted to glycogen by its conversion to common intermediates of glucose metabolism *via* Leloir pathway (Hellerstein *et al.* 1988; Wehrli *et al.* 2007). It is converted to UDP-glucose without acquiring label from either glucose tracers or ^2H_2O. Unlabeled UDP-glucose derived from galactose dilutes the enrichment or specific activity originating from G6P. In the case of glucose tracers, this dilution reduces the enrichment or specific activity of UDP-glucose relative to plasma glucose resulting in an underestimation of the direct pathway contribution. With ^2H_2O, galactose inflow into UDP-glucose dilutes the enrichment of position 5 relative to BW, therefore the ratio of position 5 enrichment to BW underestimates the real indirect pathway contribution. These effects were recently demonstrated in rodents that were given glucose and galactose loads (Soares *et al.* 2010). Since galactose inflow also dilutes enrichment of position 2 to the same extent as position 5, the $^2H5/^2H2$ ratio is unaltered and indirect pathway estimates by this method are therefore unaffected. The dilution of position 2 relative to BW reveals the contribution of galactose to glycogen synthesis allowing galactose contributions to be resolved from those of direct and indirect pathways. However, this analysis is critically dependent on the complete equivalence of G6P and BW ^2H-enrichment, i.e. complete exchange of G6P with F6P. To date, this assumption has not been tested in a meal setting. In human studies to date, these approaches have not considered the effects of galactose metabolism originating from the milk component of the breakfast meal. A 200 ml glass of skimmed milk that is typically included in such meals contains sufficient galactose equivalents to contribute significantly to net hepatic glycogen synthesis (Jones *et al.* 2006b).

1.10 References

American Diabetes Association. Diagnosis and classification of diabetes *mellitus*. Diabetes Care 2011;34 Supplement 1:S62-69.

Abele JT and Fung CI. Effect of hepatic steatosis on liver FDG uptake measured in mean standard uptake values. Radiology 2010; 254:917-924.

Adkins BA, Myers SR, Williams PE and Cherrington AD. Importance of the route of intravenous glucose delivery to hepatic glucose balance. Diabetologia 1984;27:A250-A250.

Alves TC, Nunes PM, Palmeira CM, Jones JG and Carvalho RA. Estimating gluconeogenesis by NMR isotopomer distribution analysis of [^{13}C]bicarbonate and [1-^{13}C]lactate. NMR in Biomedicine 2008;21:337-344.

Baba H, Zhang XJ and Wolfe RR. Glycerol gluconeogenesis in fasting humans. Nutrition. 1995;11:149-153.

Barnett A. Dosing of insulin glargine in the treatment of type 2 diabetes. Clinical Therapeutics 2007;29:987-999.

Barosa C, Almeida M, Caldeira MM, Gomes F and Jones JG. Contribution of proteolytic and metabolic sources to hepatic glutamine by ^{2}H NMR analysis of urinary phenylacetylglutamine ^{2}H-enrichment from $^{2}H_2O$. Metabolic Engineering 2010;12:53-61.

Basu A, Basu R, Shah P, Vella A, Johnson CM, Nair KS, Jensen MD, Schwenk WF and Rizza RA. Effects of type 2 diabetes on the ability of insulin and glucose to regulate splanchnic and muscle glucose metabolism - Evidence for a defect in haptic glucokinase activity. Diabetes 2000;49:272-283.

Basu R, Barosa, C., Basu, A., Pattan, V., Saad, A., Jones, J. and Rizza, R. Transaldolase exchange and its effects on measurements of gluconeogenesis in humans. American Journal of Physiology-Endocrinology and Metabolism 2011;300:E296-303.

Bederman IR, Kelleher JK, Wasserman DH and Brunengraber H. Zonation of labeling of lipogenic acetyl-CoA in liver. Implications for measurements of lipogenesis by mass isotopomer analysis. Faseb Journal 2001;15:A750-A750.

Bhattacharya S, Ammini AC, Jyotsna V, Gupta N and Dwivedi S. Recovery of beta-cell functions with low-dose insulin therapy: study in newly diagnosed type 2 diabetes *mellitus* patients. Diabetes Technology & Therapeutics 2011;13:461-465.

Bischof MG, Bernroider E, Krssak M, Krebs M, Stingl H, Nowotny P, Yu CL, Shulman GI, Waldhausl W and Roden M. Hepatic glycogen metabolism in type 1 diabetes after long-term near normoglycemia. Diabetes 2002;51:49-54.

Bischof MG, Krssak M, Krebs M, Bernroider E, Stingl H, Waldhausl W and Roden M. Effects of short-term improvement of insulin treatment and glycemia on hepatic glycogen metabolism in type 1 diabetes. Diabetes 2001;50:392-398.

Boden G. Interaction between free fatty acids and glucose metabolism. Current Opinion in Clinical Nutrition and Metabolic Care 2002;5:545-549.

Boden G, Chen X and Iqbal N. Acute lowering of plasma fatty acids lowers basal insulin secretion in diabetic and nondiabetic subjects. Diabetes. 1998;47:1609-1612.

Boden G and Zhang M. Recent findings concerning thiazolidinediones in the treatment of diabetes. Expert Opinion on Investigational Drugs 2006;15:243-250.

Burgess SC, Weis B, Jones JG, Smith E, Merritt ME, Margolis D, Sherry AD and Malloy CR. Noninvasive evaluation of liver metabolism by ^{2}H and ^{13}C NMR isotopomer analysis of human urine. Analytical Biochemistry 2003;312:228-234.

Carvalho RA, Jeffrey FM, Sherry AD and Malloy CR. ^{13}C isotopomer analysis of glutamate by heteronuclear multiple quantum coherence-total correlation spectroscopy (HMQC-TOCSY). FEBS Letters 1998;440:382-386.

Carvalho RA, Zhao P, Wiegers CB, Jeffrey FMH, Malloy CR and Sherry AD. TCA cycle kinetics in the rat heart by analysis of ^{13}C- isotopomers using indirect ^{1}H [^{13}C] detection. American Journal of Physiology-Heart and Circulatory Physiology 2001;281:H1413-H1421.

Chandramouli V, Ekberg K, Schumann WC, Kalhan SC, Wahren J and Landau BR. Quantifying gluconeogenesis during fasting. American Journal of Physiology 1997;273:E1209-E1215.

Chen NG and Reaven GM. Fatty acid inhibition of glucose-stimulated insulin secretion is enhanced in pancreatic islets from insulin-resistant rats. Metabolism 1999;48:1314-1317.

Chevalier S, Burgess SC, Malloy CR, Gougeon R, Marliss EB and Morais JA. The greater contribution of gluconeogenesis to glucose production in obesity is related to increased whole-body protein catabolism. Diabetes 2006;55:675-681.

Chiarelli F and Di Marzio D. Peroxisome proliferator-activated receptor-gamma agonists and diabetes: current evidence and future perspectives. Vasc Health Risk Manag 2008;4:297-304.

Chiasson JL, Liljenquist JE, Lacy WW, Jennings AS and Cherrington AD. Gluconeogenesis - methodological approaches *in vivo*. Federation Proceedings 1977;36:229-235.

Cobelli C, Toffolo G and Ferrannini E. A model of glucose kinetics and their control by insulin, compartmental and noncompartmental approaches. Mathematical Biosciences 1984;72:291-315.

Comte B, Kasumov T, Pierce BA, Puchowicz MA, Scott ME, Dahms W, Kerr D, Nissim I and Brunengraber H. Identification of phenylbutyrylglutamine, a new metabolite of phenylbutyrate metabolism in humans. Journal of Mass Spectrometry 2002;37:581-590.

Consoli A, Nurjhan N, Capani F and Gerich J. Predominant role of gluconeogenesis in increased hepatic glucose-production in NIDDM. Diabetes 1989;38:550-557.

Cusi K, Consoli A and DeFronzo RA. Metabolic effects of metformin on glucose and lactate metabolism in noninsulin-dependent diabetes *mellitus*. Journal of Clinical Endocrinology & Metabolism 1996;81:4059-4067.

Davila-Roman VG, Vedala G, Herrero P, de las Fuentes L, Rogers JG, Kelly DP and Gropler RJ. Altered myocardial fatty acid and glucose metabolism in idiopathic dilated cardiomyopathy. Journal of the American College of Cardiology 2002;40:271-277.

DeFronzo RA. From the triumvirate to the ominous octet: a new paradigm for the treatment of type 2 diabetes *mellitus*. Diabetes 2009;58:773-795.

Degrado TR, Coenen HH and Stocklin G. 14(*R,S*)-[^{18}F]Fluoro-6-thia-heptadecanoic acid (FTHA) - evaluation in mouse of a new probe of miocardial utilization of long-chain fatty-acids. Journal of Nuclear Medicine 1991;32:1888-1896.

Delgado T, Carvalheiro M, Bastos M, Baptista C, Fagulha A, Barros L, Silva C, Barosa C, Geraldes C, Castro M and Jones JG. Unexpectedly high indirect pathway contribution to hepatic glycogen synthesis in healthy subjects after oral glucose tolerance test. Diabetes 2008a;57:A11-A12.

Delgado TC, Barosa C, Castro M, Geraldes C, Bastos M, Baptista C, Fagulha A, Barros L, Mota A, Carvalheiro M, Jones JG and Merritt M. Sources of hepatic glucose production by $^{2}H_2O$ ingestion and Bayesian analysis of ^{2}H glucuronide enrichment. Magnetic Resonance in Medicine 2008b;60:517-523.

Delgado TC, Silva C, Fernandes I, Caldeira M, Bastos M, Baptista C, Carvalheiro M, Geraldes C and Jones JG. Sources of hepatic glycogen synthesis during an oral glucose tolerance test: effect of transaldolase exchange on flux estimates. Magnetic Resonance in Medicine 2009;62:1120-1128.

Diani AR, Sawada G, Wyse B, Murray FT and Khan M. Pioglitazone preserves pancreatic islet structure and insulin secretory function in three murine models of type 2 diabetes. American Journal of Physiology-Endocrinology and Metabolism 2004;286:E116-E122.

Dresner A, Laurent D, Marcucci M, Griffin ME, Dufour S, Cline GW, Slezak LA, Andersen DK, Hundal RS, Rothman DL, Petersen KF and Shulman GI. Effects of free fatty acids on glucose transport and IRS-1-associated phosphatidylinositol 3-kinase activity. Journal of Clinical Investigation 1999;103:253-259.

Dugelay S, Yang D, Soloviev MV, Previs SF, Agarwal KC, Fernandez CA and Brunengraber H. Assay of the concentration and ^{13}C-labeling pattern of phenylacetylglutamine by nuclear magnetic resonance. Analytical Biochemistry 1994;221:368-373.

Ebert A, Herzog H, Stocklin GL, Henrich MM, Degrado TR, Coenen HH and Feinendegen LE. Kinetics of 14(*R,S*)-fluorine-18-fluoro-6-thia-heptadecanoic acid in normal human hearts at rest, during exercise and after dipyridamole injection Journal of Nuclear Medicine 1994;35:51-56.

Egan W, Shindo H and Cohen JS. ^{13}C Nuclear magnetic-resonance studies of proteins. Annual Review of Biophysics and Bioengineering 1977;6:383-417.

Ekberg K, Chandramouli V, Kumaran K, Schumann WC, Wahren J and Landau BR. Gluconeogenesis and glucuronidation in liver *in vivo* and the heterogeneity of hepatocyte function. Journal of Biological Chemistry 1995;270:21715-21717.

Ekberg K, Landau BR, Wajngot A, Chandramouli V, Efendic S, Brunengraber H and Wahren J. Contributions by kidney and liver to glucose production in the postabsorptive state and after 60 h of fasting. Diabetes. 1999;48:292-298.

Ferdinand KC. Management of cardiovascular risk in patients with type 2 diabetes *mellitus* as a component of the cardiometabolic syndrome. Journal of the Cardiometabolic Syndrome. 2006;1:133-140.

Finegood DT, McArthur MD, Kojwang D, Thomas MJ, Topp BG, Leonard T and Buckingham RE. beta-cell mass dynamics in Zucker diabetic fatty rats - Rosiglitazone prevents the rise in net cell death. Diabetes 2001;50:1021-1029.

Gabbay RA, Sutherland C, Gnudi L, Kahn BB, Obrien RM, Granner DK and Flier JS. Insulin regulation of phosphoenolpyruvate carboxykinase gene expression does not require activation of the Ras mitogen-activated protein kinase signaling pathway. Journal of Biological Chemistry 1996;271:1890-1897.

Gastaldelli A, Ferrannini E, Miyazaki Y, Matsuda M, Mari A and DeFronzo RA. Thiazolidinediones improve beta-cell function in type 2 diabetic patients. American Journal of Physiology-Endocrinology and Metabolism 2007;292:E871-E883.

Gastaldelli A, Miyazaki Y, Pettiti M, Santini E, Ciociaro D, DeFronzo RA and Ferrannini E. The effect of rosiglitazone on the liver: decreased gluconeogenesis in patients with type 2 diabetes. Journal of Clinical Endocrinology and Metabolism 2006;91:806-812.

Gastaldelli A, Toschi E, Pettiti M, Frascerra S, Quinones-Galvan A, Sironi AM, Natali A and Ferrannini E. Effect of physiological hyperinsulinemia on gluconeogenesis in nondiabetic subjects and in type 2 diabetic patients. Diabetes 2001;50:1807-1812.

Gavin JR, Alberti K, Davidson MB, DeFronzo RA, Drash A, Gabbe SG, Genuth S, Harris MI, Kahn R, Keen H, Knowler WC, Lebovitz H, Maclaren NK, Palmer JP, Raskin P, Rizza RA and Stern MP. Report of the Expert Committee on the Diagnosis and Classification of Diabetes *Mellitus*. Diabetes Care 1997;20:1183-1197.

Genuth S, Alberti K, Bennett P, Buse J, DeFronzo R, Kahn R, Kitzmiller J, Knowler WC, Lebovitz H, Lernmark A, Nathan D, Palmer J, Rizza R, Saudek C, Shaw J, Steffes M, Stern M, Tuomilehto J, Zimmet P and Expert Committee on the Diagnosis and

Classification of Diabetes *Mellitus*. Follow-up report on the diagnosis of diabetes *mellitus*. Diabetes Care 2003;26:3160-3167.

Graaf AA, Mahle, M., Mollney, M., Wiechert, W., and Stahmann P, Sahm, H. Determination of full ^{13}C isotopomer distributions for metabolic flux analysis using heteronuclear spin echo difference NMR spectroscopy. Journal of Biotechnology 2000;77:25-35.

Griffin ME, Marcucci MJ, Cline GW, Bell K, Barucci N, Lee D, Goodyear LJ, Kraegen EW, White MF and Shulman GI. Free fatty acid-induced insulin resistance is associated with activation of protein kinase-C-theta and alterations in the insulin signaling cascade. Diabetes 1999;48:1270-1274.

Halama JR, Holden JE, Gatley SJ, Bernstein D, Ohora KT, Ng CK and Degrado TP. Validation of F-18-3-deoxy-3-fluoro-D-glucose (3FDG) as an agent for measurement of glucose-transport by Positron Emission Tomography. Journal of Nuclear Medicine 1983;24:P52-P52.

He YX and Guo QY. Clinical applications and advances of positron emission tomography with fluorine-18-fluorodeoxyglucose (^{18}F-FDG) in the diagnosis of liver neoplasms. Postgraduate Medical Journal 2008;84:246-251.

Hellerstein MK, Greenblatt DJ and Munro HN. Glycoconjugates as noninvasive probes of intrahepatic metabolism: I. Kinetics of label incorporation with evidence of a common precursor UDP-glucose pool for secreted glycoconjugates. Metabolism 1987;36:988-994.

Hellerstein MK and Munro HN. Glycoconjugates as noninvasive probes of intrahepatic metabolism: III. Application to galactose assimilation by the intact rat. Metabolism 1988;37:312-317.

Hellerstein MK and Neese RA. Mass isotopomer distribution analysis at eight years: theoretical, analytic, and experimental considerations. American Journal of Physiology 1999;39:E1146-E1170.

Hellerstein MK, Neese RA, Letscher A, Linfoot P and Turner S. Hepatic glucose-6-phosphatase flux and glucose phosphorylation, cycling, irreversible disposal, and net balance *in vivo* in rats. Measurement using the secreted glucuronate technique. Metabolism. 1997a;46:1390-1398.

Hellerstein MK, Neese RA, Linfoot P, Christiansen M, Turner S and Letscher A. Hepatic gluconeogenic fluxes and glycogen turnover during fasting in humans. A stable isotope study. Journal of Clinical Investigation 1997b;100:1305-1319.

Herrero P, Sharp TL, Dence C, Haraden BM and Gropler RJ. Comparison of 1-^{11}C-glucose and ^{18}F-FDG for quantifying myocardial glucose use with PET. Journal of Nuclear Medicine 2002;43:1530-1541.

Hundal RS, Krssak M, Dufour S, Laurent D, Lebon V, Chandramouli V, Inzucchi SE, Schumann WC, Petersen KF, Landau BR and Shulman GI. Mechanism by which metformin reduces glucose production in type 2 diabetes. Diabetes 2000;49:2063-2069.

Hwang JH, Perseghin G, Rothman DL, Cline GW, Magnusson I, Petersen KF and Shulman GI. Impaired net hepatic glycogen synthesis in insulin-dependent diabetic subjects during mixed meal ingestion. A ^{13}C nuclear magnetic resonance spectroscopy study. Journal of Clinical Investigation 1995;95:783-787.

Inzucchi S, Bergenstal R, Fonseca V, Gregg E, Mayer-Davis B, Spollett G, Wender R and American Diabetes Association. Diagnosis and Classification of Diabetes *Mellitus*. Diabetes Care 2010;33:S62-S69.

Inzucchi SE, Maggs DG, Spollett GR, Page SL, Rife FS, Walton V and Shulman GI. Efficacy and metabolic effects of metformin and troglitazone in type II diabetes *mellitus*. New England Journal of Medicine 1998;338:867-872.

Jones JG, Barosa C, Gomes F, Mendes AC, Delgado TC, Diogo L, Garcia P, Bastos M, Barros L, Fagulha A, Baptista C, Carvalheiro M and Caldeira MM. NMR derivatives for quantification of ^{2}H and ^{13}C-enrichment of human glucuronide from metabolic tracers. Journal of Carbohydrate Chemistry 2006a;25:203-217.

Jones JG, Carvalho RA, Sherry AD and Malloy CR. Quantitation of gluconeogenesis by ^{2}H nuclear magnetic resonance analysis of plasma glucose following ingestion of $^{2}H_2O$. Analytical Biochemistry 2000;277:121-126.

Jones JG, Cottam GL, Miller BC, Sherry AD and Malloy CR. A method for obtaining 13C isotopomer populations in ^{13}C-enriched glucose. Analytical Biochemistry 1994;217:148-152.

Jones JG, Fagulha A, Barosa C, Bastos M, Barros L, Baptista C, Caldeira MM and Carvalheiro M. Noninvasive analysis of hepatic glycogen kinetics before and after breakfast with deuterated water and acetaminophen. Diabetes 2006b;55:2294-2300.

Jones JG, Garcia P, Barosa C, Delgado TC, Caldeira MM and Diogo L. Quantification of hepatic transaldolase exchange activity and its effects on tracer measurements of indirect pathway flux in humans. Magnetic Resonance in Medicine 2008;59:423-429.

Jones JG, Garcia P, Barosa C, Delgado TC and Diogo L. Hepatic anaplerotic outflow fluxes are redirected from gluconeogenesis to lactate synthesis in patients with type 1a glycogen storage disease. Metabolic Engineering 2009;11:155-162.

Jones JG, Hansen J, Sherry AD, Malloy CR and Victor RG. Determination of acetyl-CoA enrichment in rat heart and skeletal muscle by ^{1}H nuclear magnetic resonance analysis of glutamate in tissue extracts. Analytical Biochemistry 1997;249:201-206.

Jones JG, Merritt, M. and Malloy, C.R. Quantifying tracer levels of $^{2}H_2O$ enrichment from microliter amounts of plasma and urine by ^{2}H NMR. Magnetic Resonance in Medicine 2001a;45:156-158.

Jones JG, Sherry AD, Jeffrey FM, Storey CJ and Malloy CR. Sources of acetyl-CoA entering the tricarboxylic acid cycle as determined by analysis of succinate ^{13}C isotopomers. Biochemistry 1993;32:12240-12244.

Jones JG, Solomon M.A., Cole, S.M., Sherry, A.D., Malloy, C.R. An integrated ^{2}H and ^{13}C NMR study of gluconeogenesis and TCA cycle flux in humans. American Journal of Physiology: Endocrinology and Metabolism 2001b;281:E848-E851.

Jones JG, Solomon MA, Sherry AD, Jeffrey FM and Malloy CR. ^{13}C NMR measurements of human gluconeogenic fluxes after ingestion of [U-^{13}C]propionate, phenylacetate, and acetaminophen. American Journal of Physiology 1998;275:E843-E852.

Jungermann K. Functional heterogeneity of periportal and perivenous hepatocytes. Enzyme 1986;35:161-180.

Katz J, Lee WN, Wals PA and Bergner EA. Studies of glycogen synthesis and the Krebs cycle by mass isotopomer analysis with [U-^{13}C]glucose in rats. Journal of Biological Chemistry 1989;264:12994-13004.

Katz J, Wals P and Lee WN. Isotopomer studies of gluconeogenesis and the Krebs cycle with ^{13}C-labeled lactate. Journal of Biological Chemistry 1993;268:25509-25521.

Kawasaki F, Matsuda M, Kanda Y, Inoue H and Kaku K. Structural and functional analysis of pancreatic islets preserved by pioglitazone in db/db mice. American Journal of Physiology-Endocrinology and Metabolism 2005;288:E510-E518.

Krssak M, Brehm A, Bernroider E, Anderwald C, Nowotny P, Man CD, Dalla Man C, Cline GW, Shulman GI, Waldhausl W and Roden M. Alterations in postprandial hepatic glycogen metabolism in type 2 diabetes. Diabetes 2004a;53:3048-3056.

Krssak M and Roden M. The role of lipid accumulation in liver and muscle for insulin resistance and type 2 diabetes *mellitus* in humans. Reviews in Endocrine & Metabolic Disorders 2004b;5:127-134.

Kunert O, Stingl H, Rosian E, Krssak M, Bernroider E, Seebacher W, Zangger K, Staehr P, Chandramouli V, Landau BR, Nowotny P, Waldhausl W, Haslinger E and Roden M. Measurement of fractional whole-body gluconeogenesis in humans from blood samples using ^{2}H nuclear magnetic resonance spectroscopy. Diabetes 2003;52:2475-2482.

Kunnecke B (1999). Carbon-13 NMR Spectrocopy of Biological Systems, Academic Press, Inc.

Landau BR, Fernandez CA, Previs SF, Ekberg K, Chandramouli V, Wahren J, Kalhan SC and Brunengraber H. A limitation in the use of mass isotopomer distributions to measure gluconeogenesis in fasting humans. American Journal of Physiology 1995a;269:E18-E26.

Landau BR and Wahren J. Quantification of the pathways followed in hepatic glycogen formation from glucose. Faseb Journal 1988;2:2368-2375.

Landau BR, Wahren J, Chandramouli V, Schumann WC, Ekberg K and Kalhan SC. Use of $^{2}H_2O$ for estimating rates of gluconeogenesis. Application to the fasted state. Journal of Clinical Investigation 1995b;95:172-178.

Landau BR, Wahren J, Chandramouli V, Schumann WC, Ekberg K and Kalhan SC. Contributions of gluconeogenesis to glucose production in the fasted state. Journal of Clinical Investigation 1996;98:378-385.

Lang V, Vaugelade P, Bernard F, Darcy-Vrillon B, Alamowitch C, Slama G, Duee PH and Bornet FRJ. Euglycemic hyperinsulinemic clamp to assess posthepatic glucose appearance after carbohydrate loading. 1. Validation in pigs. American Journal of Clinical Nutrition 1999;69:1174-1182.

Magnusson I, Chandramouli V, Schumann WC, Kumaran K, Wahren J and Landau BR. Quantitation of the pathways of hepatic glycogen formation on ingesting a glucose load. Journal of Clinical Investigation 1987;80:1748-1754.

Magnusson I, Chandramouli V, Schumann WC, Kumaran K, Wahren J and Landau BR. Pentose pathway in human liver. Proceedings of the National Academy of Sciences of the United States of America 1988;85:4682-4685.

Magnusson I, Rothman DL, Katz LD, Shulman RG and Shulman GI. Increased rate of gluconeogenesis in type II diabetes *mellitus*. A ^{13}C nuclear magnetic resonance study. Journal of Clinical Investigation 1992;90:1323-1327.

Mari A, Stojanovska L, Proietto J and Thorburn AW. A circulatory model for calculating non-steady-state glucose fluxes. Validation and comparison with compartmental models. Computer Methods and Programs in Biomedicine 2003;71:269-281.

Moldes M, Cerdan S, Erhard P and Seelig J. 1H-2H exchange in the perfused rat liver metabolizing [3-^{13}C]alanine and $^{2}H_2O$ as detected by multinuclear NMR spectroscopy. NMR in Biomedicine 1994;7:249-262.

Napoli R, Capaldo, B., Picardi, A., Piscione, F., Bigazzi, M.C., Dascia, C., and Sacca, L. . Indirect pathway of liver glycogen synthesis in humans is predominant and independent of β-adrenergic mechanisms. Clinical Physiology 1992;12:641-652.

Nguyen N, Magno, C., Lane, K., Hinojosa, M., Lane, L. Association of hypertension, diabetes, dyslipidemia, and metabolic syndrome with obesity: findings from the national health and nutrition examination survey, 1999 to 2004. Journal of the American College of Surgeons 2008;207:928–934.

Perdigoto R, Furtado AL, Porto A, Rodrigues TB, Geraldes C and Jones JG. Sources of glucose production in cirrhosis by $^{2}H_2O$ ingestion and ^{2}H NMR analysis of plasma glucose. Biochimica Et Biophysica Acta-Molecular Basis of Disease 2003a;1637:156-163.

Perdigoto R, Rodrigues TB, Furtado AL, Porto A, Geraldes C and Jones JG. Integration of [U-^{13}C]glucose and $^{2}H_2O$ for quantification of hepatic glucose production and gluconeogenesis. NMR in Biomedicine 2003b;16:189-198.

Petersen KF, Cline, G.W., Gerard, D.P., Magnusson, I., Rothman, D.L., Shulman, G.I. Contribution of net hepatic glycogen synthesis to disposal of an oral glucose load in humans Metabolism 2001;50:598-601.

Petersen KF, Price T, Cline GW, Rothman DL and Shulman GI. Contribution of net hepatic glycogenolysis to glucose production during the early postprandial period. American Journal of Physiology 1996;270:E186-E191.

Petersen KF and Shulman GI. Cellular mechanism of insulin resistance in skeletal muscle. Journal of the Royal Society of Medicine 2002;95:8-13.

Phelps ME, Huang SC, Hoffman EJ, Selin C, Sokoloff L and Kuhl DE. Tomographic measurement of local cerebral glucose metabolic-rate in humans with (^{18}F)2-fluoro-2-deoxy-D-glucose - validation of method. Annals of Neurology 1979;6:371-388.

Puchowicz MA, Bederman IR, Comte B, Yang DW, David F, Stone E, Jabbour K, Wasserman DH and Brunengraber H. Zonation of acetate labeling across the liver: implications for studies of lipogenesis by MIDA. American Journal of Physiology-Endocrinology and Metabolism 1999;277:E1022-E1027.

Radziuk J, Norwich KH and Vranic M. Experimental validation of measurements of glucose turnover in nonsteady state. American Journal of Physiology 1978;234:E84-E93.

Ribeiro A, Caldeira MM, Carvalheiro M, Bastos M, Baptista C, Fagulha A, Barros L, Barosa C and Jones JG. Simple measurement of gluconeogenesis by direct ^{2}H NMR analysis of menthol glucuronide enrichment from $^{2}H_2O$. Magnetic Resonance in Medicine 2005;54:429-434.

Roden M. Mechanisms of Disease: hepatic steatosis in type 2 diabetes - pathogenesis and clinical relevance. Nature Clinical Practice Endocrinology & Metabolism 2006;2:335-348.

Roden M, Petersen KF and Shulman GI. Nuclear magnetic resonance studies of hepatic glucose metabolism in humans. Recent Progress in Hormone Research, Vol 56 2001;56:219-237.

Rodrigues TB, Gray HL, Benito M, Garrido S, Sierra A, Geraldes CF, Ballesteros P and Cerdan S. Futile cycling of lactate through the plasma membrane of C6 glioma cells as detected by (^{13}C, ^{2}H) NMR. Journal of Neuroscience Research 2005;79:119-127.

Roglic G and Unwin N. Mortality attributable to diabetes: Estimates for the year 2010. Diabetes Research and Clinical Practice 87:15-19.

Roglic G, Unwin N, Bennett PH, Mathers C, Tuomilehto J, Nag S, Connolly V and King H. The burden of mortality attributable to diabetes - Realistic estimates for the year 2000. Diabetes Care 2005;28:2130-2135.

Rothman DL, Magnusson I, Katz LD, Shulman RG and Shulman GI. Quantitation of hepatic glycogenolysis and gluconeogenesis in fasting humans with ^{13}C NMR. Science. 1991;254:573-576.

Saad MJA, Hartmann LGC, Decarvalho DS, Galoro CAO, Brenelli SL and Carvalho CRO. Effect of glucagon on insulin-receptor substrate-1 (IRS-1) phosphorylation and association with phosphatidylinositol 3-kinase (PI-3-kinase). FEBS Letters 1995;370:131-134.

Saisho Y, Kou K, Tanaka K, Abe T, Kurosawa H, Shimada A, Meguro S, Kawai T and Itoh H. Postprandial serum C-peptide to plasma glucose ratio as a predictor of subsequent insulin treatment in patients with type 2 diabetes. Endocrine Journal 2011;58:315-322.

Saltiel AR and Olefsky JM. Thiazolidinediones in the treatment of insulin resistance and type II diabetes. Diabetes 1996;45:1661-1669.

Samuel VT, Liu ZX, Qu XQ, Elder BD, Bilz S, Befroy D, Romanelli AJ and Shulman GI. Mechanism of hepatic insulin resistance in non-alcoholic fatty liver disease. Journal of Biological Chemistry 2004;279:32345-32353.

Schleucher J, Vanderveer PJ and Sharkey TD. Export of carbon from chloroplasts at night. Plant Physiology 1998;118:1439-1445.

Setacci C, de Donato G, Setacci F and Chisci E. Diabetic patients: epidemiology and global impact. Journal of Cardiovascular Surgery 2009;50:263-273.

Shimabukuro M, Zhou YT, Lee Y and Unger RH. Troglitazone lowers islet fat and restores β-cell function of Zucker diabetic fatty rats. Journal of Biological Chemistry 1998;273:3547-3550.

Shiota M, Jackson PA, Bischoff H, McCaleb M, Scott M, Monohan M, Neal DW and Cherrington AD. Inhibition of glycogenolysis enhances gluconeogenic precursor uptake by the liver of conscious dogs. American Journal of Physiology-Endocrinology and Metabolism 1997;273:E868-E879.

Shulman GI, Cline G, Schumann WC, Chandramouli V, Kumaran K and Landau BR. Quantitative comparison of pathways of hepatic glycogen repletion in fed and fasted humans. American Journal of Physiology 1990;259:E335-E341.

Siler SQ, Neese RA, Christiansen MP and Hellerstein MK. The inhibition of gluconeogenesis following alcohol in humans. American Journal of Physiology 1998;275:E897-E907.

Soares AF, Carvalho RA, Veiga FJ and Jones JG. Effects of galactose on direct and indirect pathway estimates of hepatic glycogen synthesis. Metabolic Engineering 2010;12:552-560.

Soares AF, Veiga FJ, Carvalho RA and Jones JG. Quantifying hepatic glycogen synthesis by direct and indirect pathways in rats under normal ad libitum feeding conditions. Magnetic Resonance in Medicine 2009;61:1-5.

Sokoloff L, Reivich M, Kennedy C, Desrosiers MH, Patlak CS, Pettigrew KD, Sakurada O and Shinohara M. [Deoxyglucose-^{14}C] method for measurement of local cerebral glucose-utilization - theory, procedure, and normal values in conscious and anesthetized albino-rat. Journal of Neurochemistry 1977;28:897-916.

Steele R. Influences of glucose loading and of injected insulin on hepatic glucose output. Annals of the New York Academy of Sciences 1959;82:420-430.

Stingl H, Chandramouli V, Schumann WC, Brehm A, Nowotny P, Waldhausl W, Landau BR and Roden M. Changes in hepatic glycogen cycling during a glucose load in healthy humans. Diabetologia 2006;49:360-368.

Strominger JL. nucleotide intermediates in the biosynthesis of heteropolymeric polysaccharides. Biophysical Journal 1964;4:139-153.

Taylor R, Magnusson I, Rothman DL, Cline GW, Caumo A, Cobelli C and Shulman GI. Direct assessment of liver glycogen storage by ^{13}C nuclear magnetic resonance spectroscopy and regulation of glucose homeostasis after a mixed meal in normal subjects. Journal of Clinical Investigation 1996;97:126-132.

Waugh N, Scotland G, McNamee P, Gillett M, Brennan A, Goyder E, Williams R and John A. Screening for type 2 diabetes: literature review and economic modelling. Health Technology Assessment 2007;11.

Wehrli S, Reynolds R and Segal S. Metabolic fate of administered [^{13}C]galactose in tissues of galactose-1-phosphate uridyl transferase deficient mice determined by nuclear magnetic resonance. Molecular Genetics and Metabolism 2007;90:42-48.

Wild S, Roglic G, Green A, Sicree R and King H. Global prevalence of diabetes - Estimates for the year 2000 and projections for 2030. Diabetes Care 2004;27:1047-1053.

Woerle HJ, Szoke E, Meyer C, Dostou JM, Wittlin SD, Gosmanov NR, Welle SL and Gerich JE. Mechanisms for abnormal postprandial glucose metabolism in type 2 diabetes. American Journal of Physiology-Endocrinology and Metabolism 2006;290:E67-E77.

Yang D, Beylot M, Agarwal KC, Soloviev MV and Brunengraber H. Assay of the human liver citric acid cycle probe phenylacetylglutamine and of phenylacetate in plasma by gas chromatography-mass spectrometry. Analytical Biochemistry 1993;212:277-282.

Yang D, Previs SF, Fernandez CA, Dugelay S, Soloviev MV, Hazey JW, Agarwal KC, Levine WC, David F, Rinaldo P, Beylot M and Brunengraber H. Noninvasive probing of citric acid cycle intermediates in primate liver with phenylacetylglutamine. American Journal of Physiology 1996;270:E882-E889.

Yu CL, Chen Y, Cline GW, Zhang DY, Zong HH, Wang YL, Bergeron R, Kim JK, Cushman SW, Cooney GJ, Atcheson B, White MF, Kraegen EW and Shulman GI. Mechanism by which fatty acids inhibit insulin activation of insulin receptor substrate-1 (IRS-1)-associated phosphatidylinositol 3-kinase activity in muscle. Journal of Biological Chemistry 2002;277:50230-50236.

Chapter 2

Sources of Hepatic Glycogen Synthesis Following a Mixed Breakfast Meal in Healthy Subjects

2.1 Objective 61

2.2 Materials and methods 61

2.2.1 Human studies 61

2.2.2 Sample processing 62

2.2.3 NMR spectroscopy 65

2.2.4 Urinary glucuronide, plasma glucose and plasma water enrichment analysis. 65

2.3 Metabolic model and calculations 66

2.4 Quantification of G6P-F6P and G6P-F6P-transaldolase exchanges with [U-$^{2}H_{7}$]glucose 68

2.5 Quantifying the sources of hepatic glycogen synthase flux 69

2.6 Results and discussion 72

2.6.1 Quantification of $G6P_{F6P}$ and $G6P_{TA}$ exchanges with [U-$^{2}H_{7}$]glucose 72

2.6.2 Enrichment of glucose and glucuronide from [1-^{13}C]glucose and $^{2}H_{2}O$ tracers 73

2.6.3 Sources of hepatic glycogen synthesis following a breakfast meal 76

2.6.4 Effects of galactose metabolism on direct and indirect pathway measurements with [1-^{13}C]glucose 77

2.6.5 Effects of G6P-F6P and transaldolase exchange on measurements of glycogen synthesis sources with $^{2}H_{2}O$ 78

2.6.6 Assessing dietary galactose contribution to hepatic glycogen synthesis with $^{2}H_{2}O$ 80

2.7 Conclusions 83

2.8 References 84

This Chapter is based on:
Barosa, C., Silva, C., Fagulha, A., Barros, L., Caldeira, M., Carvalheiro, M, and Jones, JG.
Sources of hepatic glycogen synthesis following a mixed breakfast meal in healthy subjects.
(submitted for publication).

2.1 Objective

The objectives of this study were to evaluate the deuterated water method (^2H_2O) for resolving the contribution of galactose from those of direct and indirect pathway fluxes following a breakfast meal that included milk. To this end, the completeness of hepatic glucose-6-phosphate-fructose-6-phosphate (G6P-F6P) exchange was quantified in this setting. Also, transaldolase (TA) exchange was quantified and its effect on direct and indirect pathway fractions obtained from the glucuronide $^2H5/^2H2$ ratio was evaluated. These estimates were compared with values obtained with the [1-^{13}C]glucose method (Bischof *et al.* 2002) which is insensitive to transaldolase exchange activity. Our studies revealed that hepatic G6P-F6P exchange was sufficiently complete for the quantification of galactose contributions to glycogen synthesis by the ^2H_2O method. However, direct and indirect pathway estimates derived from the glucuronide $^2H5/^2H2$ ratio were significantly distorted by transaldolase activity. Based on these findings, a combination of ^2H_2O and [1-^{13}C]glucose tracers is suggested for resolving galactose, direct and indirect pathway fluxes of hepatic glycogen synthesis.

2.2 Materials and methods

2.2.1 Human studies

Study protocols were approved by the Ethics Committees of the University Hospital of Coimbra and were performed after informed consent from the subjects. Six overnight-fasted healthy young subjects (gender: 4 males, 2 females; age: 21-24 years; BMI: 21.8-24.8 Kg/m^2) took breakfast (540 Kcal, 60% CHO/20% fat/20% protein containing 200 ml skimmed milk) at 08:00 the following morning. The CHO portion

included 10 grams of 50%-enriched [1-^{13}C]glucose. A $^{2}H_2O$ load divided in two doses at 01:00 and 03:00 was ingested to attain body water ^{2}H-enrichment of 0.3%. This enrichment was maintained throughout the study by providing drinking water enriched with 0.3% $^{2}H_2O$. 1000 mg of paracetamol were taken together with the breakfast meal. A 10 ml blood sample was drawn at 10:00 and a urine sample was collected between 10:00-12:00 and the study was finished. Measurements of G6P-F6P and F6P-transaldolase exchanges were performed in a different group of six healthy subjects that were age- and weight matched to the first group (1 male and 5 females; age: 23-25 years; BMI: 17.9.-24.3 Kg/m^2) where an identical breakfast meal was supplemented with 10 grams of glucose enriched to 30% with [U-$^{2}H_7$]glucose and two 200 mg peppermint oil capsules. Urine was collected between 10:00 and 12:00 for analysis of menthol glucuronide as previously described (Ribeiro *et al.* 2005; Delgado *et al.* 2009).

2.2.2 Sample processing

2.2.2.1 Blood samples

After being drawn, total blood was mixed with 1.5 volumes of cold 0.3 N $ZnSO_4$ followed by addition of 1.5 volumes of cold 0.3 N $Ba(OH)_2$. The mixture was centrifuged and the supernatant passed through two sequential columns, the first containing 20 ml of Dowex-50X8-200-H^+ ion-exchange resin and the second containing 10 ml of Amberlite. The eluate was evaporated to dryness at 37ºC then derivatized to monoacetone glucose (MAG). For that, a mixture of 5 ml of 2% deuterated acetone and 200 µl of 2% deuterated sulphuric acid was prepared and added to the dry glucose sample and the mixture was stirred for 18 hours. The acetonation reaction was quenched with 5 ml of water. To hydrolyze diacetone glucose to MAG, the solution pH was adjusted to 2.1-2.3 and the mixture was maintained at 40°C for 5 hours. The pH was then adjusted to 8-9 and the solution

evaporated until dryness. MAG was extracted from the residue with boiling ethyl acetate and the solvent was then evaporated. MAG from the residue was purified by solid phase extraction (SPE). After prewash with 3 ml acetonitrile (CH_3CN) followed by 10 ml of water, the sample dissolved in 200 µl of water was applied to the column. The sample vial was rinsed two times with 200 µl of water and applied to the column. The column was flushed with 1 ml of water and the hydrophilic impurities removed. MAG was eluted with 2 ml of 10% CH_3CN/90% H_2O. For ^{13}C NMR analysis the MAG residue was resuspended in 600 µl of 45% CH_3CN/45% C^2H_3CN/10% H_2O. For ^1H NMR analysis, the MAG residue was resuspended in 600 µl of 99.9% ^2H_2O.

2.2.2.2 Urine samples

Isolation and derivatization of paracetamol glucuronide to MAG was performed as previously described (Delgado *et al.* 2008). Urine was concentrated to 10% of its original volume and then mixed with 9 volumes of 100% ethanol for salt precipitation. After centrifugation, the supernatant was evaporated to approximately 10 ml, and the pH was adjusted to 8.0–9.0. The supernatant was applied to an 18 × 1 cm Dowex-1X8-200-acetate column. To remove salts and other metabolites, the column was washed with 35 ml of water, and the paracetamol glucuronide eluted with 35 ml of 10 M acetic acid. This fraction was evaporated to dryness at 40ºC. The residue was resuspended in 45 ml water and the pH adjusted to 4.5–5.0. Two thousand units of β-glucuronidase (*H. Pomatia*, Sigma Chemical, St. Louis, MO) were added and the solution was incubated at 40°C for 48-72 hours. Then, the solution containing the glucuronic acid obtained by hydrolysis, was passed through 10 ml Dowex-50X8-200-H^+ ion-exchange resin and evaporated to complete dryness at less than 40°C, resulting in the conversion of the glucuronic acid to monoacetoneglucuronolactone (MAGL) by adding a mixture of 5 ml of 2% deuterated acetone and 100 µl of 2% deuterated sulphuric acid and stirred for 24

hours (Jones *et al.* 2006a). 5 ml of water was added, the pH adjusted to 4.5-5.0 and evaporated to dryness at less than 40°C. MAGL was extracted with CH_3CN, and then evaporated. For derivatization of MAGL to MAG, the MAGL preparation was dissolved in 5 ml of tetrahydrofuran (THF) containing lithium borohydride ($LiBH_4$) at a proportion of 1mol of MAGL: 2 mol of $LiBH_4$. The mixture was stirred for 2 hours at 62ºC. 5 ml of water was added to quench the reaction and the mixture was then passed through 1 ml of Dowex-50X8-200-H^+ ion-exchange resin and evaporated to dryness at 40ºC. Borate was removed as a volatile methyl ester, by adding 5x10 ml of methanol and evaporating each portion successively. To the final extract, 1 ml of water was added, the pH adjusted to between 7 and 8 and the solution evaporated. MAG was extracted by the addition of boiling ethyl acetate and then evaporated. MAG was then purified by SPE as described and evaporated until dryness (Jones *et al.* 2006a). For ^{13}C NMR analysis, the MAG residue was dissolved in 600 µl of 45% CH_3CN/45% C^2H_3CN/10% H_2O. For ^2H analysis, the MAG residue was dissolved in 600 µl of 90% CH_3CN/10% H_2O and for ^1H NMR analysis, it was dissolved in 200 µl of 99.9% ^2H_2O. ^2H-enrichment of body water (BW) was quantified from the ^2H NMR analysis of urine as described (Jones *et al.* 2001).

For the studies of G6P-F6P and TA exchanges, where hepatic UDP-glucose was sampled as menthol glucuronide (Mendes *et al.* 2006; Delgado *et al.* 2009) urine samples were concentrated to final volumes of 10-20 ml, neutralized to pH 7.0 and centrifuged to remove salts and solids. The supernatant was acidified to pH 1.5 with 2M HCl, and applied to a 20 gram Isolute HM-N column. The column was washed with 80 ml diethyl ether and the ether fraction was evaporated. The residue was dissolved in 600 µl CH_3CN for ^2H NMR analysis.

2.2.3 NMR spectroscopy

Proton-decoupled ^{13}C NMR spectra were obtained with a Varian Unity 500 MHz NMR spectrometer equipped with a High Field Switchable Broadband 5 mm probe. Spectra were acquired with a 60° pulse angle, a sweep width of 200 ppm, an acquisition time of 1.5 sec, a pulse delay of 1.5 sec and a temperature of 25ºC. To determine if these conditions generated different intensities for the carbon 1 and 6 signals due to T_1 and NOE differences, unlabeled glucose was derivatized to MAG and natural abundance ^{13}C signal intensities were measured. The carbon 6 to carbon 1 signal ratio estimated from two samples ran at different times was 1.06 and hence on this basis, the carbon 1 to carbon 6 signal ratio was uncorrected.

Proton-decoupled ^{2}H NMR spectra were acquired with a Varian VNMRS 600 MHz NMR spectrometer equipped with a High Field Switchable Broadband 3 mm probe. Parameters included a 90º pulse angle, a sweep width of 10 ppm, an acquisition time of 1.6 sec, a pulse delay of 0.1 sec and a temperature of 50ºC. Field-frequency stability was maintained using the Varian SCOUT acquisition sequence. ^{1}H NMR spectra were acquired with the same spectrometer equipped with a High Field Indirect Detection 3 mm probe, a sweep width of 10 ppm, an acquisition time of 3.0 sec, a pulse delay of 0.1 sec and a temperature of 25ºC.

2.2.4 Urinary glucuronide, plasma glucose and plasma water enrichment analysis

Positional ^{13}C-enrichments of MAG derived from plasma glucose and urinary glucuronide were calculated from ^{13}C and ^{1}H NMR spectra. From the ^{13}C NMR spectra, relative ^{13}C-enrichments of positions 6 and 1 were measured from the corrected ratio of carbon 6 and carbon 1 ^{13}C signal intensities (C6/C1). Absolute ^{13}C-enrichment of position 1 was quantified from the ^{1}H NMR signals of MAG hydrogen 1. The

intensities of the ^{13}C-^{1}H spin-coupled signals (Int ^{13}C) and that of the ^{1}H central doublet signal representing ^{12}C-^{1}H (Int ^{12}C) were measured and the total ^{13}C-enrichment (%) of carbon 1 was calculated as 100 × Int ^{13}C/(Int ^{13}C + Int ^{12}C). Total carbon 6 enrichment was estimated as C6/C1 × total carbon 1 enrichment. Excess ^{13}C-enrichments of carbons 1 and 6 were calculated by subtracting 1.11 from their respective total ^{13}C-enrichments. ^{2}H-enrichments of MAG signals were determined using the intramolecular methyl signals as a reference. These methyl groups have a known ^{2}H-enrichment from the reaction of the glucose or glucurolactone with a known ^{2}H-enriched deuterated acetone and deuterated sulphuric acid. The areas of these deuterated methyl groups were then compared with those of the 1-6 signals of the MAG and the absolute positional enrichments determined (Nunes *et al.* 2009). All NMR spectra were analyzed using the curve-fitting routine supplied with the NUTS PC-based NMR spectral analysis program (Acorn NMR, Fremont CA).

2.3 Metabolic model and calculations

The metabolic model representing the sources of hepatic glycogen synthesis is depicted in Figure 2.1. Hepatic glycogen is assumed to be derived from three principal sources, namely glucose, gluconeogenic precursors and galactose. Glucose may be converted to glycogen *via* the classical direct pathway and also *via* the indirect pathway. The Cori cycle can be considered to be equivalent to the indirect pathway since it results in the transformation of glucose to hepatic G6P *via* pyruvate. Gluconeogenic substrates such as glycerol or anaplerotic amino acids may also contribute to glycogen synthesis since they can feed into the same pool of metabolic intermediates as those of the indirect pathway. Finally, galactose can also contribute to net UDP-glucose synthesis *via* the LeLoir pathway. In addition to glycogen synthase contributions, the model also includes several exchange reactions, including G6P-F6P exchange catalyzed

by glucose-6-phosphate isomerase, glucose-6-phosphate - glucose-1-phosphate (G6P-G1P) exchange catalyzed by phosphoglucomutase and exchange of F6P carbons 4-5-6 and glyceraldehyde-3-phosphate (G3P) catalyzed by TA.

The model is bound by the following assumptions: 1) absence of glycogen phosphorylase flux - i.e. no simultaneous synthesis and degradation of glycogen or "glycogen cycling", 2) complete exchange between G3P and dihydroxyacetone phosphate *via* triose phosphate isomerase and 3) negligible oxidative pentose phosphate pathway flux.

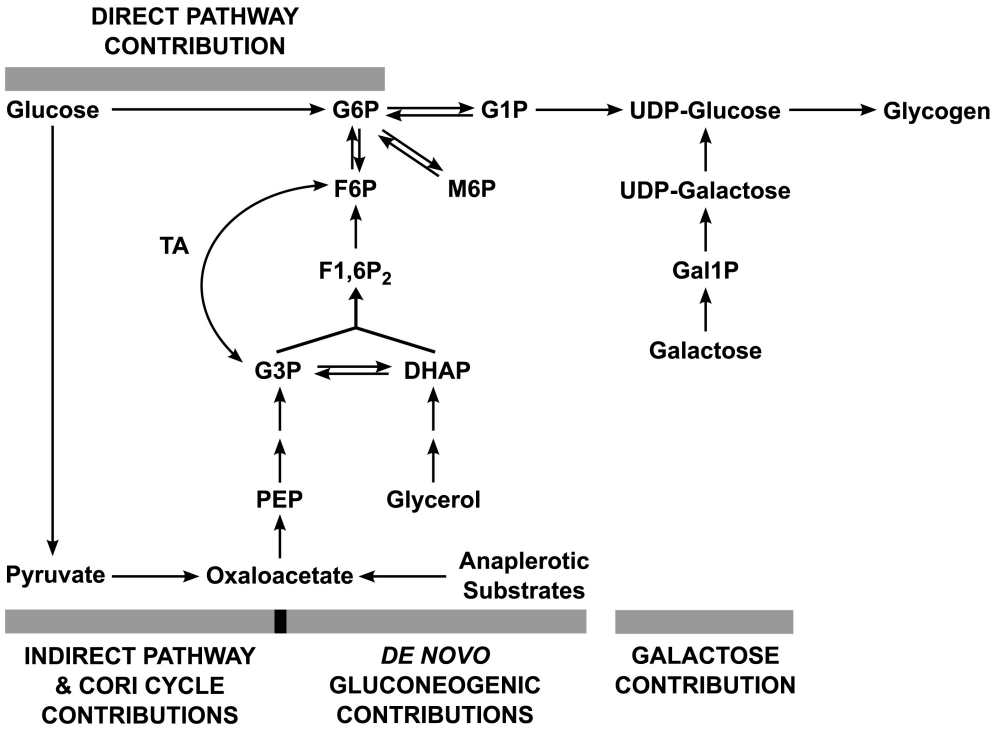

Figure 2.1: Metabolic scheme showing the principal sources and biochemical pathways involved in hepatic glycogen synthesis. Some intermediates have been omitted for clarity. Abbreviations are as follows: DHAP (dihydroxyacetone phosphate); F6P (fructose-6-phosphate); $F1,6P_2$ (fructose-1,6-bisphosphate); Gal1P (galactose-1-phosphate); G1P (glucose-1-phosphate); G6P (glucose-6-phosphate); G3P (glyceraldehydes-3-phosphate); M6P (mannose-6-phosphate); PEP (phosphoenolpyruvate); TA (transaldolase).

2.4 Quantification of G6P-F6P and G6P-F6P-transaldolase exchanges with [U-$^2H_7$]glucose

In order to correctly calculate the contributions of galactose and G6P sources (direct and indirect) to glycogen synthase flux with ^2H_2O, the extent of G6P-F6P and G6P-F6P-transaldolase exchanges must be known. It is assumed that indirect pathway metabolism of [U-$^2H_7$]glucose to G6P results in the complete loss of ^2H-enrichment to body water. Therefore the ^2H-enrichment distribution of glucuronide reflects exchanges that occurred during the direct pathway conversion of this tracer to glycogen. Position 3 enrichment is not influenced by any of the exchange mechanisms shown in Figure 2.2 (Delgado *et al.* 2009) whereas enrichment of the remaining positions may be diluted relative to that of position 3.

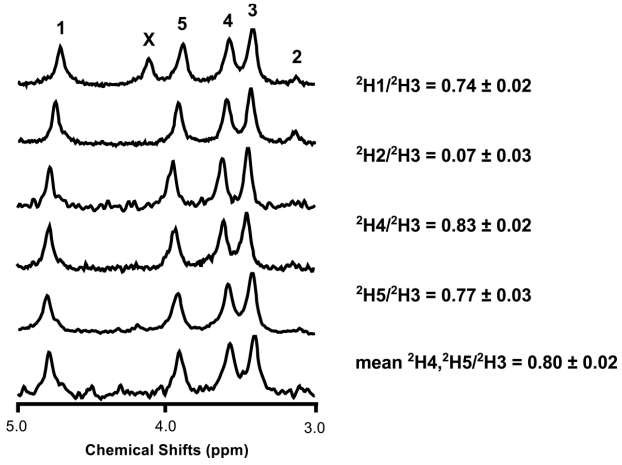

Figure 2.2: ^2H NMR spectra of menthol glucuronide obtained from the urine of six healthy subjects following ingestion of peppermint oil and a breakfast meal containing 10 grams of 30%-enriched [U-$^2H_7$]glucose. The numbers above each signal represents the position of the ^2H within the glucuronide hexose skeleton. Signal X is an impurity that is unrelated to menthol glucuronide. Also shown are the calculated ^2H-enrichment ratios of hydrogens 1, 2, 4 and 5 ($^2H1$, $^2H2$, $^2H4$, $^2H5$) to hydrogen 3 ($^2H3$) as well as that of the mean enrichments of hydrogens 4 and 5 to hydrogen 3 ($^2H4$, $^2H5$ mean/$^2H3$). Data are expressed as mean ± SEM.

Thus, the fraction of G6P molecules that participated in a particular exchange process can be determined from the ^{2}H-enrichment of the exchangeable hydrogen relative to that of position 3. For G6P-F6P exchange catalyzed by glucose-6-phosphate isomerase where hydrogen 2 of G6P is exchanged with that of water, the fraction of direct pathway G6P molecules participating in this process ($G6P_{F6P}$) was estimated as follows:

$$G6P_{F6P}\ (\%) = 100 \times [1-(^2H2/^2H3)] \quad (1)$$

where ^{2}H2/^{2}H3 is the ratio of position 2 to position 3 glucuronide ^{2}H-enrichment. The fraction of G6P that experienced TA-mediated exchange ($G6P_{TA}$) *via* isomerisation to F6P and exchange of F6P carbons 4-5-6 with G3P was estimated as follows:

$$G6P_{TA}\ (\%) = 100 \times (\text{mean } ^2H4,^2H5/^2H3) \quad (2)$$

where mean ^{2}H4,^{2}H5/^{2}H3 represents the mean ratio of positions 4 and 5 enrichment of glucuronide relative to position 3. Mean ratios were chosen over individual positional ratios (^{2}H4/^{2}H3 or ^{2}H5/^{2}H3) to give more confident estimates because of the proximity of ^{2}H4 and ^{2}H3 signals in the ^{2}H NMR spectrum of menthol glucuronide.

2.5 Quantifying the sources of hepatic glycogen synthase flux

Glycogen synthase flux is derived from net G6P and galactose fluxes into UDP-glucose and the fractional contributions of these fluxes (GS_{G6P} and GS_{Gal}) were estimated by the following equations:

$$GS_{G6P}\ (\%) = 100 \times H2/BW \div (Indirect_{corr} + (Direct_{corr} \times G6P_{F6P})) \quad (3)$$

where H2 is the enrichment of glucuronide position 2, BW is the enrichment of body water, $G6P_{F6P}$ is the fraction of direct pathway G6P that exchanged with F6P as determined by equation (1) and $Indirect_{corr}$ and $Direct_{corr}$ are corrected direct and indirect pathway fractions derived from ^{2}H enrichments in positions 5 and 2 and adjusted for $G6P_{F6P}$ and TA exchanges (see equations (10) and (11)). Inclusion of direct and indirect pathway terms in equation (3) reflects the fact that G6P is derived from both direct and indirect pathways, but only G6P formed *via* the direct pathway is dependent on G6P-F6P exchange for enrichment in position 2 while G6P derived *via* the indirect pathway is enriched to the same level as body water. When $G6P_{F6P}$ approaches 100%, as was the case for this study, equation (3) approximates to the following:

$$GS_{G6P}\ (\%) = 100 \times H2/BW \quad (4)$$

The balance represents the glycogen synthase flux contribution from galactose (GS_{Gal}).

$$GS_{Gal}\ (\%) = 100 - GS_{G6P} \quad (5)$$

G6P is derived from direct pathway, indirect pathway and *de novo* gluconeogenic contributions. The direct pathway contribution to glycogen synthesis ($G6P_{Direct}$) was estimated from the ^{13}C-excess enrichments of glucuronide and glucose from the meal [1-^{13}C]glucose tracer according to Shulman *et al.* (Shulman *et al.* 1990) with correction for the fractional contribution of G6P flux to glycogen synthesis as follows:

$$G6P_{Direct}\ (\%) = 100 \times ((C1 - C6)_{glucur}/(C1 - C6)_{gluc}) \times 100/GS_{G6P} \quad (6)$$

where (C1− C6)*glucur* is the difference between carbon 1 and carbon 6 excess ^{13}C-enrichment of glucuronide, (C1 − C6)*gluc* is the difference between carbon 1 and carbon 6 excess ^{13}C-enrichment of plasma glucose. The indirect pathway and *de novo* gluconeogenic contributions cannot be distinguished from each other and are therefore represented as the balance of glycogenic G6P flux ($G6P_{Indirect}$).

$$G6P_{Indirect}\ (\%) = GS_{G6P} - G6P_{Direct} \quad (7)$$

Direct and indirect pathway fractions were also independently calculated from the ratio of glucuronide positions 5 and 2 enrichments ($^2H5/^2H2$) from ^2H_2O as previously described (Jones *et al.* 2006b; Soares *et al.* 2009). With incomplete G6P-F6P exchange, a fraction of G6P derived *via* the direct pathway is not enriched in position 2 and is therefore not represented by the $^2H5/^2H2$ ratio. Therefore, direct and indirect pathway contributions were adjusted for this non-exchanged fraction as follows:

Indirect pathway fraction = $^2H5/^2H2$

Direct pathway, exchanged fraction = 1− ($^2H5/^2H2$)

Direct pathway, non-exchanged fraction = $((100/G6P_{F6P})-1)\times$ exchanged fraction

Total Direct pathway fraction ($Direct_{total}$) = exchanged + non-exchanged fractions

Direct Pathway (%) = $100 \times (Direct_{total}/(Direct_{total} + \text{Indirect pathway fraction})$ (8)

Indirect Pathway (%) = 100 − Direct Pathway (9)

When the fraction of G6P undergoing TA exchange ($G6P_{TA}$) is known, direct and indirect pathway estimates calculated by equations (8) and (9) may be corrected as described by (Basu *et al.* 2010).

Corrected Direct Pathway (%) = Direct pathway $\times$ $((G6P_{TA}/100) + 1)$ (10)

Corrected Indirect Pathway (%) = 100 − Corrected Direct Pathway (11)

2.6 Results and discussion

2.6.1 Quantification of $G6P_{F6P}$ and $G6P_{TA}$ exchanges with [U-$^2H_7$]glucose

Figure 2.2 shows spectra obtained from six healthy subjects following ingestion of a meal enriched with [U-$^2H_7$]glucose. The position 2 hydrogen of G6P is well known to be metabolically highly labile as a result of extensive G6P-F6P equilibration *via* glucose-6-phosphate isomerase. As expected, enrichment of this position was highly depleted, with only 7 ± 3% of ^{2}H-enrichment retained relative to that of position 3. This indicates that the fraction of G6P derived from the direct pathway that experienced G6P-F6P exchange ($G6P_{F6P}$) was 93 ± 3%. Since ~70% G6P is derived *via* the direct pathway and ~30% from the indirect pathway - which is fully equilibrated with BW – position 2 enrichment of the total glycogenic G6P pool is ~95% of BW levels.

Enrichment of glucose position 1 was also significantly depleted relative to position 3 and this can be attributed to exchange between G6P and mannose-6-phosphate (M6P) (Chandramouli *et al.* 1999). The retention of 74 ± 2% enrichment in position 1 relative to position 3 means that 26 ± 2% of G6P underwent exchange with M6P – a similar fraction to that observed by Chandramouli *et al.* in healthy subjects after 15 hours fasting (Chandramouli *et al.* 1999). Enrichment of positions 4 and 5 were also significantly smaller than that of position 3, with their mean enrichments being 80 ± 2% that of position 3. This is best explained by G6P-F6P-TA exchange activity. By this mechanism, positions 4, 5 and 6 of F6P that was generated from [U-$^2H_7$]glucose are exchanged with unlabeled G3P, resulting in a dilution of enrichment in these positions relative to position 3 (Delgado *et al.* 2009). On this basis, the fraction of glycogenic G6P that underwent TA exchange ($G6P_{TA}$) was estimated to be 20 ± 2%. This is similar to the 20% estimate reported after an oral glucose tolerance test using the same

methodology (Delgado *et al.* 2009), a 25% estimate based on glucuronide ^{13}C-enrichment analysis following a cornstarch meal enriched with [U-^{13}C]glycerol (Jones *et al.* 2008) and 25-33% during an euglycemic clamp (Bock *et al.* 2008).

In summary, these experiments demonstrate that hepatic G6P derived from labeled glucose provided as part of a meal undergoes almost complete exchange of hydrogen 2 with BW. Furthermore, 20% of G6P molecules exchanged their 4-5-6-triose moieties with G3P *via* TA. These results have important implications in estimating postprandial hepatic glycogen synthesis sources with both labeled glucose and labeled water tracers.

2.6.2 Enrichment of glucose and glucuronide from [1-^{13}C]glucose and ^2H_2O tracers

As shown by the representative ^2H and ^{13}C NMR spectra of Figure 2.3, glucose and glucuronide ^{13}C and ^2H-enrichments were well characterized by ^{13}C and ^2H NMR spectroscopy of their MAG derivatives. Table 2.1 shows the enrichment of BW and glucose metabolites for the group of subjects that received the breakfast meal accompanied by [1-^{13}C]glucose and ^2H_2O tracers. The BW ^2H-enrichment as measured by urine water analysis attained the theoretical value of 0.3%. Enrichment of glucuronide position 2 was significantly lower than that of BW. Based on the G6P-F6P exchange estimates from the [U-$^2H_7$]glucose studies, enrichment of position 2 should have approached that of BW[1]. Therefore, the difference between position 2 enrichment and BW is attributable to dilution from galactose-derived UDP-glucose.

[1] Assuming a direct pathway contribution of 72% and G6P-F6P exchange being 7% incomplete, the total fraction of glycogenic G6P that did not incorporate ^2H in position 2 *via* exchange with F6P is 5.0% (G6P derived *via* the indirect pathway fraction is fully enriched in position 2).

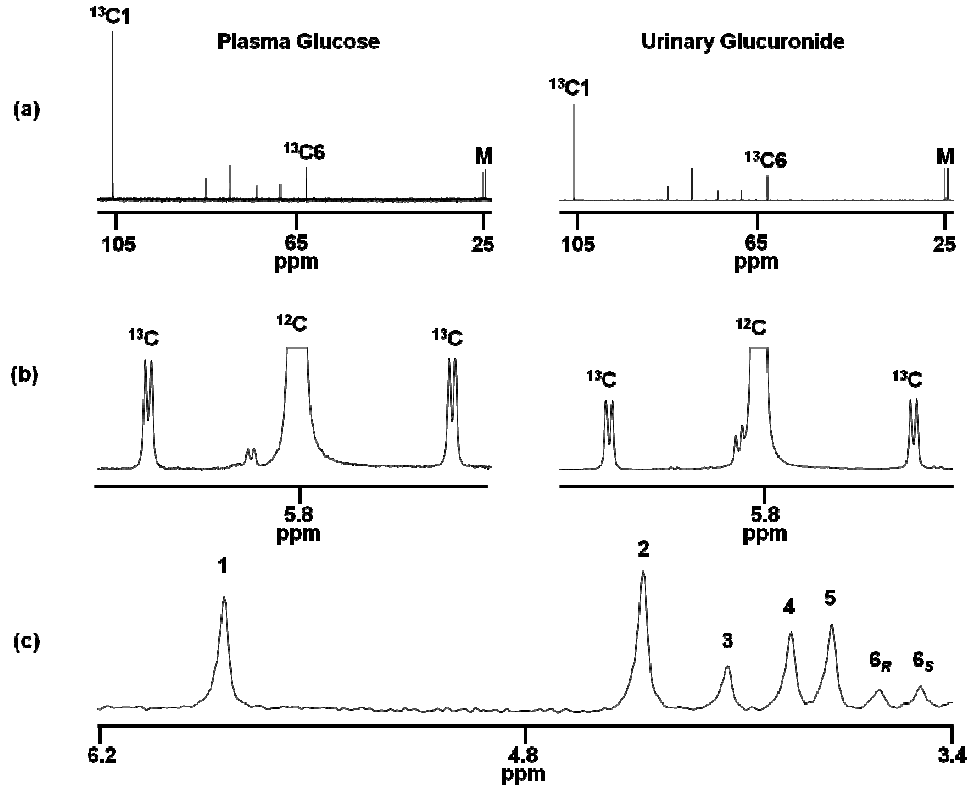

Figure 2.3: (a) ^{13}C NMR spectra of MAG derived from plasma glucose and urinary paracetamol glucuronide showing the carbon 1 and carbon 6 signals ($^{13}C1$ and $^{13}C6$) and scaled to the natural-abundance MAG methyl signals (M); **(b)** ^{1}H NMR signals of position 1 for the same MAG samples with equivalent scaling and showing the ^{12}C-^{1}H center signal (truncated to fit) and ^{13}C-^{1}H satellites and **(c)** the ^{2}H NMR spectrum of the MAG sample derived from urinary glucuronide The numbers above each signal represents the position of the ^{2}H isotope within the hexose skeleton.

Enrichment of the remaining positions was significantly less than that of position 2, consistent with the dilution of these gluconeogenic markers by direct pathway flux (Jones *et al.* 2006b). Their enrichment distribution showed a reciprocal relationship with the distribution observed from [U-$^{2}H_7$]glucose, i.e. sites that were most depleted of ^{2}H-enrichment from [U-$^{2}H_7$]glucose (positions 1, 4 and 5) had the highest enrichment from $^{2}H_2O$ whereas position 3 - the most highly enriched site from [U-$^{2}H_7$]glucose - was the least enriched from $^{2}H_2O$. These observations are

consistent with TA and M6P exchange activities that contribute to G6P ^{2}H-enrichment from $^{2}H_2O$ independently of gluconeogenic or indirect pathway fluxes.

Table 2.1: Plasma glucose and glucuronide ^{13}C and ^{2}H enrichments following $^{2}H_2O$ administration and ingestion of a meal enriched with [1-^{13}C]glucose. Urine water ^{2}H-enrichment (representing BW) is also shown.

	^{2}H Excess Enrichment (%)						^{13}C Excess Enrichment (%)			
Subject	Urine Water	Glucuronide 1	Glucuronide 2	Glucuronide 3	Glucuronide 4	Glucuronide 5	Glucose 1	Glucose 6	Glucuronide 1	Glucuronide 6
1	0.24	0.14	0.17	0.04	0.10	0.09	2.85	-0.01	1.50	-0.12
2	0.30	0.12	0.24	0.04	0.10	0.11	3.82	0.09	1.98	-0.02
3	0.24	0.15	0.20	0.03	0.09	0.10	2.82	-0.08	1.71	-0.05
4	0.23	0.09	0.17	0.03	0.05	0.08	3.54	0.00	3.22	0.00
5	0.29	0.13	0.19	0.02	0.07	0.06	3.66	0.08	1.36	-0.05
6	0.30	0.13	0.22	0.02	0.09	0.10	4.69	-0.02	2.32	-0.01
Mean	0.27	0.13	0.20**	0.03	0.08	0.09	3.36	0.01	1.84	-0.04
SEM	0.03	0.02	0.03	0.01	0.02	0.02	0.86	0.05	0.38	0.03

** Significantly less than urine water, $p < 0.05$.

Enrichment of plasma glucose and glucuronide from [1-^{13}C]glucose revealed significant excess enrichment in the carbon 1 sites of both metabolites. Significant excess ^{13}C-enrichments of the remaining carbons, including carbon 6, were not detected. Previous studies where plasma [1-^{13}C]glucose excess enrichment was

maintained at 5-7% during a hyperglycemic clamp reported low excess ^{13}C-enrichments (≤ 0.1%) in glucuronide and glucose carbon 6 sites (Shulman *et al.* 1990). This study protocol resulted in plasma glucose precursor excess enrichments that were about one-half that reported by Shulman *et al.* (Shulman *et al.* 1990) therefore the negligible glucuronide and glucose C6 excess enrichments that were observed are in accord with these previous studies. Consequently, direct and indirect pathway contributions determined from glucuronide and glucose C1 enrichments yielded identical values to those estimated with both C1 and C6 enrichment data (68 ± 4% and 32 ± 4%, respectively). C1 enrichment data are directly obtainable from ^{1}H NMR analysis of glucose and glucuronide-derived MAG, as shown in Figure 2.3(b). Compared to ^{13}C-direct detection, the ^{1}H NMR measurement has much greater sensitivity and sampling times are reduced from several hours to a few minutes with standard indirect-detection probes.

2.6.3 Sources of hepatic glycogen synthesis following a breakfast meal

The principal sources of glycogen synthase flux identified from the analysis of plasma glucose and glucuronide ^{13}C-enrichments from [1-^{13}C]glucose and enrichment of glucuronide position 2 and body water from $^{2}H_2O$ (see Table 2.1) are shown in Table 2.2. Approximately 1/5th of total glycogen synthase flux was sustained by hexose units that were unlabeled with either ^{13}C or ^{2}H. These are presumed to be derived from galactose following hydrolysis of lactose from the milk component of the breakfast meal. Of the remaining proportion derived *via* hepatic G6P, the direct pathway contribution was dominant, accounting for 72 ± 4% of glycogenic G6P flux. Meanwhile, indirect pathway and gluconeogenic sources contributed a minority of G6P and glycogen synthase fluxes. With the exception of Subject 4, who presented a remarkably high direct pathway contribution combined with a residual galactose

input, the contributions of galactose and direct and indirect pathway G6P fluxes were quite consistent for the remaining subjects.

Table 2.2: Fractional contributions of galactose and G6P sources (G6P-Total) to hepatic glycogen synthase flux in healthy subjects following a breakfast meal. G6P sources are resolved into direct (G6P-Direct) and indirect pathway and gluconeogenic contributions (G6P-Indirect). The corresponding equations used to derive these estimates are also indicated.

Subject	Galactose Equation (3)	G6P-Total Equation (4)	G6P-Direct Equation (6)	G6P-Indirect Equation (7)
1	25	75	57	18
2	16	84	54	31
3	12	88	61	27
4	8	92	91	1
5	31	69	39	30
6	23	77	49	28
Mean	19	81	58	22
SEM	3	3	5	4

2.6.4 Effects of galactose metabolism on direct and indirect pathway measurements with [1-^{13}C]glucose

The conversion of galactose to glycogen modifies direct and indirect pathway estimates derived using [1-^{13}C]glucose due to dilution of UDP-glucose ^{13}C-enrichment. As a result, the effect of galactose metabolism is to increase the apparent indirect pathway fraction and decrease the direct pathway contribution. In the present

study, the direct pathway contribution that was calculated solely from the ^{13}C-enrichment data and therefore uncorrected for galactose metabolism, tended to report lower values (58 ± 5%, $p = 0.19$ *versus* corrected values).

2.6.5 Effects of G6P-F6P and transaldolase exchange on measurements of glycogen synthesis sources with ^2H_2O

The use of ^2H_2O for characterizing glycogen synthesis pathways in humans is attractive since this inexpensive tracer is easily administered, requires only urine samples for analysis, and potentially resolves the contributions of galactose, direct and indirect pathways to glycogen synthesis. As a stand-alone method for determining these parameters, the ^2H_2O method relies on assumptions regarding G6P exchange. The galactose contribution is determined from the glucuronide position 2 ^2H-enrichment relative to that of BW with adjustment for incomplete G6P-F6P exchange (see equations (3) and (4) in the Methods section). When G6P-F6P exchange was not accounted for, (i.e. G6P and galactose contributions were calculate using the simplified form of equation (3) shown in the methods) the estimated galactose contribution was modestly higher (23 ± 3% *versus* 19 ± 3%, $p = 0.42$).

For quantifying direct and indirect pathway contributions to glycogenic G6P flux by the $^2H5/^2H2$ ratio, the ^2H_2O method is bound by two assumptions that do not apply to measurements based on [1-^{13}C]glucose. The first assumption is that G6P-F6P exchange is complete resulting in the equivalent enrichment of G6P position 2 and BW. The second assumption is that position 5 enrichment of G6P is solely attributable to indirect pathway and/or gluconeogenic contributions. This second assumption has recently been questioned on the basis that TA-mediated exchange of F6P and G3P may enrich position 5 independently of gluconeogenic activity (Bock *et al.* 2008; Basu *et al.* 2009). By quantifying $G6P_{F6P}$ and $G6P_{TA}$ under these conditions, it was possible to determine their effect on direct and indirect pathway estimates from ^2H_2O.

Estimation of direct and indirect pathways from the $^{2}H5/^{2}H2$ ratio without any corrections for exchanges yielded a direct pathway estimate of 51 ± 3% and an indirect pathway estimate of 49 ± 3%. These values are consistent with previous $^{2}H5/^{2}H2$ estimates from healthy subjects under similar conditions (Jones *et al.* 2006b). They are also significantly different to direct and indirect pathway fractions derived from the [1-^{13}C]glucose tracer, as shown in Figure 2.4. After adjusting for the observed $G6P_{F6P}$ of 93%, direct and indirect pathway contributions were calculated to be 53 ± 3% and 47 ± 3% respectively.

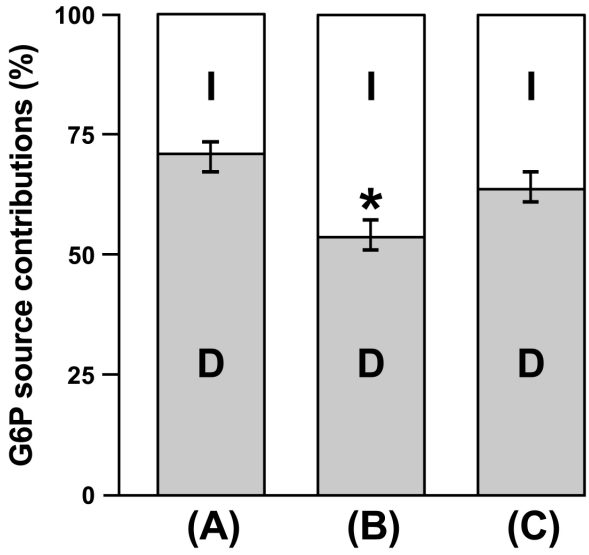

Figure 2.4: Comparison of direct (D) and indirect (I) pathway contributions to hepatic glucose-6-phosphate flux in healthy subjects by [1-^{13}C]glucose and $^{2}H_2O$ tracer methods. The percentage of glucose-6-phosphate derived *via* direct pathway is indicated by the shaded portion and that from the indirect pathway and gluconeogenesis is indicated by the unshaded portion. Column **(A)** shows estimates obtained with [1-^{13}C]glucose, column **(B)** shows estimates obtained with $^{2}H_2O$ with no correction for transaldolase exchange and column **(C)** shows estimates obtained with $^{2}H_2O$ after correction for transaldolase exchange. Error bars indicate the standard error of the mean. * (significantly different from (A), $p < 0.05$).

Thus, correction for G6P-F6P exchange did not substantially modify the direct pathway fraction and it remained significantly lower than that derived from [1-^{13}C]glucose (53 ± 3% *versus* 72 ± 4% , $p < 0.05$). When adjusted for TA exchange activity ($G6P_{TA}$) of 20%, direct pathway estimates tended to be higher compared to uncorrected values (62 ± 4% *versus* 51 ± 3%, $p = 0.15$). After adjusting for both $G6P_{F6P}$ and $G6P_{TA}$, the direct pathway fraction was 64 ± 4% ($p = 0.09$ compared to the uncorrected value) and in fair agreement with the estimate derived from [1-^{13}C]glucose, (Figure 2.4).

In conclusion, G6P-F6P exchange approached completeness hence corrections for incomplete G6P-F6P exchange had relatively minor effects on galactose and direct/indirect pathway estimates. However, the level of TA exchange measured under the study conditions required more substantial corrections for direct and indirect pathway contributions based on the ^{2}H5/^{2}H2. When these exchanges were accounted for, direct and indirect pathway fractions obtained with $^{2}H_2O$ were in reasonable agreement with those obtained with [1-^{13}C]glucose.

2.6.6 Assessing dietary galactose contribution to hepatic glycogen synthesis with $^{2}H_2O$

The $^{2}H_2O$ method was applied to determine the contribution of dietary galactose to hepatic glycogen synthesis following a breakfast meal containing a standard 200 ml portion of skimmed milk. The assay was based on measuring the enrichments of glucuronide position 2 and BW by ^{2}H NMR. The analytical precision is principally limited by the signal-to-noise (SNR) ratio of the glucuronide and BW ^{2}H NMR signals. For BW assays, SNR of 100:1 or higher for the acetone and water signals, while the glucuronide position 2 SNR´s were 30:1 or higher. A 30:1 SNR translates to a 3.33% uncertainty in the signal quantification that is attributable to the

baseline noise. In this experimental setting, where the position 2 signal intensity represented ~0.20% enrichment, this translates to an uncertainty of ± 0.007%.

The other main uncertainty of the ^2H_2O method is the assumption of complete hepatic G6P-F6P exchange. In this study, G6P-F6P exchange approached completion, but this may not be the case for different human nutritional or pathophysiological states, or for hepatic metabolism in other species. In a study of glycogen synthesis in humans infused with a glucose load and administered with ^2H_2O, G6P-F6P exchange was reported to be only 80% complete based on the values of glucuronide position 2 and BW ^2H-enrichments (Stingl *et al.* 2006). After an oral glucose tolerance test, direct pathway G6P-F6P exchange measured by the [U-$^2H_7$]glucose method was 90 ± 2% (Delgado *et al.* 2009). In fasted rats, hepatic G6P-F6P exchange after a glucose load was estimated to be only 85% complete from analysis of hepatic glycogen position 2 ^2H-enrichment from ^2H_2O (Soares *et al.* 2010). This measurement was not a direct assay of G6P-F6P exchange and required assumptions for residual hepatic glycogen levels prior to the glucose load (Soares *et al.* 2010). In principle, analysis of hepatic glycogen enrichment from [U-$^2H_7$]glucose can be applied to determine direct pathway G6P-F6P and TA exchanges in rodent and other animal models. These reports indicate that for confident assessment of glycogenic galactose utilization by the ^2H_2O method, G6P-F6P exchange needs to be verified for a particular study condition, preferably by a direct method such as the [U-$^2H_7$]glucose assay.

The results indicate that 20% of glycogenic flux was derived from galactose under these conditions. In healthy subjects, cumulative hepatic glycogen synthesis over a 4 hour period after a breakfast meal was estimated to be 28 grams (Taylor *et al.* 1996). Based on this, a galactose contribution of 20% amounts to approximately 6 grams of galactose. A 200 ml portion of reduced fat milk contains about 11 grams of lactose or 5.5 grams of galactose. Therefore, the estimates of absolute galactose contribution to glycogen synthesis closely match the amount of available galactose

from the meal. This suggests that under these conditions, essentially all of the milk galactose was recruited into hepatic glycogen. Galactose uptake and metabolism has been studied in detail with stable-isotope galactose tracers. Galactose may contribute to either hepatic glycogen or glucose synthesis. The destination of administered galactose is highly dependent on whether it is administered alone or if it is accompanied by glucose. When a galactose load is administered during the basal fasting state, a substantial fraction is converted to glucose *via* the glycogenolytic pathway (Fried *et al.* 1996; Gannon *et al.* 2001; Staehr *et al.* 2007), this fraction being higher with larger galactose loads (Sunehag *et al.* 2002). In addition, its splanchnic extraction is relatively inefficient resulting in increased blood galactose levels (Sunehag *et al.* 2002). When the galactose is co-administered with glucose, its metabolic fate is markedly altered. Both absolute and fractional splanchnic extraction rates are significantly enhanced while its appearance in plasma glucose *via* the hepatic glycogenolytic pathway is sharply reduced (Sunehag *et al.* 2002). These observations are consistent with the efficient conversion of galactose to hepatic glycogen in the presence of glucose and also support the conclusion that dietary galactose derived from lactose, and therefore accompanied by an equivalent of glucose, is also efficiently converted to glycogen.

The sensitivity of hepatic galactose metabolism to co-administered glucose highlights the potential uncertainties in inferring the glycogenic potential of dietary galactose using galactose tracers. By accounting for the true meal-derived galactose inflow into UDP-glucose, the $^{2}H_{2}O$ method may provide clearer insights into the contribution of dietary galactose to hepatic glycogen synthesis.

2.7 Conclusions

A meal that contains milk or other dairy products can provide a significant amount of galactose for hepatic glycogen synthesis. This galactose contribution is not easily traceable by classical precursor-product methods that rely on ingestion or infusion of labeled galactose. In the presence of $^{2}H_2O$, essentially all glycogen hexose precursors are enriched in position 2 to the same level as BW - with the exception of galactose, hence the galactose contribution can be assessed in a simple manner by comparing glucuronide position 2 and BW enrichments. With appropriate corrections for TA-mediated exchange, the $^{2}H_2O$ method also provides estimates direct and indirect pathway contributions to glycogen synthesis thereby allowing a more comprehensive assessment of hepatic glycogen sources from mixed meals.

These studies revealed that hepatic G6P-F6P exchange was sufficiently complete for the quantification of galactose contributions to glycogen synthesis by the $^{2}H_2O$ method. However, direct and indirect pathway estimates derived from the glucuronide $^{2}H5/^{2}H2$ ratio were significantly distorted by TA activity. Based on these findings, a combination of $^{2}H_2O$ and [1-^{13}C]glucose tracers is suggested for resolving galactose, direct and indirect pathway fluxes of hepatic glycogen synthesis.

2.8 References

Basu R, Barosa, C., Basu, A., Pattan, V., Saad, A., Jones, J. and Rizza, R. Transaldolase exchange and its effects on measurements of gluconeogenesis in humans. American Journal of Physiology-Endocrinology and Metabolism 2011; 300:E296-303.

Basu R, Chandramouli V, Schumann W, Basu A, Landau BR and Rizza RA. Additional evidence that transaldolase exchange, isotope discrimination during the triose-isomerase reaction, or both occur in humans effects of type 2 diabetes. Diabetes 2009;58:1539-1543.

Bischof MG, Bernroider E, Krssak M, Krebs M, Stingl H, Nowotny P, Yu C, Shulman GI, Waldhausl W and Roden M. Hepatic glycogen metabolism in type 1 diabetes after long-term near normoglycemia. Diabetes 2002;51:49-54.

Bock G, Schumann WC, Basu R, Burgess SC, Yan Z, Chandramouli V, Rizza RA and Landau BR. Evidence that processes other than gluconeogenesis may influence the ratio of deuterium on the fifth and third carbons of glucose - implications for the use of $^{2}H_2O$ to measure gluconeogenesis in humans. Diabetes 2008;57:50-55.

Chandramouli V, Ekberg K, Schumann WC, Wahren J and Landau BR. Origins of the hydrogen bound to carbon 1 of glucose in fasting: significance in gluconeogenesis quantitation. American Journal of Physiology 1999;277:E717-723.

Delgado TC, Barosa C, Castro M, Geraldes C, Bastos M, Baptista C, Fagulha A, Barros L, Mota A, Carvalheiro M, Jones JG and Merritt M. Sources of hepatic glucose production by $^{2}H_2O$ ingestion and Bayesian analysis of ^{2}H-glucuronide enrichment. Magnetic Resonance in Medicine 2008;60:517-523.

Delgado TC, Silva C, Fernandes I, Caldeira M, Bastos M, Baptista C, Carvalheiro M, Geraldes C and Jones JG. Sources of hepatic glycogen synthesis during an oral glucose tolerance test: effect of transaldolase exchange on flux estimates. Magnetic Resonance in Medicine 2009;62:1120-1128.

Fried R, Beckmann N, Keller U, Ninnis R, Stalder G and Seelig J. Early glycogenolysis and late glycogenesis in human liver after intravenous administration of galactose. American Journal of Physiology-Gastrointestinal and Liver Physiology 1996; 270:G14-G19.

Gannon MC, Khan MA and Nuttall FQ. Glucose appearance rate after the ingestion of galactose. Metabolism-Clinical and Experimental 2001;50:93-98.

Jones JG, Barosa C, Gomes F, Mendes AC, Delgado TC, Diogo L, Garcia P, Bastos M, Barros L, Fagulha A, Baptista C, Carvalheiro M and Caldeira MM. NMR derivatives for quantification of ^{2}H.and ^{13}C-enrichment of human glucuronide from metabolic tracers. Journal of Carbohydrate Chemistry 2006a;25:203-217.

Jones JG, Fagulha A, Barosa C, Bastos M, Barros L, Baptista C, Caldeira MM and Carvalheiro M. Noninvasive analysis of hepatic glycogen kinetics before and after breakfast with deuterated water and acetaminophen. Diabetes 2006b;55:2294-2300.

Jones JG, Garcia P, Barosa C, Delgado TC, Caldeira MM and Diogo L. Quantification of hepatic transaldolase exchange activity and its effects on tracer measurements of indirect pathway flux in humans. Magnetic Resonance in Medicine 2008;59:423-429.

Jones JG, Merritt, M. and Malloy, C.R. Quantifying tracer levels of $^{2}H_2O$ enrichment from microliter amounts of plasma and urine by ^{2}H NMR. Magnetic Resonance in Medicine 2001;45:156-158.

Mendes AC, Caldeira MM, Silva C, Burgess SC, Merritt ME, Gomes F, Barosa C, Delgado TC, Franco F, Monteiro P, Providencia L and Jones JG. Hepatic UDP-glucose ^{13}C-isotopomers from [U-^{13}C]glucose: A simple analysis by ^{13}C NMR of urinary menthol glucuronide. Magnetic Resonance in Medicine 2006;56:1121-1125.

Nunes PM and Jones JG. Quantifying endogenous glucose production and contributing source fluxes from a single ^{2}H NMR spectrum. Magnetic Resonance in Medicine 2009;62:802-807.

Ribeiro A, Caldeira MM, Carvalheiro M, Bastos M, Baptista C, Fagulha A, Barros L, Barosa C and Jones JG. Simple measurement of gluconeogenesis by direct ^{2}H NMR analysis of menthol glucuronide enrichment from $^{2}H_2O$. Magnetic Resonance in Medicine 2005;54:429-434.

Shulman GI, Cline G, Schumann WC, Chandramouli V, Kumaran K and Landau BR. Quantitative comparison of pathways of hepatic glycogen repletion in fed and fasted humans. American Journal of Physiology 1990;259:E335-E341.

Soares AF, Carvalho RA, Veiga FJ and Jones JG. Effects of galactose on direct and indirect pathway estimates of hepatic glycogen synthesis. Metabolic Engineering 2010;12:552-560.

Soares AF, Veiga FJ, Carvalho RA and Jones JG. Quantifying hepatic glycogen synthesis by direct and indirect pathways in rats under normal ad libitum feeding conditions. Magnetic Resonance in Medicine 2009;6:1-5.

Staehr P, Hother-Nielsen O, Beck-Nielsen H, Roden M, Stingl H, Holst JJ, Jones PK, Chandramouli V and Landau BR. Hepatic autoregulation: response of glucose production and gluconeogenesis to increased glycogenolysis. American Journal of Physiology-Endocrinology and Metabolism 2007;292:E1265-E1269.

Stingl H, Chandramouli V, Schumann WC, Brehm A, Nowotny P, Waldhausl W, Landau BR and Roden M. Changes in hepatic glycogen cycling during a glucose load in healthy humans. Diabetologia 2006;V49:360-368.

Sunehag AL and Haymond MW. Splanchnic galactose extraction is regulated by coingestion of glucose in humans. Metabolism-Clinical and Experimental 2002;51:827-832.

Taylor R, Magnusson I, Rothman DL, Cline GW, Caumo A, Cobelli C and Shulman GI. Direct assessment of liver glycogen storage by ^{13}C Nuclear Magnetic Resonance spectroscopy and regulation of glucose homeostasis after a mixed meal in normal subjects. Journal of Clinical Investigation 1996;97:126-132.

Chapter 3

Significant Transaldolase Exchange Activity in Human Liver:

Implications for Deuterated Water Measurements of Gluconeogenesis

3.1 Objective 93

3.2 Materials and methods 94

3.2.1 Human studies 94

3.2.2 Sample processing 96

3.3 NMR spectroscopy 97

3.3.1 Carbon-13 and proton NMR spectroscopy 97

3.3.2 Deuterium NMR spectroscopy 98

3.4 Metabolic model and calculations 99

3.5 Statistical analysis 100

3.6 Results 100

3.6.1 Comparison of plasma glucose and urinary glucuronide ^{13}C-enrichments from [1-^{13}C]acetate 100

3.6.2 Comparison of plasma glucose and urinary glucuronide ^{2}H-enrichments from $^{2}H_2O$ 103

3.6.3 Correction of position 5 enrichment for transaldolase activity and effects on estimates of gluconeogenic contribution to EGP 104

3.6.4 Relationship between position 3 and the corrected position 5 enrichments of glucose and glucuronide 105

3.7 Discussion 107

3.8 Conclusions 109

3.9 References 111

Part of the work described in this Chapter is included in the following publication:

Basu R, Barosa, C., Basu, A., Pattan, V., Saad, A., Jones, J. and Rizza, R. Transaldolase exchange and its effects on measurements of gluconeogenesis in humans. American Journal of Physiology-Endocrinology and Metabolism 2011;300:E296-303.

3.1 Objective

The deuterated water (^2H_2O) method is extensively used to measure gluconeogenesis in humans. This method assumes negligible exchange of the lower three carbons of fructose-6-phosphate (F6P) with glyceraldeyde-3-phosphate (G3P) *via* transaldolase (TA) activity. As a result, in presence of ^{2}H-enriched body water (BW) the deuterium label from G3P is transferred to position 5 of unlabeled F6P derived from glycogenolysis. This occurs independently of gluconeogenic activity. Therefore, glucose position 5 ^{2}H-enrichment, and its ^{2}H5/^{2}H2 ratio, overestimates the gluconeogenic contribution to endogenous glucose production (EGP). The effects of TA exchange are not limited to the ^2H_2O method but also influence glucose enrichment or specific activity from any labeled gluconeogenic precursor.

The present studies were performed to determine if TA exchange occurs in humans and to what extent does it alter the measurement of gluconeogenesis using the ^2H_2O method. To address this question, ^2H_2O was ingested and [1-^{13}C]acetate was infused intravenously in healthy and in insulin resistant subjects. [1-^{13}C]acetate is metabolized *via* the Krebs cycle, gluconeogenic and triose phosphate isomerase (TPI) reactions to yield equal amounts of [1-^{13}C]glyceraldehyde-3-phosphate ([1-^{13}C]G3P) and [1-^{13}C]dihydroxyacetone phosphate ([1-^{13}C]DHAP). These precursors combine to form [3-^{13}C]- and [4-^{13}C]fructose-1,6-bisphosphate ([3-^{13}C]F1,6P_2 and [4-^{13}C]F1,6P_2) then subsequently [3-^{13}C]- and [4-^{13}C]glucose. In absence of TA exchange [3-^{13}C]- and [4-^{13}C]glucose are equally labeled, therefore the ratio of ^{13}C3 to ^{13}C4 glucose enrichment (^{13}C3/^{13}C4) is equal to 1.0. In presence of TA exchange, unlabeled F6P derived from glycogenolysis becomes labeled in position 4. As a result, glucose position 4 ^{13}C-enrichment from [1-^{13}C]acetate is increased while that of position 3 is not altered. Thus, the ^{13}C3/^{13}C4 ratio is less than 1.0 and its value reflects the fraction of hepatic hexose phosphate that undergoes TA-mediated exchange for a given combination of gluconeogenic and glycogenolytic activities, as determined by the

enrichment pattern of glucose from $^{2}H_2O$. Therefore, enrichments of glucose from [1-^{13}C]acetate and from $^{2}H_2O$ were simultaneously measured using ^{13}C and ^{2}H Nuclear Magnetic Resonance (NMR) spectroscopy allowing calculation of the contribution of TA exchange to ^{2}H-enrichment of position 5 of glucose following $^{2}H_2O$ ingestion. Paracetamol was also ingested to sample uridine diphosphate glucose (UDP-glucose) into the urine in the form of paracetamol glucuronide and compared the ^{13}C and ^{2}H information obtained from the blood with that from the urine.

3.2 Materials and methods

3.2.1 Human studies

The study protocol was approved by the Mayo Clinic Institutional Review Board. The studies were performed on 16 subjects (9M, 7F; age 47 ± 4 years, body mass index 29 ± 1 kg/m^2) with normal fasting glucose and normal glucose tolerance (NFG/NGT) and without history of diabetes in first degree relatives, 17 subjects (6M, 11F; age 47 ± 3 years, body mass index 33 ± 1 kg/m^2) with impaired fasting glucose and impaired glucose tolerance (IFG/IGT) and on 13 subjects (9M, 4F; age 52 ± 4 years, body mass index 30 ± 2 kg/m^2) with impaired fasting glucose and normal glucose tolerance (IFG/NGT). Subjects were studied after giving written informed consent. Subjects were admitted the evening before to the Clinical research Unit at St. Mary's Hospital, Mayo Clinic at ~17:00 and fed a standard supper (10 total calories/kg; carbohydrate: fat: protein: 55:30:15).

$^{2}H_2O$ was ingested in 3 equal portions of 1.67 grams per lean body weight water at 22:00, 24:00, and 02:00 to attain 0.5% BW ^{2}H-enrichment. A 0.5% ^{2}H-enriched water was also provided to drink if desired but maintained in fasting.

The following morning at 06:00 (-180 minutes) [1-^{13}C]acetate infusion (5.0 μmol/kg/min) was started and continued until the end of study at 13:00. At ~ 06:30 and at ~08:45 one gram of paracetamol was ingested each time to obtain urinary glucuronide.

At time zero, somatostatin (60 ng/kg/min), insulin (0.35 mU/kg/min), glucagon (0.65 ng/kg/min) and human growth hormone (3 ng/kg/min) were started to be infused in order to ensure constant and equal portal concentrations of insulin and glucagon. In the protocol, glucagon is infused just for to maintain the insulin/glucagon ratio mimetizing that of the baseline and the clamp. Also, subjects were not given a saturating dose of insulin.

To clamp plasma glucose levels, an infusion of 50% dextrose containing [3-^{3}H]glucose and [6,6-$^{2}H_2$]glucose was started at time zero and given in amounts sufficient to maintain plasma glucose at 110 mg/dl.

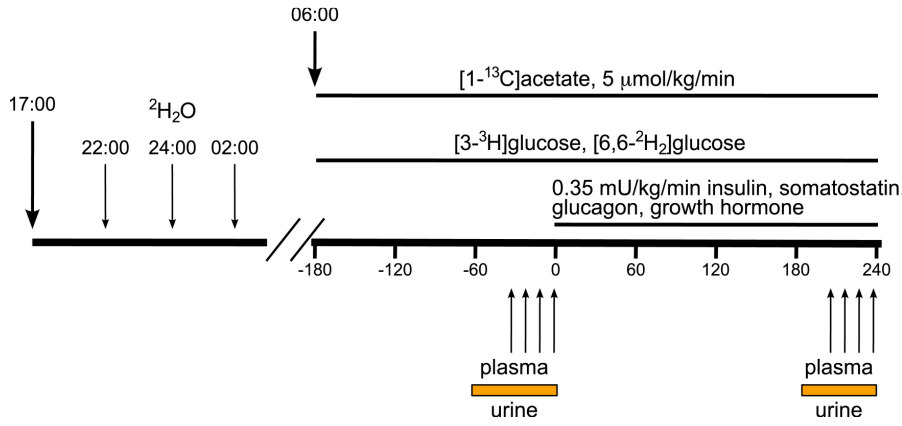

Figure 3.1: Scheme of experimental design. Subjects ingested $^{2}H_2O$ and paracetamol for to quantify the contribution of gluconeogenesis to hepatic glucose production during baseline and during clamp. An infusion of [1-^{13}C]acetate was performed to determine if TA was active. Somatostatin, insulin, glucagon and human growth hormone were infused to maintain constant and equal portal concentrations of insulin and glucagon.

Blood and urine were collected during baseline (at -60-0 min) and clamp (at 210-240 min) for determining [3-^{13}C]glucose, [4-^{13}C]glucose, [5-^{2}H]glucose and [2-^{2}H]glucose enrichments (Figure 3.1).

3.2.2 Sample processing

3.2.2.1 Blood samples

Blood samples were immediately placed on ice, centrifuged at 4ºC, separated and stored at -80ºC. Plasma was added to 1.5 volumes of cold 0.3 N $ZnSO_4$. After mixing, 1.5 volumes of cold 0.3 N $Ba(OH)_2$ was then added. The mixture was centrifuged and the supernatant kept. The supernatant was then passed through a column 20 ml of Dowex-50X8-200-H^+ ion-exchange resin above 10 ml of Amberlite. The eluate was evaporated until dryness at 37ºC and derivatized to monoacetone glucose (MAG). For that, a mixture of 5 ml of 2% deuterated acetone and 200 µl of 2% deuterated sulphuric acid was prepared and added to the dry glucose sample and stirred for 18 hours. Mixture was quenched with 5 ml of water and the pH adjusted to 2.1-2.3 and incubated for 4-5 hours at 40°C. After, the pH was adjusted to 8-9 and evaporated until dryness. MAG residue was extracted with boiling ethyl acetate and then evaporated. MAG was then purified by solid phase extraction (SPE) using a 500 mg Discovery DSC-18 cartridge, eluted with 10% CH_3CN/90% H_2O, and evaporated until dryness.

3.2.2.2 Urine samples

Urine was treated with urease and then lyophylized. To isolate the paracetamol glucuronide the lyophilyzed urine was reconstituted to approximately 10 ml. Monoacetoneglucuronolactone (MAGL) and MAG synthesis from urinary paracetamol glucuronide are already described in Chapter 2, section 2.2.2.2.

For ^{13}C NMR analysis the MAGL residue was resuspended in 600 µl of 50% C^2H_3CN and MAG residue was resuspended in 600 µl of 45% CH_3CN/45% C^2H_3CN/10% H_2O. For ^2H analysis, MAG was resuspended in 600 µl of 90% CH_3CN/10% H_2O and for ^1H NMR analysis, it was resuspended in 200 µl of 99.9% ^2H_2O.

3.3 NMR spectroscopy

3.3.1 Carbon-13 and proton NMR spectroscopy

^{13}C NMR spectra were obtained at 25ºC with Varian Unity 500 MHz NMR spectrometer equipped with a High Field Switchable Broadband 5 mm probe. Based on T_1 values of 2-4 seconds, quantitative ^{13}C signals for MAG aliphatic carbons were acquired with a 90° pulse angle, an acquisition time of 2.13 seconds during which ^1H-decoupling was applied, and a pulse delay of 21.77 seconds. ^1H NMR spectra of MAG from plasma glucose and from glucuronide in 99.9% ^2H_2O were acquired with a Varian VNMRS 600 MHz NMR spectrometer equipped with a High Field Indirect Detection 3 mm probe. Absolute ^{13}C-carbon 1 enrichment was quantified from the relative intensities of the ^{12}C-^1H central doublet and the ^{13}C-^1H satellites of position 1 ^1H signal. Absolute enrichments of carbons 3 and 4 were estimated from the ratio of their ^{13}C signals to that of carbon 1, multiplied by the absolute carbon 1-^{13}C-enrichment. Excess ^{13}C-enrichments of carbons 3 and 4 were calculated as the difference between absolute enrichment and background natural abundance value of 1.11%. %. NMR signals were quantified using the NUTS NMR spectral analysis program (Acorn NMR Inc., Fremont CA).

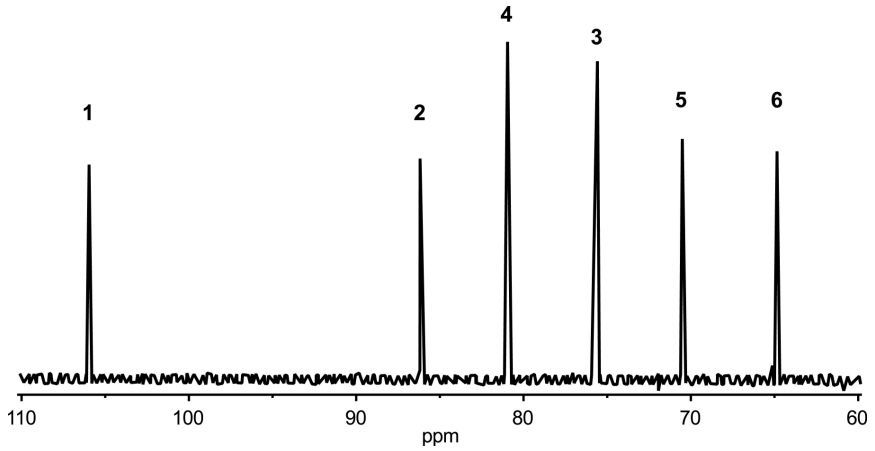

Figure 3.2: ^{13}C-spectrum of MAG derived from plasma glucose. Position 4 signal is more intense than that of position 3.

3.3.2 Deuterium NMR spectroscopy

Proton-decoupled ^{2}H NMR spectra were acquired at 50ºC with a Varian VNMRS 600 MHz NMR spectrometer equipped with a High Field Switchable Broadband 3 mm probe as previously described (see Chapter 2, section 2.2.3). ^{2}H-enrichment were calculated by comparing the hexose positional ^{2}H signal intensities with those of the MAG methyl signals, enriched to 2%. ^{2}H NMR signals were quantified using the NUTS NMR spectral analysis program (Acorn NMR Inc., Fremont CA).

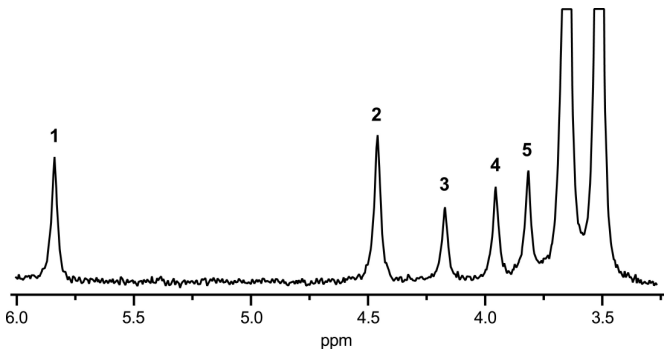

Figure 3.3: ^{2}H-spectrum of MAG derived from plasma glucose. Position 3 ^{2}H-enrichment is noticeably less than all the other positions.

3.4 Metabolic model and calculations

The gluconeogenic fractional contribution to EGP was calculated by multiplying the ratio of ^{2}H-enrichment of positions 5 and 2 of both plasma glucose and urinary glucuronide (^{2}H5/^{2}H2) and glycogenolysis contribution (1- (^{2}H5/^{2}H2)) by 100.

$$\text{Gluconeogenesis fraction (\%)} = 100 \times {}^{2}\text{H5} / {}^{2}\text{H2} \quad (1)$$

$$\text{Glycogenolysis fraction (\%)} = 100 \times [1 - ({}^{2}\text{H5} / {}^{2}\text{H2})] \quad (2)$$

The [3-^{13}C]- to [4-^{13}C] plasma glucose or glucuronide ratios (^{13}C3/^{13}C4) are sensitive to TA exchange and are used to correct the position 5 enrichment from $^{2}H_2O$ (^{2}H5$_{CORR}$):

$${}^{2}\text{H5}_{\text{CORR}} / {}^{2}\text{H2} = {}^{2}\text{H5}_{\text{OBS}} / {}^{2}\text{H2} \times {}^{13}\text{C3}/{}^{13}\text{C4} \quad (3)$$

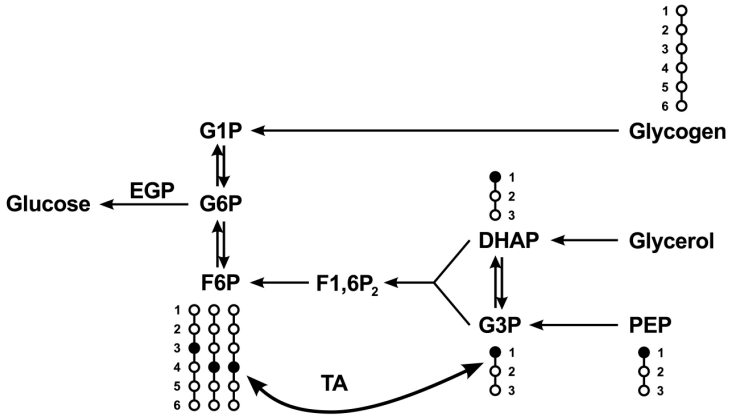

Figure 3.4: Scheme of ^{13}C-glucose label from metabolism of [1-^{13}C]acetate in the presence of TA exchange. Abbreviations are as follows: PEP (phosphoenolpyruvate), G3P (glyceraldehyde-3-phosphate), DHAP (dihydroxyacetone phosphate), F1,6P$_2$ (fructose-1,6-bisphosphate), F6P (fructose-6- phosphate), G6P (glucose-6- phosphate), G1P (glucose-1- phosphate), EGP (endogenous glucose production), TA (transaldolase). In presence of TA exchange, unlabeled fructose-6-phosphate derived from glycogen becomes enriched in position 4. The label of position 4 in glucose is increased while that of position 3 is not altered. This results in a ^{13}C3/^{13}C4 ratio of less than 1.0.

The corrected contributions of gluconeogenesis (GNG_{CORR}) and glycogenolysis (GLY_{CORR}) were then calculated as follows:

$$\text{Corrected Gluconeogenesis fraction}(GNG_{CORR})\ (\%) = 100 \times {}^{2}H5_{CORR} / {}^{2}H2 \quad (4)$$

$$\text{Corrected Glycogenolysis fraction}\ (GLY_{CORR})\ (\%) = 100 \times [1 - ({}^{2}H5_{CORR} / {}^{2}H2)] \quad (5)$$

3.5 Statistical analysis

Data in the text and figures are expressed as mean ± SEM. Values from – 30,-60- and 0 minutes were averaged as basal and 210, 220, 230, and 240 minutes as clamp for statistical analysis and representation. Wilcoxon's rank sum test was used to test the hypotheses that the plasma glucose $^{13}C3/^{13}C4$ ratio and urinary glucuronide $^{13}C3/^{13}C4$ ratio were significantly less than one. Paired t-test were used to test if [4-^{13}C]glucose or [4-^{13}C]glucuronide were significantly higher than [3-^{13}C]glucose or [3-^{13}C]glucuronide within both baseline and clamp settings. A p value of < 0.05 was considered as statistically significant.

3.6 Results

3.6.1 Comparison of plasma glucose and urinary glucuronide ^{13}C-enrichments from [1-^{13}C]acetate

For NFG/NGT subjects, plasma glucose enrichments during the clamp tended to be lower than those for the baseline. Presumably, this reflects the dilution of endogenous labeled glucose by unlabeled infused glucose used to maintain the clamp and well as insulin-mediated suppression of EGP. These effects more than offset the increase

in glucose ^{13}C-enrichment that would have occurred in the absence of the clamp due to the continuing infusion of [1-^{13}C3]acetate precursor and convergence of glucose ^{13}C-enrichment to isotopic steady-state. Plasma glucose carbon 4 ^{13}C-enrichments were significantly higher than carbon 3 for both baseline and clamp conditions and ^{13}C3/^{13}C4 were significantly less than 1.0. For the IFG/IGT and IFG/NGT groups, plasma glucose enrichment was similar to NFG/NGT at baseline, but tended to be higher after the clamp period. Glucose infusion rates are much lower for these subjects resulting in less dilution of the label. Therefore, in contrast to the NFG/NGT group, this factor opposes the progression of plasma glucose ^{13}C-enrichment from [1-^{13}C]acetate to a much lesser degree in IGT/IFG and IFG/NGT subjects. Regardless of these differences in plasma glucose enrichment kinetics, plasma glucose carbon 4 enrichment was significantly higher than that of carbon 3 and ^{13}C3/^{13}C4 was significantly less than 1.0 for both baseline and clamp conditions in all groups (Table 3.1).

Urinary glucuronide enrichment for NFG/NGT subjects showed a systematic increase between baseline and clamp conditions. This indicates that enrichment of hepatic glucose-6-phosphate (G6P) from [1-^{13}C]acetate progressed towards isotopic steady-state and was much less influenced by the clamp procedure compared to that of plasma glucose. Baseline glucuronide enrichments were also lower compared to those of plasma glucose. This may reflect the fact that the glucuronide was sampling G6P enrichment at an earlier interval compared to plasma glucose due to the lag time between synthesis in liver and appearance in urine. A similar pattern was observed for baseline glucose and glucuronide ^{13}C-enrichments of IFG/IGT subjects. With the exception of baseline NFG/NGT subjects, glucuronide carbon 4 enrichments were significantly higher than carbon 3 and the ^{13}C3/^{13}C4 ratios were significantly less than 1.0 for all other situations. Where both glucuronide and glucose were analyzed, the ^{13}C3/^{13}C4 of both metabolites were identical. These data provide strong evidence of substantial TA exchange activity in both baseline and clamp conditions and for both NFG/NGT and IFG/IGT groups.

Table 3.1: ^{13}C-Excess enrichments of carbon 3 (^{13}C3) and carbon 4 (^{13}C4) of plasma glucose and urinary glucuronide from [1-^{13}C]acetate for subjects with normal and impaired glucose tolerance. The ratio of carbon 3 to carbon 4 excess enrichment (^{13}C3/^{13}C4) for each condition is also shown.

Subjects & conditions	Analytes	Excess ^{13}C-enrichment from [1-^{13}C]acetate		
		^{13}C3(%)	**^{13}C4(%)**	**^{13}C3/^{13}C4**
NFG/NGT Baseline	**Glucose**	0.44 ± 0.05	0.62 ± 0.06 ###	0.70 ± 0.03 **
	Glucuronide	0.19 ± 0.03	0.31 ± 0.05##	0.61 ± 0.05
NFG/NGT Clamp	**Glucose**	0.35 ± 0.06	0.55 ± 0.08 ###	0.59 ± 0.04 **
	Glucuronide	0.39 ± 0.06	0.66 ± 0.06 ###	0.55 ± 0.05 *
IFG/IGT Baseline	**Glucose**	0.48 ± 0.03	0.67 ± 0.04 ###	0.71 ± 0.02 **
	Glucuronide	0.28 ± 0.02	0.39 ± 0.02 ###	0.73 ± 0.03 *
IFG/IGT Clamp	**Glucose**	0.54 ± 0.06	0.81 ± 0.07 ###	0.64 ± 0.03 **
	Glucuronide	0.37 ± 0.04	0.62 ± 0.05 ###	0.59 ± 0.04 *
IFG/NGT Baseline	**Glucose**	0.44 ± 0.05	0.56 ± 0.05 ###	0.77 ± 0.04 *
IFG/NGT Clamp	**Glucose**	0.48 ± 0.09	0.66 ± 0.09 ##	0.72 ± 0.05 *

* significantly different from 1.0 (p< 0.05), ** significantly different from 1.0 (p< 0.01), *** significantly different from 1.0 (p< 0.001).

significantly different from **^{13}C3** (p< 0.05), ## significantly different from **^{13}C3** (p< 0.01), ### significantly different from **^{13}C3** (p< 0.001).

3.6.2 Comparison of plasma glucose and urinary glucuronide ^{2}H-enrichments from ^2H_2O

As shown in Table 3.2, plasma glucose position 2 ^{2}H-enrichment obtained during baseline for NFG/NGT approached the theoretical BW enrichment of 0.5 % indicating equivalence between glucose position 2 and BW enrichments. This indicates that the plasma glucose pool was wholly derived from endogenous sources and also that it had completely turned over during the period of ^2H_2O administration. Plasma glucose position 2 enrichment measured during the clamp was significantly less ($p<0.05$), reflecting the dilution from the infused glucose. Enrichment of position 5 was also systematically reduced following the clamp. Consequently, the ratio of observed position 5 and 2 enrichments (^{2}H5/^{2}H2) remained constant throughout the experiment. For IFG/IGT subjects, position 5 and 2 enrichments were also systematically reduced following administration of the clamp, however the magnitude of this change was less than for the NFG/NGT group. This reflects a reduced dilution resulting from the smaller quantity of exogenous infused glucose required to maintain the clamp glycemic levels. ^{2}H5/^{2}H2 ratios were constant between baseline and clamp conditions and the values were not different from those of NFG/NGT subjects. For the IFG/NGT subjects, plasma glucose position 2 ^{2}H-enrichment obtained during baseline approached the theoretical BW enrichment of 0.5 % plasma glucose. However, during the clamp it was significantly less ($p<0.05$ *versus* baseline), resembling that of the NFG/NGT group. Enrichment of position 5 was also systematically reduced following the clamp, as was observed for the NFG/NGT group. The ^{2}H5/^{2}H2 ratio remained constant throughout the experiment as seen for the other two groups.

For both NFG/NGT and IFG/IGT subjects, glucuronide position 2 enrichment corresponded to the theoretical BW level of 0.5% under both baseline and clamp conditions. Also, glucuronide ^{2}H5/^{2}H2 matched those of plasma glucose. From these observed ^{2}H5/^{2}H2 values, the estimated contribution of gluconeogenesis

to EGP was ~50% under both baseline and clamp conditions and for both NFG/NGT and IFG/IGT subjects. For the baseline NFG/NGT group, these estimates of the gluconeogenic contribution to EGP are highly concordant with previously published data from overnight-fasted healthy subjects (Chandramouli *et al.* 1997; Jones *et al.* 2006).

3.6.3 Correction of position 5 enrichment for transaldolase activity and effects on estimates of gluconeogenic contribution to EGP

Under conditions where there is significant production of hepatic G6P from glycogenolysis that is not enriched with ^{2}H in position 5, such as after overnight fasting, TA exchange may account for a significant fraction of the observed glucose position 5 enrichment ($^{2}H5_{obs}$) independently of gluconeogenic activity. The extent of TA exchange may be evaluated by integrating the $^{13}C3/^{13}C4$-enrichment data representing TA exchange activity with position 5 ^{2}H-enrichment – representing both TA and gluconeogenic activities. From this analysis, a corrected estimate of position 5 enrichment representing the real gluconeogenic contribution ($^{2}H5_{corr}$) was derived.

Plasma glucose and urinary glucuronide position 5 ^{2}H-enrichments that were directly measured ($^{2}H5_{obs}$) and after correction for TA exchange ($^{2}H5_{corr}$) are shown in Table 3.2. The gluconeogenic contribution to EGP, represented by $^{2}H5_{obs}/^{2}H2$ and the gluconeogenic contribution corrected for TA exchange, represented by $^{2}H5_{corr}/^{2}H2$, are also shown. For all groups, $^{2}H5_{obs}$ for plasma glucose and clamp was significantly higher than $^{2}H5_{corr}$. With the exception of the baseline NFG/NGT group, $^{2}H5_{obs}$ measured for urinary glucuronide was also significantly higher than $^{2}H5_{corr}$. Consequently, the fractional contribution of gluconeogenesis determined after correction for TA exchange activity was significantly less than the uncorrected estimate. Overall, correction for TA exchange reduced the estimated gluconeogenic fraction from about one-half to about 1/3rd of total EGP.

Table 3.2: ^{2}H-Enrichments of position 2 (^{2}H2) and position 5 (^{2}H5) of plasma glucose and urinary glucuronide from subjects with normal and impaired glucose tolerance. Position 5 enrichment corrected for transaldolase exchange ($^2H5_{corr}$) and the corrected position 5 to position 2 enrichment ratio ($^2H5_{corr}/^2H2$) are also shown.

Subjects & conditions	Analytes	Observed ^{2}H-enrichment from ^2H_2O			Corrected position 5 enrichment and $^2H5/^2H2$ ratio	
		^{2}H2(%)	^{2}H5(%)	$^2H5/^2H2$	$^2H5_{corr}$(%)	$^2H5_{corr}/^2H2$
NFG/NGT Baseline	Glucose	0.47 ± 0.01	0.23 ± 0.02	0.49 ± 0.03	0.16 ± 0.02	0.34 ± 0.03 ***
	Glucuronide	0.49 ± 0.02	0.25 ± 0.02	0.50 ± 0.04	0.15.±0.02	0.31 ± 0.04 *
NFG/NGT Clamp	Glucose	0.22 ± 0.03	0.11 ± 0.02	0.49 ± 0.03	0.06 ± 0.01	0.28 ± 0.03 **
	Glucuronide	0.51 ± 0.01	0.25 ± 0.01	0.50 ± 0.03	0.15 ± 0.02	0.28 ± 0.04 **
IFG/IGT Baseline	Glucose	0.46 ± 0.01	0.21 ± 0.01	0.47 ± 0.02	0.15 ± 0.01	0.33 ± 0.02 ***
	Glucuronide	0.49 ± 0.02	0.26 ± 0.02	0.53 ± 0.03	0.19 ± 0.02	0.40 ± 0.03 *
IFG/IGT Clamp	Glucose	0.36 ± 0.03	0.16 ± 0.01	0.48 ± 0.03	0.11 ± 0.01	0.31 ± 0.02 ***
	Glucuronide	0.49 ± 0.02	0.27 ± 0.02	0.55 ± 0.02	0.16 ± 0.02	0.33 ± 0.03 ***
IFG/NGT Baseline	Glucose	0.47 ± 0.01	0.27 ± 0.01	0.57 ± 0.02	0.21 ± 0.01	0.44 ± 0.03 **
IFG/NGT Clamp	Glucose	0.29 ± 0.04	0.15 ± 0.02	0.53 ± 0.03	0.11 ± 0.02	0.39 ± 0.04 **

* significantly different from **$^2H5/^2H2$** ($p< 0.05$),** significantly different from **$^2H5/^2H2$** ($p< 0.01$), *** significantly different from **$^2H5/^2H2$** ($p< 0.001$).

3.6.4 Relationship between position 3 and the corrected position 5 enrichments of glucose and glucuronide

Position 3 of glucose is enriched from ^2H_2O by a specific exchange of solvent and the 1 pro-*S* hydrogen of dihydroxyacetone phosphate (DHAP) *via* TPI. Unlike position 5, enrichment of position 3 is unaffected by TA exchange. On this basis it is hypothesized that position 3 ^{2}H-enrichment should provide estimates of

gluconeogenesis that are comparable to that obtained from the corrected position 5 enrichment.

Table 3.3: ^{2}H-Enrichments of position 3 (^{2}H3) and position 5 enrichment corrected for transaldolase exchange ($^2H5_{corr}$) and fractional gluconeogenic contribution to endogenous glucose production calculated from the ration of position 3 to position 2 enrichment (^{2}H3/^{2}H2) and position 5 to position 2 enrichment after correcting for transaldolase exchange ($^2H5_{CORR}/^2$H2).

Subjects & conditions	Analytes	^{2}H-enrichment distributions and ratios			
		^{2}H3(%)	**$^2H5_{CORR}$(%)**	**^{2}H3/^{2}H2**	**$^2H5_{CORR}/^2$H2**
NFG/NGT Baseline	**Glucose**	0.15 ± 0.01	0.16 ± 0.02	0.30 ± 0.03	0.34 ± 0.03
	Glucuronide	0.13 ± 0.02	0.15 ± 0.02	0.27 ± 0.04	0.31 ± 0.04
NFG/NGT Clamp	**Glucose**	0.06 ± 0.01	0.06 ± 0.01	0.28 ± 0.03	0.28 ± 0.03
	Glucuronide	0.14 ± 0.02	0.15 ± 0.02	0.28 ± 0.03	0.28 ± 0.03
IFG/IGT Baseline	**Glucose**	0.13 ± 0.01	0.15 ± 0.01	0.27 ± 0.02	0.33 ± 0.02 **
	Glucuronide	0.13 ± 0.01	0.19 ± 0.02	0.27 ± 0.03	0.40 ± 0.03 ***
IFG/IGT Clamp	**Glucose**	0.09 ± 0.01	0.11 ± 0.01	0.25 ± 0.02	0.31 ± 0.02 *
	Glucuronide	0.13 ± 0.01	0.16 ± 0.02	0.27 ± 0.02	0.33 ± 0.03 **
IFG/NGT Baseline	**Glucose**	0.17 ± 0.01	0.21 ± 0.01	0.36 ± 0.02	0.44 ± 0.03 *
IFG/NGT Clamp	**Glucose**	0.09 ± 0.01	0.11 ± 0.02	0.32 ± 0.03	0.39 ± 0.04

* significantly different from **^{2}H3/^{2}H2** (p< 0.05),** significantly different from **^{2}H3/^{2}H2** (p< 0.01), *** significantly different from **^{2}H3/^{2}H2** (p< 0.001).

The results of this comparison are shown in Table 3.3 for NFG/NGT, IFG/IGT and IFG/NGT groups as well as for plasma glucose and urinary glucuronide analyses. With the exception of baseline and clamp for both plasma glucose and glucuronide analysis from NFG/NGT, and for clamp plasma glucose for IFG/NGT, position 3 enrichment was significantly lower than that of corrected position 5. However, these differences were substantially smaller compared to that of uncorrected and corrected position 5 enrichments. Therefore, it can be concluded that the $^{2}H3/^{2}H2$ ratio provides a more precise estimate of gluconeogenic fraction compared to $^{2}H5_{obs}/^{2}H2$, but there is a slight, but significant under-reporting of the gluconeogenic fraction compared to $^{2}H5_{corr}/^{2}H2$.

3.7 Discussion

Enrichment of plasma glucose or urinary glucuronide from gluconeogenic tracers provides the basis for estimating the gluconeogenic and glycogenolytic contributions to EGP. Regardless of the tracer used, one of the fundamental assumptions of this approach is that enrichment of gluconeogenically-derived G6P is diluted by unlabeled G6P derived from glycogenolysis. From this dilution, the fractional contributions of gluconeogenesis and glycogenolysis to EGP are obtained. By converting an unlabeled G6P molecule into a molecule enriched with the gluconeogenic tracer, TA exchange invalidates this assumption. The data indicate that 23-27% of unlabeled G6P underwent TA exchange. This resulted in substantial overestimates of the gluconeogenic fraction, with the mean corrected value being ~39% lower than the uncorrected value for NFG/NGT subjects and ~33% lower for the IFG/IGT group, and ~25% lower for IFG/NGT. These corrections are based on measurements of excess ^{13}C-enrichment in positions 3 and 4 of glucose and glucuronide from [1-^{13}C]acetate by quantitative ^{13}C NMR spectroscopy of two

different derivatives (MAG from plasma glucose and MAGL from glucuronide). The excess ^{13}C-enrichments of these positions ranged from 0.19% to 0.81%. The ^{13}C NMR signals of both derivatives consistently showed significantly excess enrichment in carbon 4 compared to carbon 3 with the sole exception of the baseline NFG/NGT glucuronide. This sample had the lowest levels of excess ^{13}C-enrichment which resulted in the highest uncertainty of the measured values. This fact, rather than any real difference in TA activity between this and the other sampling times, was the reason that the difference between carbon 3 and 4 enrichments did not reach statistical significance.

The extent of TA exchange revealed by these ^{13}C-enrichment data has significant effects on the ^{2}H-enrichment distribution of glucose and glucuronide from $^{2}H_2O$ in overnight fasted subjects. This is because there is substantial influx of unlabeled hepatic G6P from glycogenolysis, a significant fraction of which will become enriched in positions 4, 5 and 6 by gluconeogenic tracers as a result of TA exchange. Since enrichment of positions 1, 2 and 3 of G6P from the same tracers are not affected by TA, enrichment levels of these sites should in principle be insensitive to TA exchange. With $^{2}H_2O$, both positions 1 and 2 of glucose become enriched by exchanges at the level of hepatic G6P (Landau *et al.* 1996; Chandramouli *et al.* 1999) therefore enrichment at either of these sites does not inform the gluconeogenic contribution to G6P. However, position 3 enrichment is solely derived from exchanges at the triose phosphate level and is therefore specific for gluconeogenic activity. For enrichment of position 3 to be a quantitative measure of gluconeogenesis, DHAP and G3P must be completely exchanged *via* TPI. There is evidence that TPI exchange is extensive for in situ human livers (Jones *et al.* 2008). Incorporation of ^{2}H from BW into 1*R*-DHAP *via* TPI may also be subject to a significant kinetic isotope effect (Albery *et al.* 1976; Fisher *et al.* 1976; Herlihy *et al.* 1976). This may discriminate ^{2}H incorporation into this site relative to ^{1}H resulting in a lower enrichment of the 1*R*-DHAP hydrogen compared to BW. To the extent that

TPI exchange is incomplete and/or ^{2}H-enrichment of DHAP is hindered by isotope effects, enrichment of position 3 underestimates the true gluconeogenic contribution to G6P flux. When position 3 enrichment is compared with that of the corrected position 5 (Table 3.3) the overall tendency is for to be less enriched.

The $^{2}H_2O$ method was developed as a simple and robust analysis of the contributions of hepatic gluconeogenesis and glycogenolysis to fasting glucose production. Enrichment of position 5 can be measured by both NMR and GC-MS and informs contributions from all gluconeogenic sources including glycerol. However, TA exchange contributes to the position 5 enrichments of glucose and glucuronide independently of gluconeogenic G6P production. Correcting the position 5 enrichment for TA exchange requires administration of an additional tracer such as [1-^{13}C]acetate and analysis of both ^{13}C and ^{2}H enrichment distributions of glucose and therefore substantially increases the complexity and cost of the measurement.

Position 3 enrichment of glucose from $^{2}H_2O$ *via* gluconeogenesis is insensitive to TA exchange activity and can be quantified by ^{2}H NMR (but not by GC-MS at this time). However, for this to be a quantitative marker of the gluconeogenic contribution to G6P synthesis, assumptions of complete triose phosphate exchange *via* TPI and absence of isotopic discrimination against ^{2}H incorporation into DHAP are required. It remains uncertain if these assumptions hold under different physiological and pathophysiological conditions.

3.8 Conclusions

Substantial TA exchange occurs in humans resulting in an overestimation of contribution of gluconeogenesis when measured with the $^{2}H_2O$ method. Following an overnight fast, glucose enrichment from infused [1-^{13}C]acetate was significantly higher in carbon 4 compared to carbon 3. The use of appropriate ^{13}C-tracers provides a potential means of correcting for this overestimate. The plasma [3-^{13}C]glucose to [4-

^{13}C]glucose ratio as well the urinary [3-^{13}C]glucuronide to [4-^{13}C]glucuronide ratio was less than 1.0 in all subjects both before and during the insulin infusion indicating substantial TA exchange. This resulted in an overestimation of the contribution of gluconeogenesis and an underestimation of contribution of glycogenolysis. Therefore, unless TA exchange is taken into account, the deuterated water method does not accurately measure the contribution of gluconeogenesis in non-diabetic and in insulin resistant subjects. Enrichment of glucose and glucuronide position 3 from $^{2}H_2O$ is insensitive to TA exchange and may therefore be a potential novel marker for gluconeogenic activity. However, incomplete exchange between BW and the gluconeogenic precursor hydrogen destined to become glucose position 3 may result in modest underestimates of the gluconeogenic contribution to G6P.

3.9 References

Albery WJ and Knowles JR. Deuterium and tritium exchange in enzyme-kinetics. Biochemistry 1976;15:5588-5600.

Chandramouli V, Ekberg K, Schumann WC, Kalhan SC, Wahren J and Landau BR. Quantifying gluconeogenesis during fasting. American Journal of Physiology 1997;273:E1209-E1215.

Chandramouli V, Ekberg K, Schumann WC, Wahren J and Landau BR. Origins of the hydrogen bound to carbon 1 of glucose in fasting: significance in gluconeogenesis quantitation. American Journal of Physiology 1999;277:E717-723.

Fisher LM, Albery WJ and Knowles JR. Energetics of triosephosphate isomerase - nature of proton-transfer between catalytic base and solvent water. Biochemistry 1976;15:5621-5626.

Herlihy JM, Maister SG, Albery WJ and Knowles JR. Energetics of triosephosphate isomerase - fate of 1(*R*)-^{3}H- label of tritiated dihydroxyacetone phosphate in isomerase reaction. Biochemistry 1976;15:5601-5607.

Jones JG, Fagulha A, Barosa C, Bastos M, Barros L, Baptista C, Caldeira MM and Carvalheiro M. Noninvasive analysis of hepatic glycogen kinetics before and after breakfast with deuterated water and acetaminophen. Diabetes 2006;55:2294-2300.

Jones JG, Garcia P, Barosa C, Delgado TC, Caldeira MM and Diogo L. Quantification of hepatic transaldolase exchange activity and its effects on tracer measurements of indirect pathway flux in humans. Magnetic Resonance in Medicine 2008;59:423-429.

Landau BR, Wahren J, Chandramouli V, Schumann WC, Ekberg K and Kalhan SC. Contributions of gluconeogenesis to glucose production in the fasted state. Journal of Clinical Investigation 1996;98:378-385.

Chapter 4

Contribution of Proteolytic and Metabolic Sources to Hepatic Glutamine

4.1 Objective 117

4.2 Introduction 117

4.3 Materials and methods 121

4.3.1 Human studies 121

4.3.2 Sample processing 122

4.3.3 NMR spectroscopy 123

4.3.4 Calculation of positional glutamate ^{2}H-enrichment 123

4.3.5 Calculation of hepatic glutamine flux parameters from ^{2}H-enrichment data 124

4.4 Results 126

4.5 Discussion 132

4.5.1 Analytical considerations 132

4.5.2 Intra-*versus* extrahepatic sources of PAGN 132

4.5.3 Glutamine ^{2}H-enrichment from $^{2}H_2O$ 133

4.5.4 PAGN ^{2}H-enrichment levels and sources of glutamyl carbon skeletons 135

4.5.5 Enrichment of acetyl-CoA from ^{2}H-enriched body water 137

4.5.6 Whole-body glutamine production and hepatic gluconeogenesis 138

4.6 Conclusions 140

4.7 References 141

This Chapter is based on:
Barosa, C., Almeida, M., Caldeira, M., Gomes, F., Jones, JG.
Contribution of proteolytic and metabolic sources to hepatic glutamine by ^{2}H NMR analysis of urinary phenylacetylglutamine ^{2}H-enrichment from $^{2}H_2O$.
Metabolic Engineering, 2010. 12(1): p. 53-61.

4.1 Objective

Proteolytic and cataplerotic sources of hepatic glutamine were determined by ^{2}H NMR analysis of urinary phenylacetylglutamine (PAGN) ^{2}H-enrichments in eight healthy subjects after deuterated water (^2H_2O) and phenylbutyric acid ingestion. Body water (BW) enrichment was 0.49 ± 0.03%. PAGN was enriched to lower levels with significant differences between the various glutamine positions. PAGN position 2 enrichment = 0.33 ± 0.02%; 3*R* = 0.27 ± 0.02%; 3*S* = 0.27 ± 0.02% and position 4 = 0.17 ± 0.01%. Position 3*R,S* enrichments are conditional with the net conversion of citrate to glutamate and are therefore markers of cataplerosis. From the ratio of positions 3*R,S* to BW enrichment, 55 ± 3% of hepatic glutamine was derived from cataplerosis and 45 ± 3% from proteolysis. In conclusion, enrichment of PAGN 3*R,S* hydrogens relative to that of BW reflects the contribution of cataplerotic and proteolytic sources to hepatic glutamine.

4.2 Introduction

Glutamine is an abundant non-essential amino acid that is highly involved in carbon and nitrogen transfer between different organs and tissues. Skeletal muscle is the principal source of whole body glutamine production, accounting for 50-70% of the glutamine rate of appearance (R_a) (Nurjhan *et al.* 1995; Biolo *et al.* 2005). The glutamine carbon skeleton is utilized by the gut as an energy source and by the liver as a gluconeogenic precursor. Thermodynamically, glutamine is a potent gluconeogenic amino acid since its conversion to sugar phosphates is accompanied by a net gain of adenosine-triphosphate (ATP) and reducing equivalents. There is evidence that glutamine derived from peripheral tissues is a significant source of carbon for hepatic gluconeogenesis (Nurjhan *et al.* 1995; Hankard *et al.* 1997; Perriello *et al.* 1997).

Therefore, alterations in whole body glutamine production may have a significant effect on gluconeogenic activity and hepatic glucose metabolism. Glutamine can be derived from both metabolic and proteolytic sources hence its R_a may be influenced by changes in peripheral metabolic activity or in whole-body protein kinetics. These could include the balance between whole-body protein anabolism and catabolism as well as the intermediary metabolic flux activities of various peripheral tissues.

Skeletal muscle has a relatively large pool of free glutamine that is in rapid turnover (Biolo *et al.* 1995). The glutamine content of alkali-soluble muscle protein is about 4%, hence proteolysis provides a direct source of glutamine. In addition, glutamine can be synthesized from other amino acids that are released during proteolysis, including proline, histidine, asparagine and glutamate. Of these precursors, glutamate is quantitatively the most important since its abundance in skeletal muscle protein is ~4 fold higher than that of glutamine (Kuhn *et al.* 1999). Consequently, each equivalent of glutamine that is directly released by skeletal muscle proteolysis is accompanied by four of glutamate, which can be potentially converted to glutamine. Indeed, much of the glutamate released by proteolysis is likely rapidly converted to glutamine as seen by the 10-fold greater concentration and higher R_a of plasma glutamine compared to plasma glutamate. Glutamine can also be derived from Krebs cycle intermediates *via* amination of α-ketoglutarate and amidation of glutamate. Net glutamine production from this source requires that the cataplerotic removal of carbon skeletons from the Krebs cycle is balanced by anaplerotic inflow. Sources of anaplerotic carbons include amino acids derived from proteolysis, such as glutamate, aspartate and alanine, as well as pyruvate derived from glycolysis. Skeletal muscle has the capacity for anaplerotic utilization of pyruvate - as seen by pyruvate carboxylase and malic enzyme activities (Sahlin *et al.* 1995). Anaplerotic flux in skeletal muscle has been demonstrated by ^{13}C isotope studies (Jucker *et al.* 1997) and by mass balance measurements of Krebs cycle intermediates (Sahlin *et al.* 1995; Gibala *et al.* 2000). Therefore, to the extent that anaplerotic outflow contributes to muscle

glutamine synthesis, the production of glutamine by skeletal muscle reflects metabolic as well as proteolytic activity.

The principal fate of glutamine released from muscle and other peripheral tissues is metabolism by splanchnic tissues including liver, intestine and kidney. There is high interest in relating the sources of whole body glutamine carbons to hepatic gluconeogenic activity. Critical illness is characterized by a loss of lean body mass (Reeds *et al.* 2006) hence there is potential for an increased generation of glutamine from proteolysis. This setting is also frequently characterized by hyperglycemia and elevated rates of hepatic gluconeogenesis (Leij-Halfwerk *et al.* 2000; Norrelund *et al.* 2006; Reeds *et al.* 2006). Given that glutamine may be a significant contributor to hepatic gluconeogenesis in healthy subjects (Nurjhan *et al.* 1995; Hankard *et al.* 1997; Perriello *et al.* 1997) an increased availability of hepatic glutamine during illness could contribute to elevated hepatic gluconeogenic fluxes. However, it is unclear to what extent whole-body protein breakdown and cataplerotic Krebs cycle fluxes contribute to hepatic glutamine availability.

It is hypothesized that cataplerotic and proteolytic contributions to hepatic glutamine can be inferred from the analysis of hepatic glutamine ^{2}H-enrichment from $^{2}H_2O$. When BW is enriched with $^{2}H_2O$ for a few hours, free amino acids become enriched with ^{2}H in various positional hydrogens (Previs *et al.* 2004). In many cases, enrichment of any given amino-acid hydrogen occurs *via* a specific metabolic transformation which can provide information on the amino acid source. Thus, glutamine that is derived from the Krebs cycle *via* cataplerosis will have predictable ^{2}H-enrichment levels in positions 2, 3 and 4 reflecting the incorporation of water hydrogens by specific Krebs cycle enzymes and by amination of α-ketoglutarate (see Figure 4.1). In contrast, amino acid residues of proteins are not significantly enriched with ^{2}H because over the experimental time scale, the fraction of protein that has turned over is very small and there are no known mechanisms for ^{2}H-enrichment of

the majority of non-exchangeable protein hydrogens other than through the incorporation of ^{2}H-enriched amino acids.

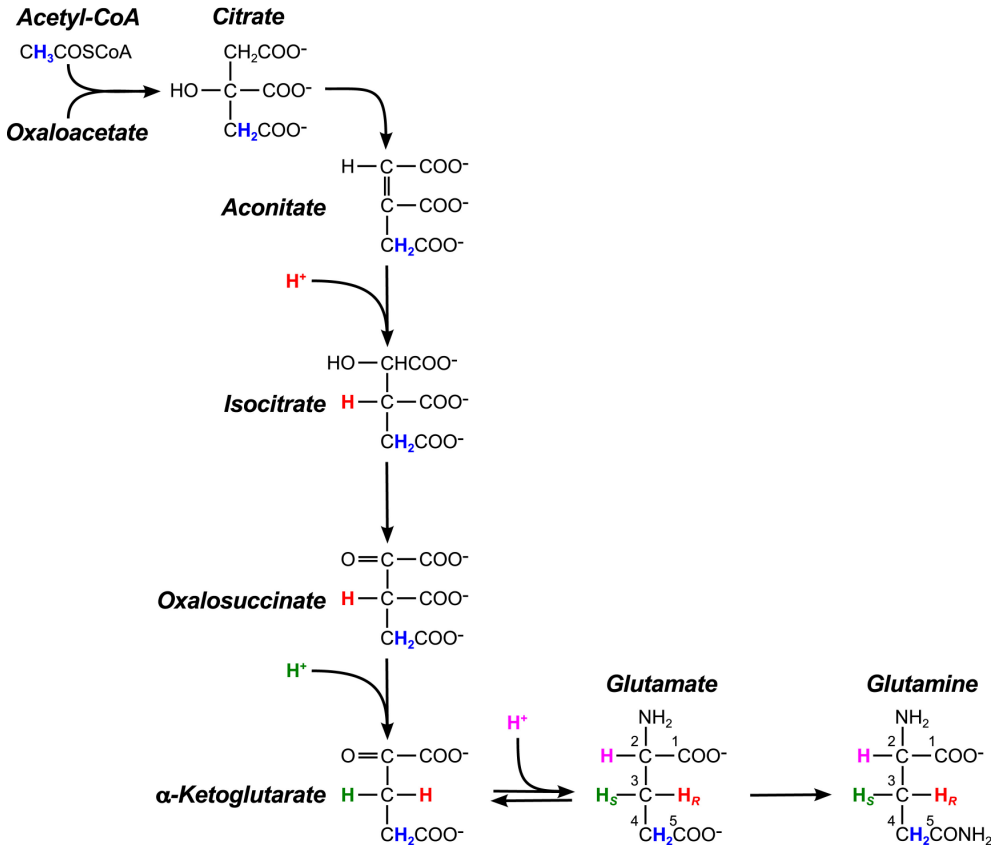

Figure 4.1: Sources of glutamine hydrogen enrichment from exchanges or addition of body water protons to Krebs cycle intermediates. The two hydrogen 4 atoms of glutamine (shown in blue) originate from the methyl hydrogens of acetyl-CoA. Hydrogen 3*R* (shown in red) is incorporated from bulk water during the conversion of aconitate to isocitrate *via* aconitase and hydrogen 3*S* (shown in green) is incorporated during the conversion of oxalosuccinate to α-ketoglutarate *via* isocitrate dehydrogenase. Hydrogen 2 (shown in pink) is incorporated *via* the amination of α-ketoglutarate to glutamate by either transaminase or glutamate dehydrogenase.

Since the ^{2}H-enrichment distributions are preserved during the conversion of glutamate to glutamine, the ^{2}H-enrichment level of glutamine reflects carbon skeletons that originated from the Krebs cycle and/or participated in transaminase

exchanges. Meanwhile, glutamine carbon skeletons that are not deuterated could not have originated from the Krebs cycle and did not undergo transaminase exchange. It is postulated that the most probable source of such precursors are C5 amino acids (principally glutamine and glutamate) released by proteolysis.

Hepatic glutamine can be noninvasively sampled as the urinary phenylacetylglutamine (PAGN) conjugate following ingestion of aspartame, sodium phenylacetate or sodium phenylbutyrate (Yang *et al.* 1993; Dugelay *et al.* 1994; Yang *et al.* 1996; Comte *et al.* 2002a). Enrichment of hepatic glutamine from ^2H_2O is preserved in the glutamine moiety of PAGN. The glutamine hydrogens of PAGN have well resolved NMR signals allowing positional enrichment in the backbone hydrogens to be analyzed by ^2H NMR. Analysis of low levels of ^2H-enrichments by NMR requires the recovery of ~0.1-0.2 mmol of analyte (Jones *et al.* 2001b; Perdigoto *et al.* 2003; Ribeiro *et al.* 2005; Jones *et al.* 2006). This quantity of PAGN may be conveniently recovered by the ingestion of a single capsule containing 0.3-0.5 grams of phenylbutyric acid followed by urine collection 2-4 hours afterwards (Perdigoto *et al.* 2003). In this Chapter, is demonstrate that analysis of the PAGN ^2H-enrichment pattern following ^2H_2O ingestion provides a practical and novel insight on the sources of hepatic glutamine in humans. The results indicate that in healthy postabsorptive subjects, a substantial portion of hepatic glutamine originates from proteolytic C5 amino acids.

4.3 Materials and methods

4.3.1 Human studies

All studies were performed in accordance with a protocol approved by the Ethics Committees of the University Hospital of Coimbra following informed consent from each subject. Subjects began fasting at 20:00 following a standard dinner. During the night, each subject ingested 5.0 g/kg body-water of ^2H_2O as a

35% solution in non-carbonated spring water (~350 ml total volume) divided into equal 2 portions: The first portion was given at 01:00 and the second portion was given at 03:00. For the remainder of the study, the subject drank water containing 0.5% ^2H_2O to maintain BW enrichment. At 07:00 the subjects ingested a gelatin capsule containing 300 mg phenylbutyric acid. Urine was collected between 09:00 and 11:00.

4.3.2 Sample processing

4.3.2.1 Urine samples

Isolation and processing of urinary PAGN: Urine was concentrated to 10-15 ml by rotary evaporation, the pH of the concentrate was adjusted to 7 with 5M NaOH and the sample was centrifuged. After removal of precipitate, the supernatant pH was adjusted to 1.5 with 2M HCl and applied to a 20 ml solid-phase extraction (SPE) column (Isolute HM-N, Symta, S.A.L.,Spain). PAGN was eluted with 80 ml ethyl acetate and the ethyl acetate was evaporated to dryness. For hydrolysis of PAGN to glutamate, the ethyl acetate extract was dissolved in 5 ml of 6M HCl and heated for 24 hours at 105ºC. The solution was centrifuged and the supernatant mixed with ~35 ml water. The pH was raised to 1.0 by addition of 2M NH_4OH and the solution was passed through an 18cm x 1cm column of Dowex-50X8-200-H^+ cation-exchange resin. The column was washed with 40 ml of water, glutamate was eluted with 40 ml of 2M NH_4OH and the solvent was evaporated to dryness. The same hydrolysis and purification procedure was applied to a set of [2,3,3,4,4-$^2H_5$] glutamine samples to generate [2,3,3,4,4-$^2H_5$]glutamate standards. For NMR spectroscopy, the residue containing glutamate was dissolved in ~600 µl of deuterium-depleted water containing a known amount of 0.505% deuterated dimethyl sulfoxide (DMSO) as an internal ^1H and ^2H concentration standard.

4.3.3 NMR spectroscopy

Proton-decoupled ^{2}H NMR spectra were acquired with a Varian Unity 500 MHz NMR spectrometer equipped with a High Field Switchable Broadband 5 mm probe (Varian, Palo Alto, CA). Spectra were obtained at 60°C without field-frequency lock with a 90 degree pulse angle, a sweep width of 10 ppm, an acquisition time of 2 seconds, and a pulse delay of 5 seconds. Between 1,500 and 7,600 free induction decays (fid) were acquired per sample for collection times of 3-15 hours. The summed fid´s were processed with 0.5-Hz line-broadening before Fourier transform. Fully relaxed ^{1}H NMR spectra were obtained under the same conditions with pre-saturation of the water signal. A pulse width of 45 degrees, acquisition time of 3 seconds and a delay of 16 seconds were used. Each ^{1}H spectrum was acquired with a single fid. ^{2}H-enrichment of urine water was analyzed by ^{2}H NMR as previously described (Jones *et al.* 2001a) All NMR spectra were analyzed using the curve-fitting routine supplied with the NUTS PC-based NMR spectral analysis program (Acorn NMR Inc., Fremont CA).

4.3.4 Calculation of positional glutamate ^{2}H-enrichment

Given the known ^{2}H-enrichment of the DMSO standard (0.505%) and assuming equal DMSO and glutamate proton equivalents[1], the ^{2}H-enrichment of any glutamate signal is simply the DMSO enrichment multiplied by the ratio of DMSO and glutamate ^{2}H-signal intensities. In the case of glutamate position 2 (G2), the enrichment would be equal to $0.505 \times {}^{2}H\ signal_{G2}/{}^{2}H\ signal_{DMSO}$. To account for the unequal amounts of DMSO and glutamate molecules present in the sample, this expression is multiplied by the relative amounts of DMSO and glutamate, obtained

[1] The DMSO ^{1}H or ^{2}H signal represents 6 equivalent proton or deuterium atoms per molecule

from the ratio of DMSO and glutamate ^{1}H NMR signals (^{1}H signal$_{DMSO}$/^{1}H signal$_{G2}$). Thus, percent enrichment of glutamate hydrogen 2 was calculated from equation (1).

$$\text{G2 Enrichment (\%)} = 0.505 \times (^{2}\text{H signal}_{G2}/^{2}\text{H signal}_{DMSO}) \times (^{1}\text{H signal}_{DMSO}/^{1}\text{H signal}_{G2}) \quad (1)$$

The positional ^{2}H-enrichments of the resolvable prochiral hydrogen 3 positions (G3*R*, G3*S*) were quantified likewise (equations (2) and (3)). Since the ^{1}H signals of the 3*R* and 3*S* sites consist of complex multiplets due to ^{1}H-^{1}H spin-spin coupling and are therefore difficult to quantify precisely, the simpler G2 ^{1}H signal (which is theoretically equivalent in intensity to each of the G3 ^{1}H multiplets), was used instead.

$$\text{G3}R\text{ Enrichment (\%)} = 0.505 \times (^{2}\text{H signal}_{G3R}/^{2}\text{H signal}_{DMSO}) \times (^{1}\text{H signal}_{DMSO}/^{1}\text{H signal}_{G2}) \quad (2)$$

$$\text{G3}S\text{ Enrichment (\%)} = 0.505 \times (^{2}\text{H signal}_{G3S}/^{2}\text{H signal}_{DMSO}) \times (^{1}\text{H signal}_{DMSO}/^{1}\text{H signal}_{G2}) \quad (3)$$

The hydrogen pair of glutamate position 4 (G4) are magnetically equivalent hence the G4 deuterium signal represents the summed ^{2}H-enrichment at these two sites and the mean enrichment per position 4 hydrogen is represented by one-half of the G4 signal intensity as shown by equation (4):

$$\text{G4 Enrichment (\%)} = 0.505 \times 0.5 \times (^{2}\text{H signal}_{G4}/^{2}\text{H signal}_{DMSO}) \times (^{1}\text{H signal}_{DMSO}/^{1}\text{H signal}_{G4}) \quad (4)$$

4.3.5 Calculation of hepatic glutamine flux parameters from ^{2}H-enrichment data

Metabolic parameters were estimated from glutamate and BW ^{2}H-enrichments with equations (5)-(10). The underlying assumptions are a): BW ^{2}H-enrichment is at

isotopic steady-state during the interval that hepatic glutamine was sampled as PAGN and b): the hepatic glutamine pool has completely turned over before being sampled. With the ^2H_2O administration protocol, BW enrichment was verified to be at isotopic steady state from 06:00 onwards (i.e. 3-5 hours before PAGN sampling, data not shown). Although there is no direct information for hepatic glutamine half-life in humans, studies of PAGN enrichment from ^{13}C tracers suggested that it is relatively short (Jones *et al.* 1998; Jones *et al.* 2001b) compared to the BW isotopic steady state interval of several hours. Hence there is confidence that the hepatic glutamine pool being sampled as PAGN has completely turned over during this period.

The fraction of hepatic glutamine derived from cataplerotic outflow of the Krebs cycle was estimated by equation (5):

$$\text{Krebs cycle fraction (\%)} = 100 \times \text{G3}R,S \text{ Enrichment} / \text{BW} \quad (5)$$

BW is the ^2H enrichment level of BW. The fraction of hepatic glutamine derived from proteolytic sources was estimated as the difference:

$$\text{Proteolytic contribution (\%)} = 100 - \text{Krebs cycle contribution} \quad (6)$$

By definition, all glutamine molecules labeled in positions 3 *via* the Krebs cycle are also enriched in position 2 following the conversion of α-ketoglutarate to glutamate (i.e. G3*R* = G3*S* = G2 enrichment for these molecules). For position 2 to be more enriched than positions 3*R* and 3*S* (as was observed in our experiments), a portion of glutamate molecules that were not derived from the Krebs cycle must undergo a specific exchange of position 2 hydrogen with that of BW. The most plausible mechanism is *via* transaminase-mediated exchange in the cytosol (see discussion). The difference between positions 2 and 3 enrichment therefore reflects the fraction of unlabeled (i.e. proteolytic) glutamate molecules that participated in transaminase-mediated exchange *en route* to being converted to glutamine, as described by equations (7)-(9):

$$\text{Glutamine enriched in position 2 } \textit{via} \text{ Krebs cycle + transaminase (\%)} = 100 \times \text{G2 Enrichment /BW} \quad (7)$$

$$\text{Glutamine enriched in position 2 } \textit{via} \text{ Krebs cycle only (\%)} = 100 \times \text{G3}\textit{R,S} \text{ Enrichment /BW} \quad (8)$$

$$\text{Glutamine enriched in position 2 } \textit{via} \text{ transaminase only (\%)} = 100 \times (\text{G2-G3}\textit{R,S} \text{ Enrichment) /BW} \quad (9)$$

Equation (9) refers to the fraction of molecules enriched solely *via* transaminase in relation to the total glutamine population (proteolytic + Krebs cycle). However, since only unlabeled glutamate molecules derived from proteolysis can be enriched in position 2 alone *via* transaminase-mediated exchange, the fraction of these molecules enriched by this process can be estimated by equation (10):

$$\text{Proteolytic fraction enriched } \textit{via} \text{ transaminase (\%)} = \text{Glutamine enriched } \textit{via} \text{ transaminase only/Proteolytic fraction} \quad (10)$$

Glutamate molecules derived from the Krebs cycle are already enriched in position 2 to the same level as BW hence their participation in transaminase-mediated exchange will not alter position 2 enrichment.

4.4 Results

^{2}H NMR analysis of urinary PAGN: Glutamate was recovered from urinary phenylacetylglutamine in quantities ranging from 170 to 500 μmol. For ^{2}H NMR spectroscopy, optimal signal linewidths were obtained with glutamate amounts of 300 μmol or less (~0.5 M concentration for the sample volumes). In contrast to a recent study by Comte *et al.* (Comte *et al.* 2002a) there were no detectable levels of phenylbutyrylglutamine in the samples as determined by ^{1}H NMR analysis of concentrated urine fractions. The phenylbutyrate dose used in our study (0.3 grams

per subject) was much lower than that used study of Comte *et al.* and may explain its quantitative conversion to PAGN. In any case, since both phenylbutyryl- and phenylacetylglutamine are hydrolyzed to glutamate for NMR spectroscopy, our analysis is applicable to subjects or conditions that generate phenylbutyrylglutamine, PAGN, or a mixture of both. Following desalting, acid hydrolysis and ion-exchange chromatography, the sample was characterized by ^{1}H NMR signals of glutamate and an unknown metabolite with a resonance that was adjacent to the glutamate hydrogen 2. For ^{2}H NMR spectroscopy, optimal ^{2}H-signal linewidths (~3 Hz) and dispersion were obtained by directly dissolving the glutamate eluted from the final cation-exchange column (essentially mono-ammonium glutamate) in water and acquiring the spectra at 60 °C. Under these conditions, the hydrogen 3*R* and 3*S* signals are resolved, allowing the ^{2}H-enrichment in each prochiral position to be determined. To check that the hydrolysis procedure did not alter the ^{2}H-enrichment levels of the glutamyl hydrogens, a set of glutamine standards enriched with [2,3,3,4,4-$^{2}H_5$]glutamine were hydrolyzed and the resulting glutamate was purified by cation-exchange chromatography and analyzed by ^{1}H and ^{2}H NMR. The mean ^{2}H signal ratios (relative to an arbitrary hydrogen 2 value of 100) were 100 ± 3.3 (hydrogen 3*R*), 112 ± 2.8 (hydrogen 3*S*) and 188 ± 2.3 (hydrogen 4), which are all within ~10% of the theoretical 1:1:1:2 ratio. Moreover, the ^{2}H-enrichment estimates for hydrogen 2 derived by NMR showed an excellent correlation with the real enrichment values as shown in Figure 4.2.

Enrichment of the other positions also were well correlated with the line of identity (hydrogen 3*R*; $y = 1.03x + 0.01$, $R^2 = 0.97$; hydrogen 3*S*; $y = 0.98x - 0.02$, $R^2 = 0.93$ and hydrogen 4; $y = 1.13x - 0.01$, $R^2 = 0.96$). These data demonstrate that 1) the positional ^{2}H-enrichment distribution among the glutamine aliphatic hydrogens is preserved following purification and hydrolysis, and 2); the NMR method provides a precise and accurate measurement of absolute ^{2}H-enrichment values.

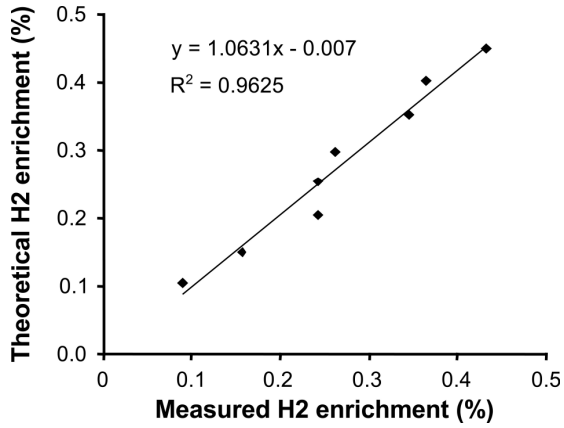

Figure 4.2: Relationship between the theoretical and experimental ^{2}H-enrichments of glutamate hydrogen 2 as measured by ^{2}H NMR spectroscopy of a series of glutamate standards. The standards were prepared from glutamine precursors containing known fractions of [2,3,3,4,4-$^{2}H_5$]glutamine ranging from 0.1-0.5%.

Figure 4.3 shows ^{1}H and ^{2}H NMR spectra of glutamate prepared from PAGN obtained from a healthy human subject who had previously ingested $^{2}H_2O$ and phenylbutyric acid. The 1.5-4.0 ppm region of the spectrum that features the glutamate signals had an additional single resonance at 3.4 ppm from an unknown compound (labeled X in Figure 4.3). The presence of both ^{1}H and ^{2}H NMR signals indicates that this site was enriched with ^{2}H, consistent with a metabolite that underwent exchange with ^{2}H-enriched BW and co-purified with PAGN and glutamate. The most likely identity of this signal is the methylene hydrogens of glycine derived from phenylacetylglycine hydrolysis. Glycine has been shown to be conjugated with phenylacetate in both primate and humans and phenylacetylglycine has been identified in urine (Webster *et al.* 1976). The methylene hydrogens of glycine can be enriched with ^{2}H during its formation from glycolytic intermediates *via* serine.

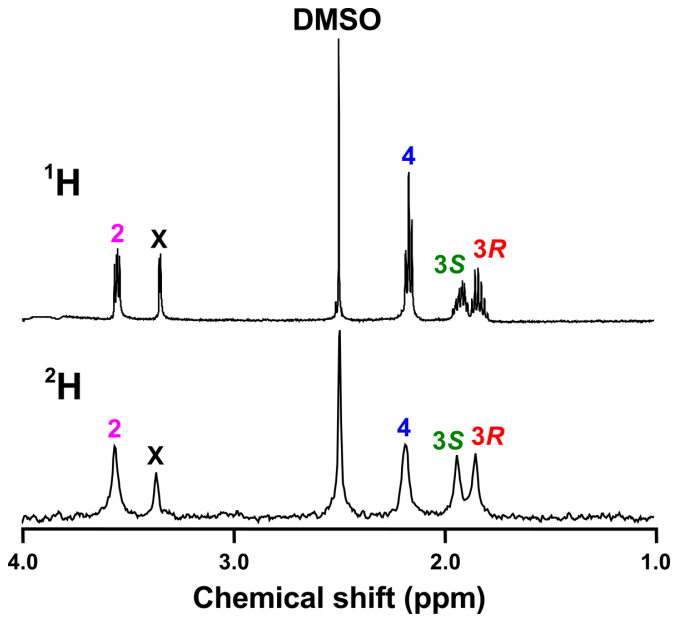

Figure 4.3: ^{1}H and ^{2}H NMR spectra of glutamate obtained from the hydrolysis of urinary phenylacetylglutamine of an overnight fasted subject. Both spectra were processed with 0.5 Hz line-broadening. The ^{1}H spectrum represents one acquisition while the ^{2}H spectrum represents 7,608 free-induction decays. The number above each resonance identifies the positional aliphatic glutamyl hydrogen and the colour of the number represents the metabolic origin of each positional ^{2}H-enrichment site as depicted in Figure 4.1.

The glutamate ^{2}H signals derived from PAGN did not show an even distribution of ^{2}H-enrichment, reflecting the specificity of exchange reactions that mediate the transfer of ^{2}H from bulk water into the various positions of the glutamyl backbone hydrogens. The estimated fractional ^{2}H-enrichments of each site, shown in Table 4.1, indicate that the position 2 hydrogen had the highest enrichment levels, followed by the hydrogen 3*R* and 3*S* sites, with the lowest enrichment values found for the position 4 hydrogens.

Table 4.1: Positional ^2H-enrichments of glutamate obtained from urinary PAGN for the eight healthy overnight fasted subjects given ^2H_2O and phenylbutyrate. Body water (BW) ^2H-enrichment is also shown.

Subject	PAGN Hydrogen 2 enrichment%	PAGN Hydrogen 3*S* enrichment%	PAGN Hydrogen 3*R* enrichment%	PAGN Hydrogen 4 enrichment%	BW%
1	0.25	0.21	0.21	0.14	0.47
2	0.44	0.39	0.42	0.25	0.67
3	0.35	0.25	0.25	0.16	0.51
4	0.35	0.27	0.27	0.17	0.57
5	0.32	0.23	0.23	0.16	0.40
6	0.30	0.26	0.24	0.18	0.42
7	0.32	0.30	0.29	0.19	0.41
8	0.28	0.23	0.23	0.15	0.44
Mean	**0.33***	**0.27**	**0.27**	**0.17**	**0.49**
SEM	**0.02**	**0.02**	**0.02**	**0.01**	**0.03**

* Significantly higher than H3*S* and H3*R* enrichments ($p< 0.05$), paired Student t-test).

Table 4.2: Sources of hepatic glutamine from the cataplerotic flux of the Krebs cycle and from proteolysis as estimated from the fractional ^2H-enrichments in positions 2 and 3*R*,*S* relative to that of body water (equations 5 and 6). Also shown is the fraction of proteolytic amino acids that participated in transaminase exchange before conversion to glutamine (equation 10). By definition, glutamine molecules derived from the Krebs cycle will have complete incorporation of deuterium from body water in to position 2 (i.e. equivalent to 100% exchange).

Subject	Glutamine carbon sources		Exchange *via* transaminase	
	Krebs cycle	Proteolysis	Krebs cycle sources	Proteolytic sources
1	44	56	100	17
2	60	40	100	17
3	49	51	100	38
4	47	53	100	27
5	58	43	100	53
6	60	40	100	29
7	72	28	100	22
8	52	48	100	24
Mean	**55**	**45**	**100**	**28**
SEM	**3**	**3**		**4**

The range of enrichments were substantially less that of BW indicating that a significant fraction of hepatic glutamine molecules had not undergone exchange with ^{2}H-BW and therefore could not have originated *via* the Krebs cycle but instead was derived from a metabolically inert glutamine pool (Figure 4.4).

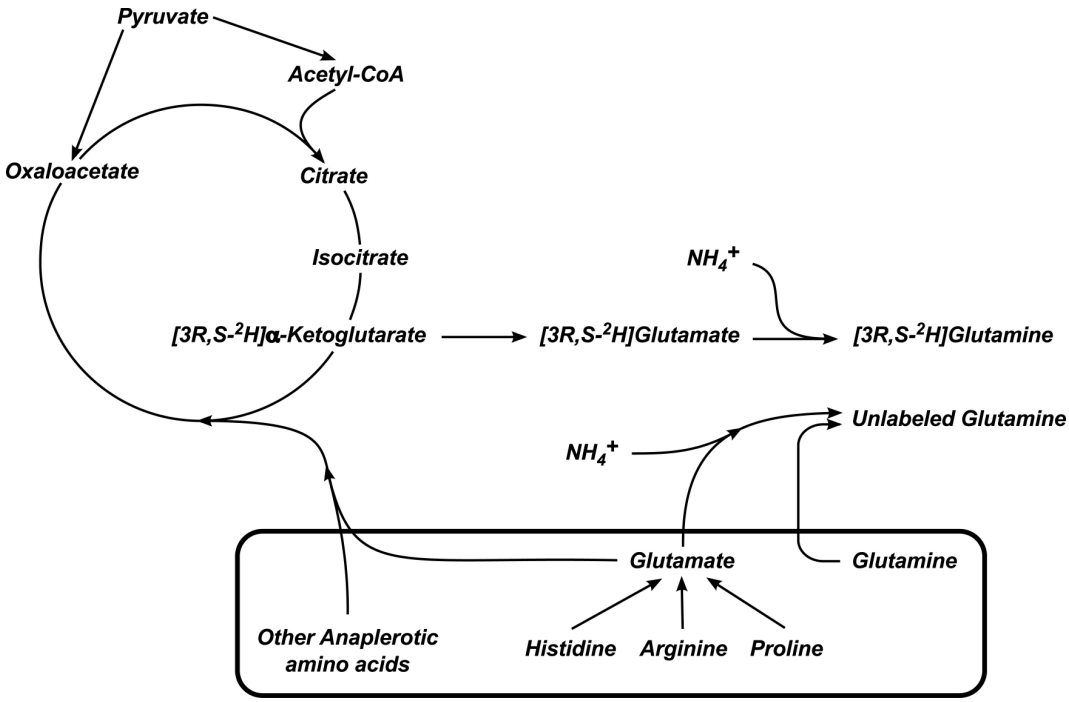

Figure 4.4: Schematic model depicting the principal sources of the glutamine carbon skeleton of phenylacetylglutamine from the Krebs cycle and from protein amino acid residues.

4.5 Discussion

4.5.1 Analytical considerations

It was demonstrated that positional ^{2}H-enrichment of human hepatic glutamine from ^{2}H-enriched BW can be measured by ^{2}H NMR following a relatively simple purification procedure. In principle, the analysis can be directly applied to PAGN since this molecule has well resolved chemical shifts for the glutamyl backbone hydrogens. In practice, it is found difficult to purify PAGN to a sufficient degree by the methodology used, to avoid contamination from other urinary metabolites. In addition, a portion of PAGN can undergo isomerization to form phenylacetylisoglutamine (Revelle *et al.* 1996) during sample drying resulting in a mixture of the two compounds and dispersion of the NMR signals. Finally, with the use of phenylbutyric acid as the metabolite biopsy agent, there is always the possibility that phenylbutyrylglutamine could be produced in addition to PAGN (Comte *et al.* 2002a), again potentially increasing the complexity of the NMR spectrum. Hydrolysis of SPE-purified PAGN (or phenylbutyrylglutamine) followed by isolation of the glutamate product by cation exchange greatly reduces background contributions from other urinary metabolites and generates a single analyte in good yield. Moreover, the recovered glutamate can be analyzed directly by NMR as an aqueous solution without need for pH adjustment or other manipulations aside from addition of the internal standard.

4.5.2 Intra-*versus* extrahepatic sources of PAGN

Glutamine that is recruited for PAGN synthesis can originate from both hepatic and extra-hepatic sources. There is evidence that the hepatic glutamine pool has a significant contribution from peripheral sources and is highly exchanged with

plasma glutamine. Tracers that are extensively metabolized by skeletal muscle, such as [2-^{14}C]acetate, are recovered in glutamine that is sampled in the liver as PAGN (Schumann *et al.* 1991). Conversely, with tracers that are preferentially metabolized by the hepatic Krebs cycle such as [U-^{13}C]propionate and [3-^{14}C]lactate, hepatic glutamine ^{13}C-enrichment or ^{14}C-specific activity was found to be substantially less than that of other anaplerotic products such as glucose-6-phosphate (G6P) (Magnusson *et al.* 1991; Jones *et al.* 1998; Jones *et al.* 2001b). The lower enrichment/specific activity of hepatic glutamine compared to hepatic G6P is consistent with the dilution of labeled glutamine derived from the hepatic Krebs cycle by unlabeled glutamine from peripheral sources.

4.5.3 Glutamine ^{2}H-enrichment from $^{2}H_2O$

Figure 4.1 shows the metabolic steps that are involved in the transfer of ^{2}H-enrichment from ^{2}H-enriched BW into the five aliphatic hydrogens of glutamine. Enrichment of hydrogen 2 is achieved by the conversion of α-ketoglutarate to glutamate. This can be catalyzed by glutamate dehydrogenase, or alternatively, any transaminase that utilizes α-ketoglutarate as an amine receptor such as alanine aminotransferase or aspartate aminotransferase. In all cases, it is assumed that the incorporation of BW into position 2 is quantitative given the fact that there is essentially complete exchange between the precursor nicotinamide adenine dinucleotide (NADH) hydrogen and that of bulk water (in the case of glutamate dehydrogenase) and the pyridoxal aldimine/ketimine intermediates and bulk water (in the case of transaminases). As a result, it can be assumed that ^{2}H-enrichment level at position 2 reflects glutamine molecules that originated from the α-ketoglutarate pool of the Krebs cycle and from glutamate molecules that had participated in glutamate-α-ketoglutarate exchange.

For a glutamine molecule to be enriched in the 3*R* and 3*S* hydrogens, its carbon skeleton must have originated from citrate either *via* the Krebs cycle or *via* cytosolic aconitase and isocitrate dehydrogenase. The 3*R* hydrogen is incorporated during the conversion of citrate to isocitrate, catalyzed by aconitase. The 3*S* hydrogen is incorporated following the conversion of isocitrate to α-ketoglutarate *via* proton addition to the transient oxalosuccinate intermediate. During a single turn of the Krebs cycle, both sites become enriched with BW resulting in equivalent enrichment of the 3*R* and 3*S* positions. While aconitase and isocitrate dehydrogenase activities are also present in the cytosol and could in principle result in enrichment of these sites independently of mitochondrial citrate metabolism (Garcia-Martin *et al.* 2002), the rapid equilibration of cytosolic and mitochondrial metabolite pools *via* citrate transport and malate-aspartate shuttles ensure that cytosolic and mitochondrial α-ketoglutarate pools are equivalently enriched from ^{2}H-BW under steady-state conditions. In any case, mitochondrial citrate synthase is the common source of citrate for both mitochondrial and cytosolic citrate metabolism. Enrichment of α-ketoglutarate 3*R* and 3*S* sites is assumed to reflect the net conversion of citrate to α-ketoglutarate hence glutamine molecules that are enriched in these positions also represent net products of citrate. As a result, the export of [3*R*,*S*-^{2}H] α-ketoglutarate from the Krebs cycle pool has to be balanced by an equivalent import of anaplerotic carbon skeletons[2].To the extent that the citrate–isocitrate–α-ketoglutarate–glutamate transformation is reversible, enrichment of the 3*R* and 3*S* positions represents exchange of glutamate and citrate in addition to net glutamate synthesis from citrate, therefore overestimating the cataplerotic contribution. While recent studies have

[2] Glutamate-α-ketoglutarate exchange will initially generate [3*R*,*S*]glutamate without net anaplerotic flux but under isotopic steady-state conditions, the exchanging glutamate pool is equivalently enriched to α-ketoglutarate and can therefore be considered as part of the Krebs cycle metabolites pool. Removal of [3*R*,*S*]glutamate from this system *via* conversion to [3*R*,*S*]glutamine depletes the pool and is therefore defined as cataplerosis. Maintenance of the Krebs cycle pool requires an equivalent anaplerotic inflow, which may include proteolytic glutamate.

demonstrated the reversibility of citrate–α-ketoglutarate–glutamate transformation in several tissues (Des Rosiers *et al.* 1994; Comte *et al.* 2002b; Yoo *et al.* 2008), in cardiac muscle it represents only a minor fraction (3-7%) of forward Krebs cycle flux (Comte *et al.* 2002b). Assuming similar conditions in skeletal muscle, enrichment of glutamate 3*R* and 3*S* positions by glutamate-citrate exchange is relatively insignificant.

For glutamine derived from the Krebs cycle, the origin of carbon 4 can be traced to the methyl carbon of acetyl-CoA. The methyl hydrogens of acetyl-CoA have been shown to partially exchange with those of BW, as seen by the partial loss of deuterium following the metabolism of [2-^{13}C, 2-$^{2}H_3$]acetate to glutamate and glutamine (Chapa *et al.* 2000). In addition, precursors of acetyl-CoA such as pyruvate can become enriched in the methyl position (Cooper 1976). In contrast to the aconitase and isocitrate dehydrogenase reactions, the incorporation of BW hydrogens by this mechanism is not obligatory.

4.5.4 PAGN ^{2}H-enrichment levels and sources of glutamyl carbon skeletons

In the context of enrichment from ^{2}H-BW, the glutamyl moiety of PAGN can be considered to be derived from three distinct biochemical sources. To the extent that there is transfer of glutamine from peripheral tissues to the liver, the location of these sources may be extrahepatic as well as intrahepatic since the $^{2}H_2O$ tracer is present in all tissues. Glutamyl moieties can be derived from 1) the direct release of glutamine from protein breakdown; 2) amination of glutamate produced by protein breakdown (glutamate that is directly released in addition to glutamate produced from the catabolism of histidine, proline and asparagine) and 3) amination of a glutamate molecule derived from the Krebs cycle *via* cataplerosis. Glutamine carbon skeletons derived from the Krebs cycle will be enriched in both 3*R* and 3*S* hydrogens whereas those derived from protein breakdown, be it in the form of glutamine or glutamate,

will not be enriched in these sites. Therefore, the enrichment of glutamine 3*R* or 3*S* relative to that of BW is equivalent to the fraction of glutamine derived from the Krebs cycle. To the extent that proteolytic amino acids such as glutamate, alanine and aspartate are utilized as anaplerotic substrates by the Krebs cycle, the cataplerotic fraction will include the contributions of these carbons in addition to other anaplerotic sources such as pyruvate. In this study, enrichment of the 3*R*,*S* sites relative to that of BW enrichment was ~55% indicating that at least 45% of hepatic glutamine was derived from proteolysis. In the study of Kuhn *et al.*, the rate of appearance of proteolytic glutamine was assessed by measuring the total protein turnover *via* [1-^{13}C]leucine and multiplying this by the fraction of protein glutamine residues (Kuhn *et al.* 1999). This rate represented ~14% of whole body glutamine R_a indicating that proteolysis accounted for 14% and *de novo* synthesis accounted for 86% of glutamine R_a. In this analysis, *de novo* synthesis includes glutamine synthesized from both cataplerotic activity and from proteolytic amino acid precursors such as glutamate. Since the fraction of protein glutamate residues is ~4 times that of glutamine (Kuhn *et al.* 1999), the release of one equivalent of glutamine *via* proteolysis is accompanied by four of glutamate. Were this glutamate quantitatively converted to glutamine, it would account for ~56% of total glutamine R_a. On this basis, proteolytic carbon skeletons (glutamine, glutamate plus other amino acid precursors) could potentially contribute over 70% of whole-body glutamine R_a. Under these conditions plasma glutamine enrichment of position 3 relative to that of BW would be low since only a minority (~30%) of glutamine molecules would be derived from cataplerosis. The experimental finding that 28-56% of hepatic glutamine was unlabeled is consistent with a sizable inflow of proteolytically-derived glutamine. While this could in principle be derived from both intra- and extra-hepatic proteolysis, extra-hepatic sources are expected to be important contributors given the active uptake of plasma glutamine by the liver (van de Poll *et al.* 2007).

Enrichment of glutamine position 2 originates during the conversion of α-ketoglutarate to glutamate and can be catalyzed by glutamate dehydrogenase and various transaminases that couple glutamate/α-ketoglutarate with other amino acids and their keto-acid equivalents. Therefore, glutamine molecules whose carbon skeletons are derived from the Krebs cycle will be enriched in this position as well as in position 3. The observation that position 2 enrichment was significantly higher than that of position 3 is best explained by the participation of unlabeled glutamate in transaminase exchange prior to being converted to glutamine. Moreover, this exchange must have involved glutamate pools that were not exchanging with Krebs cycle metabolites otherwise there would be no selective enrichment of position 2. It can be speculated that cytosolic transaminases might provide the opportunity for rapid glutamate/α-ketoglutarate exchange in isolation from the mitochondrial Krebs cycle intermediates. From the difference in enrichment between positions 2 and 3 of hepatic glutamine, it was estimated that about one-quarter of the proteolytic glutamyl precursors participated in transaminase exchange before conversion to glutamine. Since hydrogen 2 is enriched independently of cataplerotic Krebs cycle flux, its enrichment level relative to BW overestimates the fraction of glutamine derived from cataplerosis.

4.5.5 Enrichment of acetyl-CoA from ^{2}H-enriched body water

Carbon 4 of glutamate and its pair of hydrogens are derived from the methyl carbon and hydrogens of acetyl-CoA, a common product of pyruvate and fatty acid oxidation. Incorporation of acetyl-CoA into citrate *via* citrate synthase is accompanied by the loss of one of the methyl hydrogens. The remaining two hydrogens that are bound to the carbon do not participate in any of the reactions that transform citrate to glutamine. To the extent that these hydrogens do not exchange with those of BW during the conversion of citrate to α-ketoglutarate and glutamate, enrichment of

position 4 reflects the enrichment of the acetyl-CoA molecules that entered the Krebs cycle. The extent of acetyl-CoA enrichment can be determined by comparing the relative enrichments of position 4 and position 3, since for every α-ketoglutarate molecule that is derived from the Krebs cycle, the position 3 hydrogens are fully exchanged with those of BW. From the PAGN positional enrichment levels presented in Table 4.1 the mean ratio of position 4 to position 3 ^{2}H-enrichments was 0.66 indicating that exchange between the acetyl-CoA methyl hydrogens that fed the Krebs cycle and BW was 66% complete. This value may reflect a weighted contribution of acetyl-CoA from pyruvate, *via* pyruvate dehydrogenase, and from acyl sources *via* β-oxidation. The methyl hydrogens of acetyl-CoA derived from pyruvate are expected to be almost quantitatively exchanged with those of water as a result of alanine aminotransferase activity (Cooper 1976). For acetyl-CoA derived from β-oxidation of fatty acids, the extent of methyl hydrogen enrichment from ^{2}H-BW is not known. The β-oxidation sequence involves the incorporation of 2 water hydrogens per acetyl-CoA molecule released[3] giving a theoretical enrichment of 66% that of BW. This is identical to our experimental estimate and suggests that the acetyl-CoA entering the hepatic Krebs cycle was derived from acyl sources rather than pyruvate. This is concordant with ^{14}C and ^{13}C tracer studies of human Krebs cycle fluxes that estimated an 80-90% contribution of acyl substrates to acetyl-CoA production in the fasted state (Magnusson *et al.* 1991; Diraison *et al.* 1999).

4.5.6 Whole-body glutamine production and hepatic gluconeogenesis

For healthy, postabsorptive subjects, glutamine R_a is 4.5-6.0 μmol/kg/min (Nurjhan *et al.* 1995; Hankard *et al.* 1997; Williams *et al.* 1998). In comparison, gluconeogenic flux is ~5.0 μmol/kg/min (10 μmol/kg/min of triose-P equivalents)

[3] Hydration of trans-delta-2-enoyl-CoA by *S*-3-hydroxyacyl-CoA hydrolase and cleavage of acetyl CoA from 3-ketoacyl-CoA by 3-ketothiolase.

of which 90%, or ~9μmol/kg/min, is derived *via* the anaplerotic pathways of the Krebs cycle. Therefore, glutamine could potentially provide up to two thirds of anaplerotic carbons for gluconeogenesis. In healthy subjects infused with ^{13}C-enriched glutamine, the contribution of glutamine to endogenous glucose production was estimated to be 8% after 18 hours of fasting rising to 16% after 42 hours of fasting (Hankard *et al.* 1997). To the extent that the ^{13}C-tracer is diluted as a result of exchanges at the level of the hepatic Krebs cycle and amino acid pools, these values likely underestimate the true contribution of glutamine to gluconeogenesis. Glutamine R_a is significantly increased in several kinds of critical illness. In HIV-infected subjects, muscle wasting was associated with a ~50% increase in glutamine R_a (Yarasheski *et al.* 1998). During sepsis, there is an increased efflux of glutamine from skeletal muscle which is associated with a net loss of protein (Biolo *et al.* 1997). In other critical illness settings, glutamine R_a may lie within the normal range but the source contributions can be significantly altered. For a group of critically ill subjects with gastrointestinal damage, glutamine R_a was not significantly different to that of healthy controls, but the fractional contribution of proteolytic sources to glutamine R_a was significantly higher for the critically ill group (Jackson *et al.* 1999). In lung cancer patients experiencing loss of lean body mass, both endogenous glucose production and gluconeogenesis from alanine were significantly elevated compared to lung-cancer patients that were weight-stable (Leij-Halfwerk *et al.* 2000). Insulin-resistant subjects who are not critically ill may also have an increased availability of amino acids for gluconeogenesis due to impaired stimulation of protein synthesis by insulin (Chevalier *et al.* 2005; Chevalier *et al.* 2006). These studies underline the increased role of gluconeogenic amino acids derived from peripheral tissues on hepatic glucose metabolism in a range of disease conditions. To the extent that the hepatic glutamine pool is connected to whole-body glutamine fluxes and sources, its enrichment from ^2H_2O could be sensitive to systemic alterations in glutamine metabolism.

4.6 Conclusions

In conclusion, in this Chapter, is present a simple and noninvasive method for resolving the contributions of whole-body metabolic and proteolytic activities to the supply of hepatic glutamine carbon skeletons based on the ingestion of ^2H_2O and phenylbutyrate followed by the analysis of urinary PAGN. This analysis may allow the role of peripheral intermediary metabolism and protein synthesis/degradation on the sources of hepatic glutamine carbons to be better defined. PAGN recovery and analysis can be integrated with ^2H_2O measurements of hepatic gluconeogenesis (Jones *et al.* 1998; Jones *et al.* 2001b; Perdigoto *et al.* 2003) therefore in principle, the relationship between hepatic glutamine sources and gluconeogenic activity can be explored in a variety of physiological and pathophysiological settings.

4.7 References

Biolo G, Fleming RYD, Maggi SP and Wolfe RR. Transmembrane transport and intracellular kinetics of amino-acids in human skeletal-muscle. American Journal of Physiology-Endocrinology and Metabolism 1995;31:E75-E84.

Biolo G, Toigo G, Ciocchi B, Situlin R, Iscra F, Gullo A and Guarnieri G. Metabolic response to injury and sepsis: Changes in protein metabolism. Nutrition 1997;13:S52-S57.

Biolo G, Zorat F, Antonione R and Ciocchi B. Muscle glutamine depletion in the intensive care unit. International Journal of Biochemistry & Cell Biology 2005;37:2169-2179.

Chapa F, Cruz F, Garcia-Martin ML, Garcia-Espinosa MA and Cerdan S. Metabolism of [1-^{13}C]glucose and [2-^{13}C, 2-$^{2}H_3$]acetate in the neuronal and glial compartments of the adult rat brain as detected by [^{13}C, ^{2}H] NMR spectroscopy. Neurochemistry International 2000;37:217-228.

Chevalier S, Burgess SC, Malloy CR, Gougeon R, Marliss EB and Morais JA. The greater contribution of gluconeogenesis to glucose production in obesity is related to increased whole-body protein catabolism. Diabetes 2006;55:675-681.

Chevalier S, Marliss EB, Morais JA, Lamarche M and Gougeon R. Whole-body protein anabolic response is resistant to the action of insulin in obese women. American Journal of Clinical Nutrition 2005;82:355-365.

Comte B, Kasumov T, Pierce BA, Puchowicz MA, Scott ME, Dahms W, Kerr D, Nissim I and Brunengraber H. Identification of phenylbutyrylglutamine, a new metabolite of phenylbutyrate metabolism in humans. Journal of Mass Spectrometry 2002a;37:581-590.

Comte B, Vincent G, Bouchard B, Benderdour M and Des Rosiers C. Reverse flux through cardiac NADP^{+}-isocitrate dehydrogenase under normoxia and ischemia. American Journal of Physiology - Heart and Circulatory Physiology 2002b;283:H1505-H1514.

Cooper AJ. Proton magnetic resonance studies of glutamate-alanine transaminase-catalyzed deuterium exchange. Evidence for proton conservation during prototropic transfer from the alpha carbon of L-alanine to the C4-position of pyridoxal 5'-phosphate. Journal of Biological Chemistry 1976;251:1088-1096.

Des Rosiers C, Fernandez CA, David F and Brunengraber H. Reversibility of the mitochondrial isocitrate dehydrogenase reaction in the perfused rat liver. Evidence from isotopomer analysis of citric acid cycle intermediates. Journal of Biological Chemistry 1994;269:27179-27182.

Diraison F, Large V, Maugeais C, Krempf M and Beylot M. Noninvasive tracing of human liver metabolism: comparison of phenylacetate and apoB-100 to sample glutamine. American Journal of Physiology 1999;277:E529-536.

Dugelay S, Yang D, Soloviev MV, Previs SF, Agarwal KC, Fernandez CA and Brunengraber H. Assay of the concentration and ^{13}C-labeling pattern of phenylacetylglutamine by Nuclear Magnetic Resonance. Analytical Biochemistry 1994;221:368-373.

Garcia-Martin ML, Garcia-Espinosa MA, Ballesteros P, Bruix M and Cerdan S. Hydrogen turnover and subcellular compartmentation of hepatic [2-^{13}C]glutamate and [3-^{13}C]aspartate as detected by ^{13}C NMR. Journal of Biological Chemistry 2002;277:7799-7807.

Gibala MJ, Young ME and Taegtmeyer H. Anaplerosis of the citric acid cycle: role in energy metabolism of heart and skeletal muscle. Acta Physiologica Scandinavica 2000;168:657-665.

Hankard RG, Haymond MW and Darmaun D. Role of glutamine as a glucose precursor in fasting humans. Diabetes. 1997;46:1535-1541.

Jackson NC, Carroll PV, Russell-Jones DL, Sönksen PH, Treacher DF and Umpleby AM. The metabolic consequences of critical illness: acute effects on glutamine and protein metabolism. American Journal of Physiology - Endocrinology and Metabolism 1999;276:E163-E170.

Jones JG, Barosa C, Gomes F, Mendes AC, Delgado TC, Diogo L, Garcia P, Bastos M, Barros L, Fagulha A, Baptista C, Carvalheiro M and Caldeira MM. NMR derivatives for quantification of ^{2}H- and ^{13}C-enrichment of human glucuronide from metabolic tracers. Journal of Carbohydrate Chemistry 2006;25:203-217.

Jones JG, Carvalho RA, Franco B, Sherry AD and Malloy CR. Measurement of hepatic glucose output, Krebs cycle, and gluconeogenic fluxes by NMR analysis of a single plasma glucose sample. Analytical Biochemistry 1998;263:39-45.

Jones JG, Merritt, M. and Malloy, C.R. Quantifying tracer levels of $^{2}H_2O$ enrichment from microliter amounts of plasma and urine by ^{2}H NMR. Magnetic Resonance in Medicine 2001a;45:156-158.

Jones JG, Solomon M.A., Cole, S.M., Sherry, A.D., Malloy, C.R. An integrated ^{2}H and ^{13}C NMR study of gluconeogenesis and TCA cycle flux in humans. American Journal of Physiology- Endocrinology and Metabolism 2001b;281:E848-E851.

Jucker BM, Rennings AJ, Cline GW, Petersen KF and Shulman GI. *In vivo* NMR investigation of intramuscular glucose metabolism in conscious rats. American Journal of Physiology - Endocrinology And Metabolism 1997;273:E139-E148.

Kuhn KS, Schuhmann K, Stehle P, Darmaun D and Fürst P. Determination of glutamine in muscle protein facilitates accurate assessment of proteolysis and *de novo* synthesis-derived endogenous glutamine production. The American Journal of Clinical Nutrition 1999;70:484-489.

Leij-Halfwerk S, Dagnelie PC, van Den Berg JW, Wattimena JD, Hordijk-Luijk CH and Wilson JP. Weight loss and elevated gluconeogenesis from alanine in lung cancer patients. American Journal of Clinical Nutrition 2000;71:583-589.

Magnusson I, Schumann WC, Bartsch GE, Chandramouli V, Kumaran K, Wahren J and Landau BR. Noninvasive tracing of Krebs cycle metabolism in liver. Journal of Biological Chemistry 1991;266:6975-6984.

Norrelund H, Wiggers H, Halbirk M, Frystyk J, Flyvbjerg A, Botker HE, Schmitz O, Jorgensen JOL, Christiansen JS and Moller N. Abnormalities of whole body protein turnover, muscle metabolism and levels of metabolic hormones in patients with chronic heart failure. Journal of Internal Medicine 2006;260:11-21.

Nurjhan N, Bucci A, Perriello G, Stumvoll M, Dailey G, Bier DM, Toft I, Jenssen TG and Gerich JE. Glutamine - a major gluconeogenic precursor and vehicle for interorgan carbon transport in man. Journal of Clinical Investigation 1995;95:272-277.

Perdigoto R, Rodrigues TB, Furtado AL, Porto A, Geraldes C and Jones JG. Integration of [U-^{13}C]glucose and $^{2}H_2O$ for quantification of hepatic glucose production and gluconeogenesis. NMR in Biomedicine 2003;16:189-198.

Perriello G, Nurjhan N, Stumvoll M, Bucci A, Welle S, Dailey G, Bier DM, Toft I, Jenssen TG and Gerich JE. Regulation of gluconeogenesis by glutamine in normal postabsorptive humans. American Journal of Physiology 1997;272:E437-E445.

Previs SF, Fatica R, Chandramouli V, Alexander JC, Brunengraber H and Landau BR. Quantifying rates of protein synthesis in humans by use of ^2H_2O: application to patients with end-stage renal disease. American Journal of Physiology - Endocrinology and Metabolism 2004;286:E665-E672.

Reeds DN, Cade WT, Patterson BW, Powderly WG, Klein S and Yarasheski KE. Whole-body proteolysis rate is elevated in HIV-associated insulin resistance. Diabetes 2006;55:2849-2855.

Revelle LK, Davignon DA and Wilson JA. 3-[(phenylacetyl)amino]-2,6-piperidinedione hydrolysis studies with improved synthesis and characterization of hydrolysates. Journal of Pharmaceutical Sciences 1996;85:1049-1052.

Ribeiro A, Caldeira MM, Carvalheiro M, Bastos M, Baptista C, Fagulha A, Barros L, Barosa C and Jones JG. Simple measurement of gluconeogenesis by direct ^2H NMR analysis of menthol glucuronide enrichment from ^2H_2O. Magnetic Resonance in Medicine 2005;54:429-434.

Sahlin K, Jorfeldt L, Henriksson KG, Lewis SF and Haller RG. Tricarboxylic-acid cycle intermediates during incremental exercise in healthy-subjects and in patients with Mcardles-disease. Clinical Science 1995;88:687-693.

Schumann WC, Magnusson I, Chandramouli V, Kumaran K, Wahren J and Landau BR. Metabolism of [2-^{14}C]acetate and its use in assessing hepatic Krebs cycle activity and gluconeogenesis. Journal of Biological Chemistry 1991;266:6985-6990.

van de Poll MCG, Ligthart-Melis GC, Boelens PG, Deutz NEP, van Leeuwen PAM and Dejong CHC. Intestinal and hepatic metabolism of glutamine and citrulline in humans. Journal of Physiology-London 2007;581:819-827.

Webster LT, Siddiqui UA, Lucas SV, Strong JM and Mieyal JJ. Identification of separate acyl-CoA:glycine and acyl-CoA:L-glutamine N-acyltransferase activities in mitochondrial fractions from liver of rhesus monkey and man. Journal of Biological Chemistry 1976;251:3352-3358.

Williams BD, Chinkes DL and Wolfe RR. Alanine and glutamine kinetics at rest and during exercise in humans. Medicine and Science in Sports and Exercise 1998;30:1053-1058.

Yang D, Beylot M, Agarwal KC, Soloviev MV and Brunengraber H. Assay of the human liver citric acid cycle probe phenylacetylglutamine and of phenylacetate in plasma by gas chromatography-mass spectrometry. Analytical Biochemistry 1993;212:277-282.

Yang D, Previs SF, Fernandez CA, Dugelay S, Soloviev MV, Hazey JW, Agarwal KC, Levine WC, David F, Rinaldo P, Beylot M and Brunengraber H. Noninvasive probing of citric acid cycle intermediates in primate liver with phenylacetylglutamine. American Journal of Physiology 1996;270:E882-E889.

Yarasheski KE, Zachwieja JJ, Gischler J, Crowley J, Horgan MM and Powderly WG. Increased plasma Gln and Leu Ra and inappropriately low muscle protein synthesis rate in AIDS wasting. American Journal of Physiology - Endocrinology And Metabolism 1998;275:E577-E583.

Yoo H, Antoniewicz MR, Stephanopoulos G and Kelleher JK. Quantifying reductive carboxylation flux of glutamine to lipid in a brown adipocyte cell line. Journal of Biological Chemistry 2008;283:20621-20627.

Chapter 5

Concluding Remarks

Concluding Remarks

Novel noninvasive assays of glucose and glutamine fluxes were developed using stable isotopes and Nuclear Magnetic Resonance (NMR) analysis of hepatic uridine diphosphate-glucose (UDP-glucose) and glutamine, obtained *via* chemical biopsy as urinary glucuronide and phenylacetylglutamine, respectively.

In Chapters 2 and 3 these approaches were applied to study hepatic glucose and glycogen metabolism both in healthy and insulin resistant subjects. In Chapter 2, direct and indirect pathway contributions to hepatic glycogen synthesis were measured in healthy subjects by analysis of glucuronide enrichment from deuterated water (^2H_2O). The method relies on a hitherto untested assumption of complete exchange between hepatic glucose-6-phosphate and fructose-6-phosphate. This assumption was verified by observing the essentially complete depletion of glucuronide hydrogen 2 enrichment from [U-$^2H_7$]glucose. On this basis, direct and indirect contributions were calculated from the position 5 to position 2 ^{2}H-enrichment ratio. The [U-$^2H_7$]glucose analysis also indicated the presence of significant transaldolase (TA) exchange activity as seen by the significantly lower ^{2}H-enrichment of glucuronide positions 4 and 5 relative to position 3. The fraction of hepatic hexose phosphate that underwent TA exchange was estimated to be 20%. The contribution of galactose derived from the milk of the breakfast meal was also determined. Galactose is metabolized to glycogen in the liver without acquiring label, thus diluting the ^{2}H-enrichments. Its contribution to glycogen synthesis was calculated by comparing dilution of glucuronide position 2 relative to body water ^{2}H-enrichments. The galactose contribution to glycogen synthesis was found to be 20%.

In Chapter 3, current measurements of the gluconeogenic contribution to endogenous glucose production (EGP) based on enrichment of glucose position 5 from deuterated water were challenged by the demonstration of significant hepatic

TA exchange activity. TA exchange results in glucose enrichment from gluconeogenic tracers independently of gluconeogenic flux. TA exchange activity was quantified by ^{13}C NMR analysis of glucose and glucuronide positions 3 and 4 enrichments from infused [1-^{13}C]acetate. The results show that up to one-third of hepatic hexose phosphate underwent TA exchange resulting in significant overestimates of the gluconeogenic contribution to EGP with the conventional deuterated water analysis. This effect was observed for subjects with normal glucose tolerance as well as for subjects with impaired glucose tolerance. Glucose position 5 enrichment from ^2H_2O overestimates gluconeogenesis because of TA exchange. Glucose position 3 enrichment is unaffected by TA exchange and is therefore proposed to be a more precise marker of gluconeogenic activity. However, its incorporation into glucose is contingent on complete triose phosphate exchange and absence of kinetic isotope effects that are well described for triose phosphate isomerase. Comparison of glucose position 3 *versus* position 5 enrichments after correction for TA exchange indicates a modest underestimate of the true gluconeogenic contribution to EGP from analysis of position 3 enrichment.

In Chapter 4, whole-body metabolic and proteolytic contributions to the hepatic glutamine pool were accessed by ingestion of ^2H_2O. Hepatic glutamine pool was sampled with phenylbutyrate to form urinary phenylacetylglutamine and proteolytic and cataplerotic sources were determined by ^2H NMR analysis of phenylacetylglutamine. From the ratio of positions 3*R,S* ^2H-enrichments relative to that of body water, was determined that in a group of healthy subjects 55% of hepatic glutamine was derived from cataplerosis and 45% from proteolysis. The knowledge of the sources of glutamine can be applied and related with gluconeogenic fluxes in pathophysiological states such as Type 2 diabetes and cachexia.

In conclusion, the work presented in this Thesis present an advance in improving the precision and minimizing the uncertainties of hepatic glucose and glycogen synthesis metabolism by accounting for the effects of TA and dietary

galactose to the measurements. Also the establishment of proteolytic and metabolic contributions to hepatic glutamine pool in healthy subjects is of a high importance since glutamine is a gluconeogenic amino acid and may contribute to elevated rates of gluconeogenesis.

ACKNOWLEDGEMENTS/REMERCIEMENTS/AGRADECIMENTOS

To Doctor John Jones, I want to express my gratitude for giving me the opportunity to join his studies in the clinical research field, a dream I always had. The strength of his transmitted enthusiasm made me overpass all natural private barriers and accept this challenge. I underline my deep admiration for his scientific strictness. Sharing great skills and knowledge in different matters within the metabolism research area, he always carries ideas and creativity. Working with him has been very pleasant and profitable. His precious guidance, constant support, along with encouragement and optimism, were of utmost importance for the development of this work. Finally, my deep gratitude for the confidence he always deposited on me.

À Doutora Madalena Caldeira agradeço as suas palavras de incentivo, que muito contribuíram para me entusiasmar a partir para este projecto. Grata também por todos os conhecimentos que me foi transmitindo ao longo de todos estes anos. Devo salientar o seu acompanhamento, apoio e mostra de confiança durante a apresentação e divulgação do trabalho realizado.

Ao Professor Doutor Carlos Geraldes a minha gratidão por ter-me recebido no grupo de RMN, abrindo-me assim, as "portas" da Investigação. Guardo com grande apreço a sua amizade e constante apoio, já desde os tempos da minha licenciatura.

Para a Doutora Margarida Castro a minha grande amizade e gratidão. Tem sido, na sua disponibilidade e conselhos sábios, que sempre tenho encontrado todo o apoio, ao longo de um percurso de muitos anos.

Je tiens à remercier le Docteur Emeric Wasielewski, avec profonde reconnaissance et amitié, pour son indéniable support, engagement et intérêt en ce qui concerne la résolution des difficultés tout au long de ce travail de spectroscopie RMN. Son optimisme, dévouement et persévérance ont pris une importance fondamentale dans l'arrangement et l'achèvement du travail présenté dans cette Thèse.

Um agradecimento muito especial aos colegas de laboratório Ana Rita Gonçalves, Claúdia Silva, Daniela Pinheiro, Filipa Simões, Filipe Gomes, Isabel Gonçalves, Ivana Jarak, Joana Barra, Manuela Almeida, Patrícia Nunes e Teresa Delgado, assim como aos colegas "visitantes" Ana Maria Silva, Fátima Martins, Francisca Soares, e Ivan Viegas, que me acompanharam ao longo destes anos de realização do trabalho experimental, apresentado nesta Tese. Gostaria também de expressar o meu apreço às "antigas" colegas de laboratório, Ângela Ribeiro e Carina Mendes, que acompanharam os meus primeiros passos na Investigação Científica, ainda antes de empreender a árdua tarefa de um projecto de doutoramento. Toda a partilha de experiência, inter-ajuda e companheirismo foram essenciais para um ambiente particularmente agradável e inesquecíveis bons momentos. Saliento ainda a simpatia com que fui recebida pela Carla Fonseca, Giovannia Araújo, Liliana Montezinho e Pedro Coxito, aquando da minha chegada ao grupo de RMN. Um abraço, com estima, à Doutora Licínia e à Doutora Luísa.

Ao serviço de Endocrinologia, Diabetes e Metabolismo do Hospital Universitário de Coimbra, e particularmente à Professora Doutora Manuela Carvalheiro, Dr.ª Ana Fagulha, Dr.ª Luísa Barros, Dr.ª Margarida Bastos e Dr.ª Carla Baptista os meus agradecimentos pelo trabalho realizado em conjunto. Obrigada também a todos os Enfermeiros e Funcionários deste serviço que colaboraram nos estudos clínicos realizados.

Agradeço a todos os voluntários que participaram nos estudos clínicos. A sua colaboração foi fundamental para a realização do trabalho apresentado nesta Tese.

Ao meu Pai, Luís, Teresa e Luísa a minha profunda gratidão pelo permanente e incondicional apoio ao longo de todos estes anos.